

# AKARI IRC Data User Manual

Version 2.2

Fumi Egusa<sup>3</sup>,  
Rosario Lorente<sup>1</sup>, Takashi Onaka<sup>2</sup>, Yoshifusa Ita<sup>3,5,7</sup>, Youichi Ohyama<sup>3,9</sup>,  
Toshihiko Tanabé<sup>2</sup>, Chris Pearson<sup>6</sup> and Takuji Yamashita<sup>3</sup>

with contributions from:

Martin Cohen<sup>4</sup>, Daisuke Ishihara<sup>2,8</sup>, Hideo Matsuhara<sup>3</sup>, Itsuki Sakon<sup>2</sup>, Takehiko Wada<sup>3</sup>,  
and Issei Yamamura<sup>3</sup>

<sup>1</sup>European Space Astronomy Centre (ESAC), ESA

<sup>2</sup>Tokyo University, Japan

<sup>3</sup>Institute of Space and Astronautical Science (ISAS), JAXA

<sup>4</sup>University of California, Berkeley

<sup>5</sup>National Astronomical Observatory, Japan (NAOJ)

<sup>6</sup>Rutherford Appleton Laboratory (RAL)

<sup>7</sup>Astronomical Institute, Tohoku University, Japan

<sup>8</sup>Nagoya University, Japan

<sup>9</sup>Academia Sinica Institute of Astronomy and Astrophysics, Taiwan

July 6, 2016





<b>Date</b>	<b>Revision</b>	<b>Comments</b>
07 March 2007	Version 1.0	Release of version 1.0
21 March 2007	Version 1.1	Updated Table 4.6.7 (photometric conversion factors)
18 June 2007	Version 1.2	Updated Sections: 4.6.3, 4.10, 4.13, 5.13.2, 5.14, 6.1
06 September 2007	Version 1.3	Updated Chapter 4, 5 and 6 Included ghosts in Np observations (section 4.13)
28 May 2008	Version 1.4	Chapter 6 updated according to spectroscopy pipeline 20080528
26 December 2014	Version 1.6	Major updates in Chapters 3, 4, and 5 according to the revised imaging toolkit for Phase 1&2 (ver. 140003)
31 March 2015	Version 2.0	Updates in Chapters 3, 4, and 5 according to the imaging toolkit for Phase 1&2 (ver. 150331) and processed data release
01 December 2015	Version 2.1	Updated Chapter 4 Added the difference between MIR-S and -L shift values (Section 4.16)
06 July 2016	Version 2.2	Proofread some sentences in Sections 4.12.1, 4.17, 5.7.2, and 5.13.

# Contents

<b>1</b>	<b>Introduction</b>	<b>1</b>
1.1	Purpose of this document . . . . .	1
1.2	Operational phases . . . . .	1
1.3	Relevant information . . . . .	2
<b>2</b>	<b>Instrument overview</b>	<b>3</b>
2.1	Focal plane arrays . . . . .	5
2.1.1	Near-InfraRed Camera: NIR . . . . .	5
2.1.2	Short wavelength Mid-InfraRed Camera: MIR-S . . . . .	6
2.1.3	Long wavelength Mid-InfraRed Camera: MIR-L . . . . .	8
2.1.4	Arrays operation . . . . .	8
2.2	Instrument AOTs . . . . .	9
2.2.1	IRC00 . . . . .	9
2.2.2	IRC02 . . . . .	10
2.2.3	IRC03 . . . . .	10
2.2.4	IRC04 . . . . .	10
2.2.5	IRC05 . . . . .	10
2.2.6	IRC11 . . . . .	10
2.2.7	IRC51 . . . . .	10
2.2.8	AOT parameters for imaging observations . . . . .	11
2.3	In-orbit sensitivity . . . . .	11
<b>3</b>	<b>Distributed Data Products</b>	<b>13</b>
3.1	IRC FITS file naming rule . . . . .	13
3.1.1	Raw data package . . . . .	13
3.1.2	Processed data package . . . . .	13
3.2	Raw data description . . . . .	14
3.2.1	Raw data naming convention . . . . .	14
3.2.2	AKARI FITS Primary HDU (common information) rawdata header . . . . .	14
3.2.3	Raw data dimensions . . . . .	18
3.3	Quick look data . . . . .	18
3.3.1	IRC imaging: IRC00, IRC02, IRC03, and IRC05 . . . . .	19
3.3.2	IRC spectroscopy: IRC04 . . . . .	19
3.4	IRC04 image orientation and dispersion direction . . . . .	19

<b>4</b>	<b>IRC Calibration and Accuracy</b>	<b>20</b>
4.1	Dark image . . . . .	20
4.1.1	Long-term variation . . . . .	20
4.1.2	Intermediate-term variation . . . . .	22
4.1.3	Short-term variation . . . . .	22
4.2	Flatfield . . . . .	22
4.2.1	Flatfields for imaging data . . . . .	22
4.2.2	Flats for spectroscopy images . . . . .	24
4.3	Instrument linearity . . . . .	27
4.4	Instrument Point Spread Function . . . . .	27
4.5	RSRF . . . . .	30
4.6	Flux calibration for point sources . . . . .	32
4.6.1	Observed standards and data processing . . . . .	32
4.6.2	Estimation of the in-band flux . . . . .	34
4.6.3	Absolute calibration . . . . .	35
4.6.4	Overall accuracy of the flux calibration . . . . .	35
4.7	Flux calibration for extended sources . . . . .	35
4.8	Color correction . . . . .	36
4.9	Distortion . . . . .	44
4.10	Memory effects caused by bright source observations . . . . .	45
4.11	Astrometry . . . . .	46
4.12	Arrays anomalies . . . . .	46
4.12.1	NIR array . . . . .	46
4.12.2	MIR arrays . . . . .	46
4.13	Ghosts . . . . .	47
4.13.1	Arcmin-scale ghosts . . . . .	47
4.13.2	Degree-scale ghosts . . . . .	47
4.14	The earthshine light (EL) . . . . .	48
4.15	Relative shift values . . . . .	49
4.16	Difference between MIR-S and -L shift values . . . . .	52
4.17	General concerns on slit-less spectroscopy data . . . . .	54
<b>5</b>	<b>Imaging toolkit cookbook</b>	<b>57</b>
5.1	Introduction . . . . .	57
5.2	General overview of the toolkit processing . . . . .	57
5.3	Expected Data Processing Rate (minimum expectation) . . . . .	58
5.4	How to install the IRC imaging Toolkit . . . . .	58
5.4.1	Requirements . . . . .	58
5.4.2	Install IRAF . . . . .	59
5.4.3	Download IRC imaging data reduction software package . . . . .	59
5.4.4	Unpack irc.tgz . . . . .	59
5.4.5	Make irc binaries . . . . .	59
5.4.6	Run "setpath.pl" . . . . .	59
5.4.7	Perl path . . . . .	59
5.4.8	Add IRC entry to IRAF . . . . .	60
5.5	How to UPGRADE the version of IRC imaging toolkit . . . . .	61
5.6	Setting up your toolkit environment and running the pipeline . . . . .	61
5.6.1	Creating the directory structure . . . . .	61

5.6.2	Launch IRAF . . . . .	61
5.6.3	Load the IRC package . . . . .	63
5.7	The pre-pipeline processor (Red-Box) . . . . .	64
5.7.1	Configuration . . . . .	64
5.7.2	Running the prepipeline processor . . . . .	64
5.8	Before running the pipeline processor . . . . .	68
5.9	The pipeline1 processor (Green-Box) . . . . .	69
5.9.1	Parameter configuration . . . . .	69
5.9.2	Execution . . . . .	70
5.10	The pipeline2 processor (Green-Box & Blue-Box) . . . . .	75
5.10.1	Parameter configuration . . . . .	75
5.10.2	Execution . . . . .	78
5.11	The coadding processor (Blue-Box) . . . . .	81
5.11.1	The Blue-Box Co-Add Wrapper . . . . .	81
5.12	Log files produced from the toolkit . . . . .	86
5.12.1	prepipeline . . . . .	86
5.12.2	pipeline1 . . . . .	86
5.12.3	pipeline2 . . . . .	86
5.13	The IRC TOOL (irc_tool) . . . . .	88
5.14	Limitations of the functionalities in the current version of the imaging toolkit . . . . .	91
5.15	Error messages when running the pipeline and Troubleshooting . . . . .	93
5.16	Toolkit structure . . . . .	95
<b>6</b>	<b>Spectroscopy pipeline cookbook</b> . . . . .	<b>97</b>
6.1	General overview of the pipeline processing . . . . .	97
6.1.1	Dark subtraction . . . . .	98
6.1.2	Linearity correction/Saturation Masking . . . . .	98
6.1.3	(monochromatic) Flat-fielding . . . . .	98
6.1.4	Background subtraction (from individual sub-frames) . . . . .	99
6.1.5	Image screening . . . . .	99
6.1.6	Image registration (among sub-frames) . . . . .	99
6.1.7	Imaging stacking . . . . .	99
6.1.8	Target detection/position measurement . . . . .	100
6.1.9	Background subtraction (from stacked image) . . . . .	100
6.1.10	Extracting 2D spectra . . . . .	100
6.1.11	Wavelength calibration . . . . .	101
6.1.12	Flat color-term correction . . . . .	102
6.1.13	(local) Background subtraction (from extracted 2D spectra) . . . . .	102
6.1.14	Spectral tilt correction . . . . .	103
6.1.15	Spectral response calibration . . . . .	103
6.1.16	Notes on slit spectroscopy . . . . .	103
6.2	How to install and to set-up the IRC spectroscopy pipeline . . . . .	104
6.2.1	Data preparation . . . . .	104
6.3	Calibration data . . . . .	104
6.3.1	Calibration files . . . . .	104
6.4	Running the pipeline . . . . .	107
6.4.1	Data reduction order . . . . .	107
6.4.2	Running the pipeline . . . . .	108

6.4.3	Options . . . . .	109
6.4.4	Outputs . . . . .	110
6.4.5	Summary of interactive operations within the pipeline . . . . .	112
6.4.6	Warning messages of the pipeline . . . . .	113
6.5	Working on the pipeline output . . . . .	114
6.5.1	Displaying the whole images on ds9 . . . . .	114
6.5.2	Displaying the extracted images on ATV . . . . .	115
6.5.3	Checking for wavelength zero reference point with the zero-th order light image . . . . .	115
6.5.4	Spectral plotting tool . . . . .	116
6.5.5	Working on saved data . . . . .	119
6.6	(Hopefully) Useful Tips . . . . .	119
6.6.1	Getting best S/N spectra in slit (Ns, Nh) or Np spectroscopy data . . . . .	119
6.6.2	Tackling narrow spikes seen in NIR spectra (especially in slit spectra) . . . . .	119
6.6.3	Examining strange/fake features in NP spectra, especially around 2.4-3.5 $\mu\text{m}$ . . . . .	119
6.6.4	Examining flux level (in)consistency among different disperser data . . . . .	120
6.7	Appendix . . . . .	121
6.7.1	Variable name conventions . . . . .	121
6.7.2	Summary of Commands and their Options . . . . .	121
6.8	Error messages when running the pipeline and Troubleshooting . . . . .	124

# Chapter 1

## Introduction

### 1.1 Purpose of this document

This document is intended to provide a comprehensive guide to data from the Infrared Camera (IRC) onboard AKARI. It includes a brief summary of the instrumentation, a summary of the data products, and the pipeline software overview together with the calibration of the instrument. **Please note that most of this document focuses on data from pointed observations carried out during the period (so-called Phases 1 & 2, see §1.2) when the instruments were cooled with liquid Helium.** Part of the data and information given here will be updated as the data reduction and calibration will get improved. The latest information may be posted on the web until the revised version will be prepared. A comprehensive overview of the instrumentation and operation is described in the ASTRO-F Observers Manual (available from the AKARI observer's webpage, see §1.3) and **in the AKARI first result volume (PASJ, Volume 60, Issue sp2, 2008).**

### 1.2 Operational phases

---

February 22, 2006	Launch
	Lid open?
	Performance Verification (PV) 1
May 7, 2006	Phase 1 start
November 11, 2006	Phase 2 start
August 26, 2007	liquid He boil off
	PV 2
June 1, 2008	Phase 3 start
February 15, 2020	science observations end
November 24, 2011	satellite operations terminated

---



### 1.3 Relevant information

#### AKARI Observer's Web

The ISAS Web page contains the most up to date information:

URL: <http://www.ir.isas.jaxa.jp/AKARI/Observation/>

The ESAC page also includes up to date information:

URL: <http://akari.esac.esa.int/observers/>

#### Helpdesk

Any questions and comments on AKARI observations and user support are addressed to the AKARI Helpdesks:

[iris\\_help@ir.isas.jaxa.jp](mailto:iris_help@ir.isas.jaxa.jp)

<http://akari.esac.esa.int/esupport/>

## Chapter 2

# Instrument overview

The Infrared Camera (IRC) onboard AKARI was originally designed to make wide-field deep imaging and low-resolution spectroscopic observations in the pointing mode of the AKARI satellite. Its unique wide field coverage of  $10' \times 10'$  is ideal for survey-type observations or multi-object spectroscopic programs.

The capability for the use in the survey mode has later been explored and now is also being used to carry out mid-infrared all-sky survey observations.

Each channel has a filter wheel, on which medium band filters, dispersive elements, and a blank window as a shutter are installed. Table 2.0.1 summarizes the parameters of the IRC filters and dispersion elements. The NIR camera covers three independent wavelength bands that very roughly correspond to the well known K, L, and M bands. Each of the two MIR cameras have two narrow filters which cover the shorter and longer half of the wavelength range of the cameras, and a wide filter that overlaps the two narrow filters. The S9W and L18W bands are used for the all-sky survey observations.

The pixel scale and the imaging area of the focal plane arrays are summarized in Table 2.0.2. The imaging area is the rectangular area excluding the slit region.

The dispersion elements of the IRC are set into the filter wheel so that all the light in the FoV is dispersed. A spectrum is obtained in the direction parallel to the scan path (in-scan direction). Slits are provided for each camera (Figure 2.0.2) in order to avoid contamination by nearby sources / diffuse radiation. The two dispersion elements of the NIR camera provide different spectral resolutions over a similar wavelength range. In the MIR-S and MIR-L, each dispersion element covers about half of the camera's wavelength range. However, unfortunately one of the elements of MIR-L, LG1, was degraded during the ground tests. Thus only LG2 will be used for observations, resulting in a gap in the wavelength range corresponding to the LG1 element.

The slits are primarily designed for extended sources and it should not be assumed that they can be used to guide a point source into the slit, except for the NIR camera which has an aperture for point sources. The current design is the following:

- The slit for the NIR camera consists of three parts of different widths. The left most (closest to the imaging area) has a 5 arcsec width and will be mainly used for simultaneous observations of diffuse light with the MIR-S camera. This slit position is labeled as 'Ns' for IRC04 AOT observation parameter. Both the NP (low-resolution prism) and NG (high-resolution grism) will be used with this slit. The middle  $1' \times 1'$  square part, referred to as 'Np' is for spectroscopy of point sources. The aperture is large compared to the absolute pointing accuracy of the satellite (designed to be better than 30 arcsec) to ensure that the

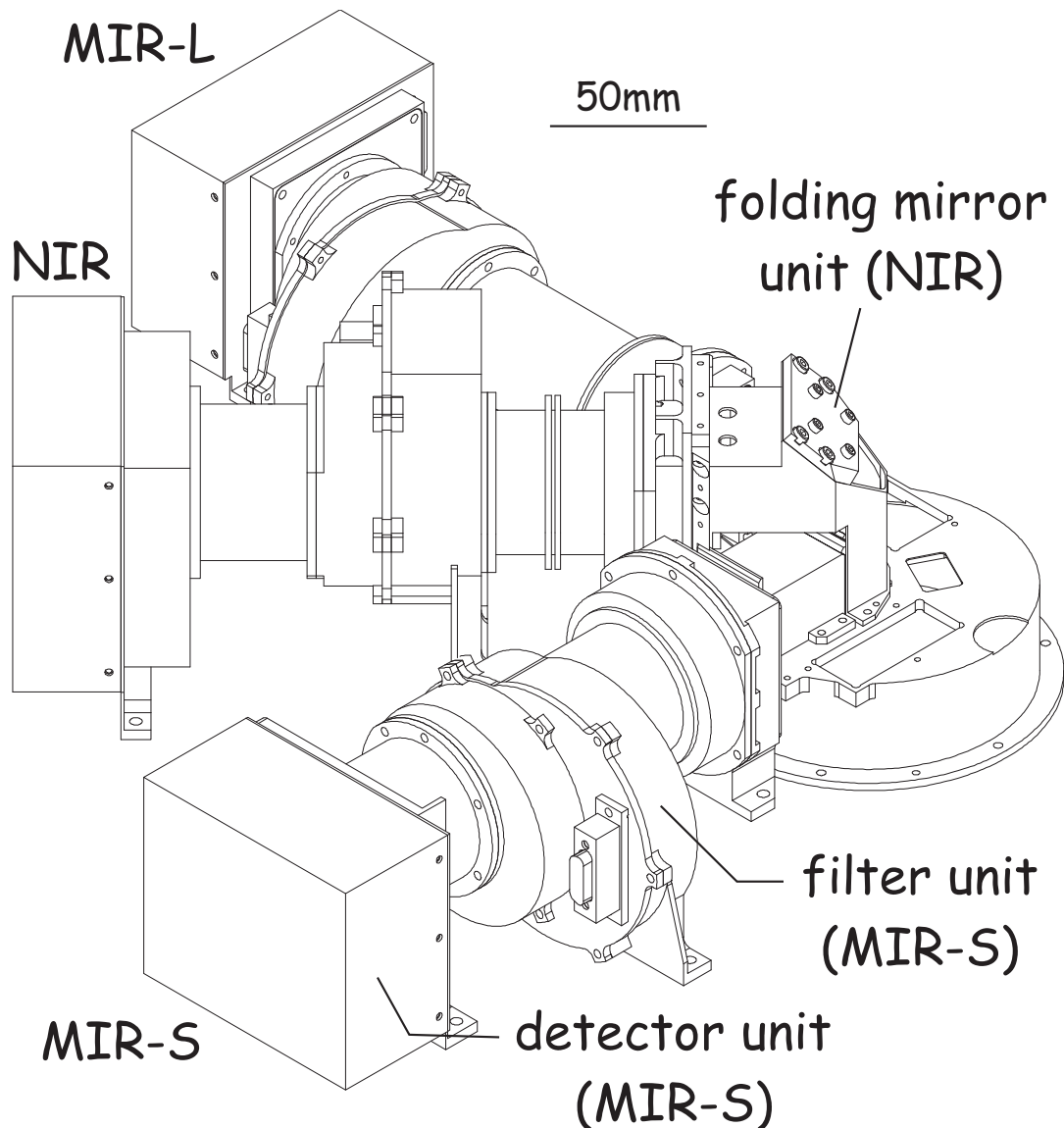


Figure 2.0.1: Bird's-eye view of the IRC camera.

target can be accurately guided into the area. Note that for observations of faint sources, confusion due to galaxies may be a serious problem. The NG (grism) is assumed to be used with this aperture. The rightmost (outer) part ('Nh') has a 3 arcsec width and is used for the highest resolution spectroscopy of diffuse radiation with the NG (grism).

- The MIR-S has a slit of 5 arcsec width for diffuse light. As this slit overlaps with the innermost slit of the NIR camera, it is also referred to as 'Ns'. We assume that the point source density in the mid-infrared range is low enough to avoid serious confusion, such that spectroscopy of point sources can be made in the imaging field.
- The MIR-L has a 7 arcsec slit for diffuse light similar to that of the MIR-S camera. This position is referred to as 'Ls'.

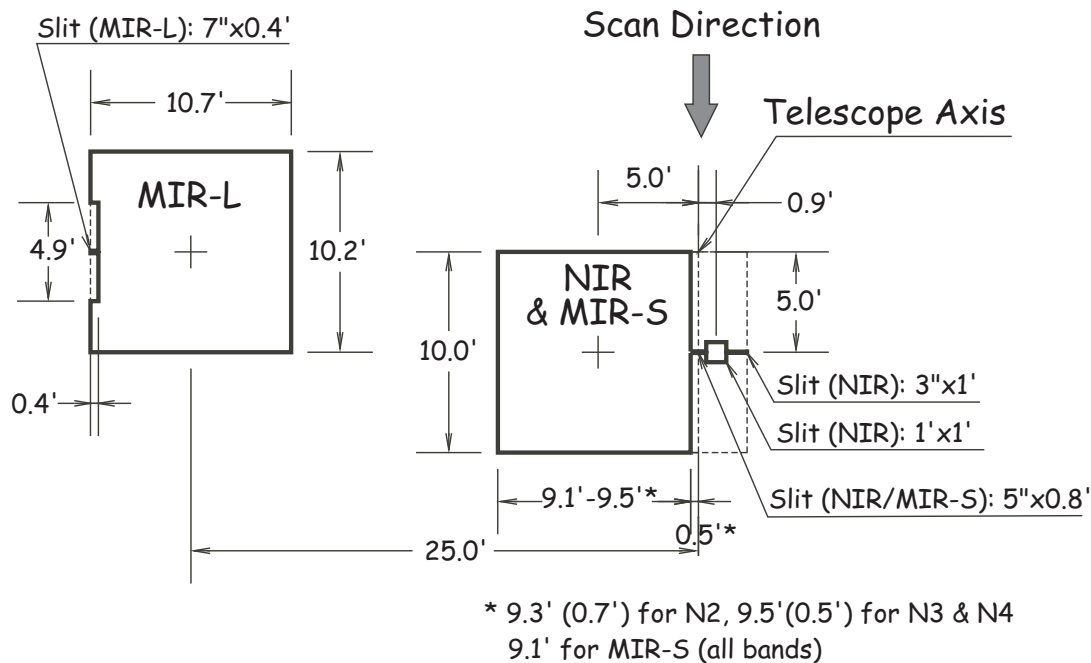


Figure 2.0.2: Field of view location of the three channels of the IRC. The vertical arrow indicates the scan direction in the survey mode. The NIR and MIR-S share the same field of view by means of a beam splitter. See text for the usage of the slits.

## 2.1 Focal plane arrays

The IRC comprises three channels (Figure 2.0.1). The near-infrared (NIR) channel operates in 2–5  $\mu\text{m}$ , the mid-infrared short (MIR-S) channel covers 5–12  $\mu\text{m}$ , and the mid-infrared long (MIR-L) channel works in 12–26  $\mu\text{m}$ . The NIR uses  $512 \times 412$  format InSb array and MIR-S and MIR-L both employ  $256 \times 256$  format Si:As impurity band conduction arrays. The three channels have a field of view of about  $10' \times 10'$  and the NIR and MIR-S share the same field of view by the beam splitter, whereas the MIR-L observes a sky about  $25'$  away from the NIR/MIR-S sky (Figure 2.0.2).

### 2.1.1 Near-InfraRed Camera: NIR

Figure 2.1.3 shows the side view of the NIR channel. The light from the telescope is split by a germanium beam splitter (see Figure 2.1.4) and the near-infrared radiation is introduced to the NIR channel. The NIR consists of silicon and germanium lenses. There are color aberrations among N2, N3, and N4 and the telescope focus is adjusted in between them. Faint ghosts of bright sources are also present, which come from internal reflections in the beam splitter. The brightness is about 0.7% of the true source and the position is well determined and in a good agreement with the ray-tracing simulation. There are also ghosts that seem to come from the internal scattering in the NIR optics. Details are under investigation.

Table 2.0.1: IRC Filters and Dispersion Elements

(1) Channel	(2) Name	(3)	(4) $\lambda_{\text{ref}}$ ( $\mu\text{m}$ )	(5) Wavelength ( $\mu\text{m}$ )	(6) $\lambda_{\text{c}}$ ( $\mu\text{m}$ )	(7) $\Delta\lambda$ ( $\mu\text{m}/\text{pix}$ )	(8) Dispersion ( $\mu\text{m}/\text{pix}$ )
NIR	N2	filter	2.4	1.9–2.8	2.34	0.71	—
	N3	filter	3.2	2.7–3.8	3.19	0.87	—
	N4	filter	4.1	3.6–5.3	4.33	1.53	—
	NP	prism		1.8–5.2	—	—	0.06 @3.5 $\mu\text{m}$
	NG	grism		2.5–5.0	—	—	0.0097
MIR-S	S7	filter	7.0	5.9–8.4	7.12	1.75	—
	S9W	filter	9.0	6.7–11.6	8.61	4.10	—
	S11	filter	11.0	8.5–13.1	10.45	4.12	—
	SG1	grism		5.4–8.4	—	—	0.057
	SG2	grism		7.5–12.9	—	—	0.099
MIR-L	L15	filter	15.0	12.6–19.4	15.58	5.98	—
	L18W <sup>1</sup>	filter	18.0	13.9–25.6	18.39	9.97	—
	L24	filter	24.0	20.3–26.5	22.89	5.34	—
	LG2	grism		17.5–25.7	—	—	0.175

(4) Reference wavelength.

(5) Defined as where the responsivity for a given energy is larger than  $1/e$  of the peak.

(6) Isophotal wavelength of the filter band.

(7) Effective bandwidth.

(8) Dispersion power of NP depends on wavelength.

The quoted value corresponds to  $3.5\mu\text{m}$

<sup>1</sup>Renamed from L20W. No change of the wavelength profile itself.

Table 2.0.2: General characteristics of the IRC focal plane arrays

Channel	NIR	MIR-S	MIR-L
Detector	InSb (SBRC-189)	Si:As (CRC-744)	Si:As (CRC-744)
Format	$512 \times 512$	$256 \times 256$	$256 \times 256$
<b>Pixel scale (<math>'' \times ''</math>)</b>	$1.446 \times 1.458$	$2.340 \times 2.340$	$2.516 \times 2.384$
Imaging area ( $\text{pixel}^2$ )	$391 \times 412$	$233 \times 256$	$246 \times 239$
Readout noise ( $e^-$ )	30.6 <sup>a</sup>	14.2 <sup>b</sup>	same as MIR-S
Dark current ( $e^-/\text{s}$ )	0.2	26	same as MIR-S
Operability(%) <sup>c</sup>	99.9	100	100

a Estimated by Fowler 1 sampling

b Estimated by Fowler 4 sampling

c Pre-launch performance

### 2.1.2 Short wavelength Mid-InfraRed Camera: MIR-S

The light reflected by the beam splitter is lead to the MIR-S. It consists of two aspherical germanium lenses. Figure 2.1.4 shows the side-view of the MIR-S channel. Part of the narrow

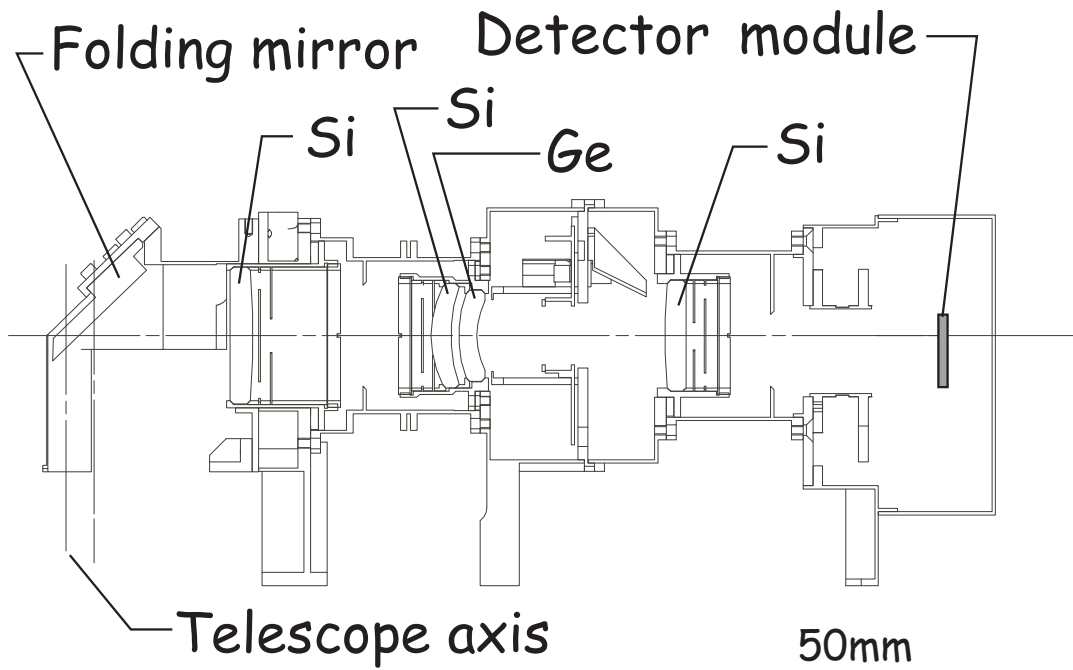


Figure 2.1.3: Side-view of the NIR channel.

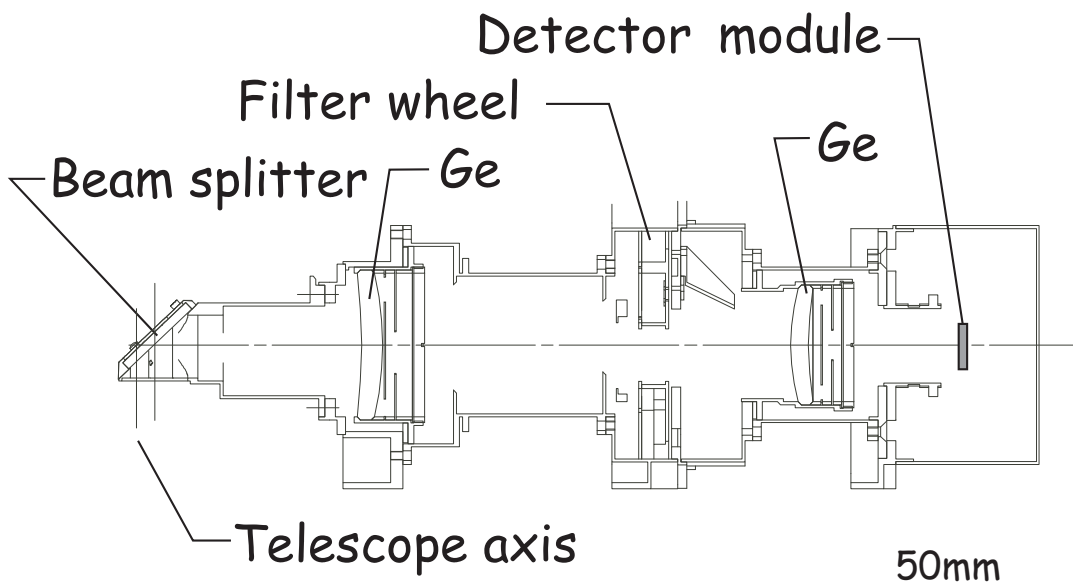


Figure 2.1.4: Side-view of the MIR-S channel. The beam splitter that splits the light into NIR and MIR-S channels acts as a folding mirror for the MIR-S.

slit used for the NIR channel (Figure 2.0.2) will also be shared by MIR-S for spectroscopy for diffuse emission. The MIR-S also has ghost images of bright sources due to the internal reflections in the beam splitter. The brightness of the ghost is about 0.8% of the true source for S7 and S9W and 3.8% for S11 band.

### 2.1.3 Long wavelength Mid-InfraRed Camera: MIR-L

The MIR-L channel consists of 5 lenses of CsI and KRS-5 (Figure 2.1.5). It also has a small slit for spectroscopy of diffuse emission (Figure 2.0.2). Unfocused ghost images are known to exist for very bright sources, whose location depends on the position of the true source in the field-of-view. The origin of the ghost is not yet clearly identified, but it is most likely to come from the scattering by the optical elements of the MIR-L channel (internal scattering).

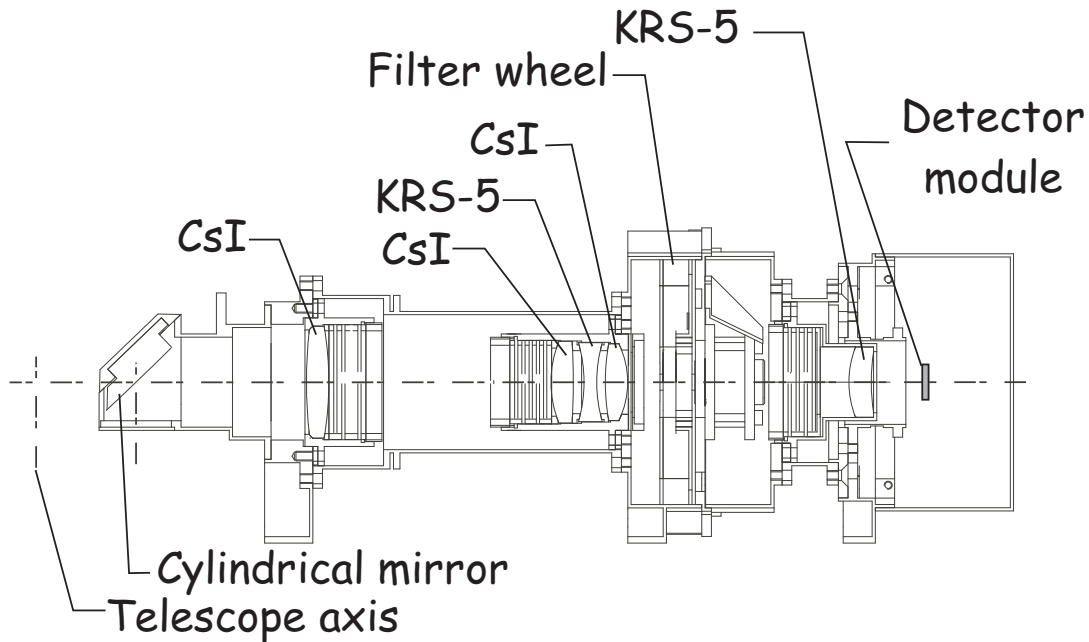


Figure 2.1.5: Side-view of the MIR-L. The folding mirror is cylindrical to correct the astigmatism. Thus the pixel scale of the MIR-L channel is not the same for the X and Y directions.

### 2.1.4 Arrays operation

The focal plane arrays are operated in a synchronized manner. The MIR-S and MIR-L arrays are operated in the same clock pattern. The array operation is made in a unit frame, which consists of short and long exposures. The short exposure is intended to increase the dynamic range by about 8 to 10 times. The clock pattern of one frame is the same for all AOTs except for IRC05, whose frame is twice the period of other AOTs (see next section). Except for IRC05, one frame is about 63 sec, in which NIR has one short and one long exposures, and MIR-S and MIR-L have one short and three long exposures. The short exposure is made with the Fowler 1 sampling scheme and the long exposure is made with the Fowler 4 sampling. For the IRC05, the clock of the MIR-S and MIR-L is the same as for other AOTs, but repeated twice in a frame. The short exposure of the NIR in IRC05 is taken once and the exposure scheme is the same for other AOTs. The long exposure of the NIR in IRC05 is made with the Fowler 16 sampling scheme and is taken once in a frame.

## 2.2 Instrument AOTs

In a pointed observation, the filter and dithering combinations for IRC have been fixed to a few patterns, which are called Astronomical Observation Template (AOT). The duration of a pointed observation and the frame time are well determined. Each AOT consists of a combination of frames of the IRC operation with dithering and filter wheel rotation operations, which is well fixed in a pointed observation. Figure 2.2.6 shows an illustration of the pre-fixed sequences in each AOT. In all the AOTs, except for AOT11, a dark frame is carried out before and after the observation (pre-dark and post-dark observations).

In a pointed staring observation, the IRC observation is started once it receives the notification of the stabilization of the attitude from the attitude and orbital controlling system. The IRC observation continues till the angle between the telescope axis and the earth rim becomes less than a certain value. Thus the last image in a pointed observation may be taken during the maneuver and cannot be used for astronomical observations. This will be correctly treated in the pipeline software.



Figure 2.2.6: Observation sequences of the AOT IRC00, 02, 03, 04 and 05. Yellow boxes labeled as “Exposure cycle” indicate exposure frames. Orange boxes with “M” are Micro-Scan (i.e. dithering) operations including stabilization, and light-blue boxes with “W” are Filter Wheel rotations. Dead time for a Filter Wheel change depends on the relative position of the elements. The Green area on the right side is the extra observation time which is not guaranteed.

### 2.2.1 IRC00

The IRC00 mode was designed for deep imaging observations. After performance investigation in orbit, it has been replaced by IRC05 and is not in use.



### 2.2.2 IRC02

The IRC02 mode was designed for general purpose imaging observations that take images with two fixed filters in a pointed observation. It provides at least three images for a filter with dithering operations.

### 2.2.3 IRC03

The IRC03 mode was designed for general purpose imaging observations that take images with three filters in a pointed observation. For each filter two imaging observations are made with dithering operations.

### 2.2.4 IRC04

The IRC04 mode was designed for general purpose spectroscopic observations. This mode does not have dithering operations. It has an imaging observation sandwiched by spectroscopic observations (observations with the dispersive elements) of 4 frames. The imaging observation will be used to determine the wavelength reference point for slit-less spectroscopy.

The parameters for this AOT are  $[a-c]; [N/L] [s/h/p/c]$ . The first character stands for the filter element; **a** for NP, **b** for NG, and **c** for both, while the latter two indicate the target position;  $[N/L]s$  for wider slit,  $Nh$  for narrower slit,  $Np$  for  $1' \times 1'$  short slit area, and  $[N/L]c$  for center of the detector array for slitless observations.

### 2.2.5 IRC05

The IRC05 mode was designed for deep imaging observations with a filter in a pointed observation. This mode has neither dithering operation nor filter change. Thus observers are requested to make a number of pointed observations for a give target for the redundancy. This mode replaces IRC00 after confirming its high performance for faint source observations for the NIR channel. The exposure times for the MIR-S and MIR-L are the same as for other AOTs for both short and long exposures, whereas that for the long exposure of NIR is longer than others and is made with the Fowler 16 sampling scheme instead of the Fowler 4 sampling.

### 2.2.6 IRC11

The IRC11 was designed for wide area observations or slow-scan observations with the IRC. Only the MIR-S and MIR-L channels can be used in the IRC11. The arrays are operated in the same manner as in the all-sky survey mode, making binning of 4 pixels in the cross-scan direction. On the orbit, the data downlink capacity was found to be sufficient to transmit the full resolution data in the IRC slow scan. The unbinning mode is now designated as IRC51 and all the IRC slow scan observations from 2007 January are executed with the IRC51 mode.

### 2.2.7 IRC51

This is the same slow-scan mode as the IRC11 except that the IRC51 provides the full spatial resolution (without binning) in the cross-scan direction. All the IRC slow-scan observations after 2007 January are executed with IRC51.

Table 2.3.3: IRC sensitivity and image quality

	N2	N3	N4	S7	S9W	S11	L15	L18W	L24
5- $\sigma$ sensitivity ( $\mu\text{Jy}$ )									
AOT02	16	16	16	74	76	132	279	273	584
AOT03	20	19	19	91	93	162	341	335	716
AOT05	5 <sup>a</sup>	5 <sup>a</sup>	9 <sup>a</sup>	43	44	76	161	158	337

The values for N2, N3, and N4 of IRC05 are tentative.

### 2.2.8 AOT parameters for imaging observations

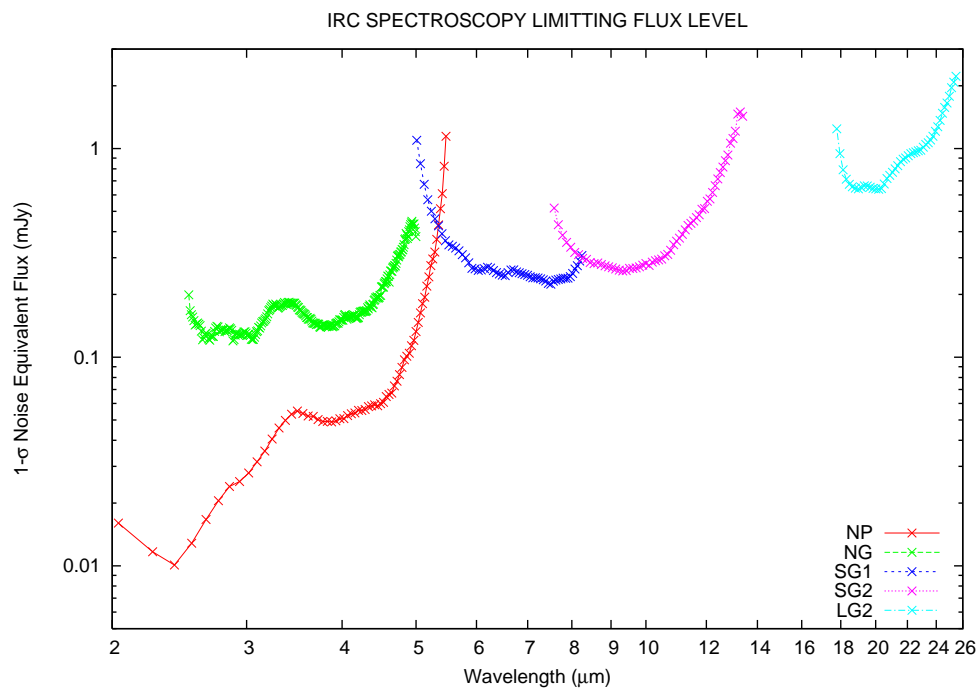
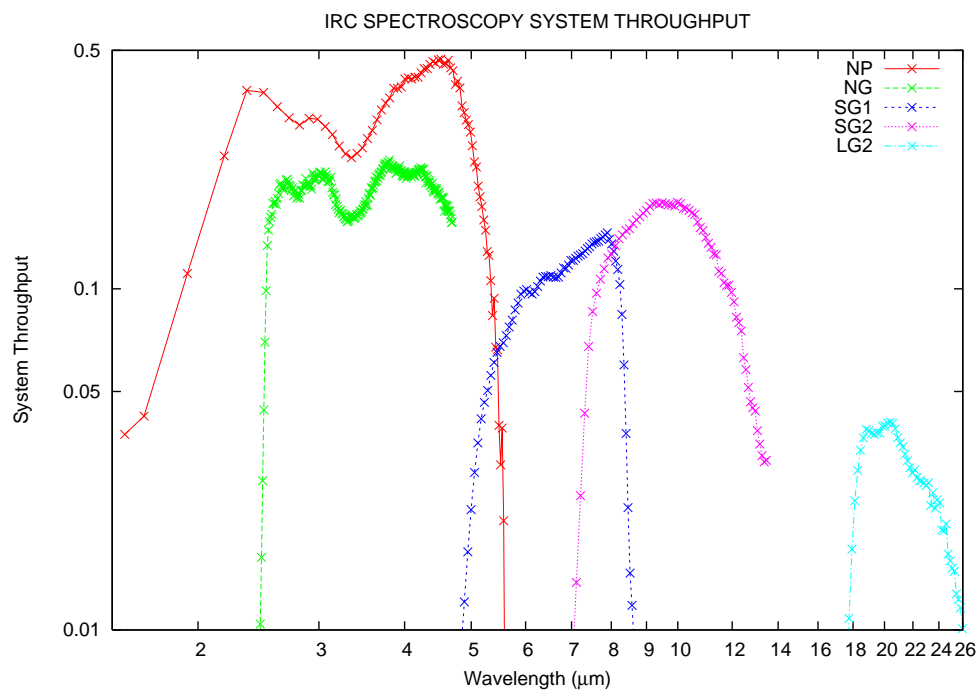
The parameters for imaging AOTs are [a-c] ; [N/L]. As for the parameters for IRC04 explained in §2.2.4, the last character N/L indicates where the target source is. Namely, the target is in the NIR and MIR-S field in the case of N and in the MIR-L field in the case of L. On the other hand, the first character a/b/c represents the filter or combination of filters used in the observations.

## 2.3 In-orbit sensitivity

Optical throughputs of all IRC channels are confirmed to be as expected by observations of standard stars

The sensitivity values for the imaging AOTs are collected in Table 2.3.3. The IRC05 numbers are preliminary.

In the case of IRC04, Figures 2.3.7 and 2.3.8 show the sensitivity ( $1\sigma$  noise with  $2 \times 2$  binning) and the throughput of the system, respectively, as a function of  $\lambda$ .

Figure 2.3.7: IRC spectroscopy sensitivity as a function of  $\lambda$ .Figure 2.3.8: IRC spectroscopy throughput as a function of  $\lambda$ .

## Chapter 3

# Distributed Data Products

Two levels of data products are delivered to the users: raw data and processed data. The raw data are intended to be used to run the pipelines described in Chapters 5 and 6 to get interactively the best science out of them. **The processed data are outputs from the latest toolkit with standard options. Users are recommended to check parameters used for their production in log files and may run pipelines with better parameters depending on science goals.**

### 3.1 IRC FITS file naming rule

Pointed observation data are distributed to the users as a tar+gz package format (hereafter 'data package') per observation. A data package contains FITS format observation data and a Readme file describing the contents etc.

**One data package is provided for one ObsID, which is a combination of 7-digit TargetID and 3-digit SubID (e.g. 1234567\_123). While the TargetID defines observational setups such as target positions and AOTs, the SubID represents the number of observations. However, note that the center and position angle of field of views of different SubIDs may not coincide due to the pointing accuracy and observational timing. Calibration templates such as dark and flat can also be different. Therefore, data from different SubIDs should be treated separately.**

#### 3.1.1 Raw data package

The naming convention for the IRC **rawdata** package is: `AKARI_IRC_TargetID_SubID.tar.gz`.

When extracting an IRC data package a directory named `AKARI_IRC_TargetID_SubID/` is created. Two subdirectories, `rawdata/` and `irc_ql/` contain the raw FITS data files and the processed result files, respectively.

#### 3.1.2 Processed data package

**The name of the processed package released in Mar. 2015 is `AKARI_IRC_TargetID_SubID_201503.tar.gz`.**

**Two subdirectories, `dark/` and `stacked_IM/` contain templates for dark current of MIR-S and -L and calibrated and stacked images for individual bands, respectively. Stacked images are named as `TargetID_SubID_filtername_long.fits`,**

where ‘long’ indicates long exposure. A process log (‘ircpipeline.log’) and readme file (‘README’) are also included in the package.

## 3.2 Raw data description

### 3.2.1 Raw data naming convention

The naming convention for the IRC raw data files is common for all the IRC AOTs as is the following:

FVVxxxxxx\_[N—M].fits

where:

- F is a fixed character
- VVVxxxxxx: Extended frame counter (decimal digits). This is a unique identifier of the exposure.
- xxxxxx: frame counter in the telemetry file.
- VVV: maintained by the FITS creation program. Incremented when xxxxxx is reset to 0.

N—M : NIR / MIR (Scan mode data may have extra characters to this).

NIR data is in a separate file, while MIR-S and MIR-L are stored in the same FITS file. The README file describes:

- file list in the data package
- observation summary extracted from the FITS file
- comments specific for the observation

### 3.2.2 AKARI FITS Primary HDU (common information) rawdata header

The contents of the AKARI FITS Primary HDU of all raw data, both IRC and FIS, is as follows:

SIMPLE	=	T	/	Standard FITS format
BITPIX	=	16	/	number of bits per data pixel
NAXIS	=	3	/	Number of axes
NAXIS1	=	412	/	Image dimension
NAXIS2	=	512	/	Image dimension
NAXIS3	=	2	/	Image frame
EXTEND	=	T	/	Extension may be present
FMTTYPE	=	'ASTRO-F IMAGE IRC'	/	Type of File Format in FITS file
FTYPEVER	=	4	/	Version of FMTTYPE
CNTTYPE	=	'IRC_NIR'	/	Type of data content
DATE	=	'2006-09-25T09:45:24'	/	File Creation Date
CREATOR	=	'TBD'	/	Data generator program name
CRTRVER	=	'1.0'	/	Version of CREATOR
PIPELINE	=	'ircpl ver. 1.0'	/	Data Processing Pipeline name
DATASTAT	=	'GOOD'	/	Data status
ORIGIN	=	'ISAS/JAXA'	/	Organization creating FITS file

TELESCOP	=	'AKARI '	/	AKARI mission
INSTRUME	=	'IRC '	/	Identifier of the instrument
DETECTOR	=	'NIR '	/	Detector name
OBSERVER	=	'PI Name '	/	PI Name (Observer's ID)
PROPOSAL	=	'PRPID '	/	Proposal ID
OBS-CAT	=	'OT '	/	Observation Category
PNTNG-ID	=	1234567	/	Pointing ID
TARGETID	=	1234567	/	Target ID
SUBID	=	1	/	Sub ID
OBJECT	=	'target '	/	Object name
OBJ-RA	=	320.5533	/	[degree] Target position
OBJ-DEC	=	-23.3325	/	[degree] Target position
AOT	=	'IRC03 '	/	Observation AOT
AOTPARAM	=	'8;0.5;70'	/	AOT Parameter
INSTMODE	=	TBD	/	Instrument operation mode
TIMESYS	=	'UTC '	/	Explicit time scale specification
DATE-OBS	=	YYYY-MM-DDTHH:MM:SS	/	Observation start date+time
DATE-END	=	YYYY-MM-DDTHH:MM:SS	/	Observation end date+time
DATE-REF	=	YYYY-MM-DDTHH:MM:SS	/	Reference time in the Observation
AFTM-OBS	=	[double]	/	DATE-OBS in ASTRO-F Time
AFTM-END	=	[double]	/	DATE-END in ASTRO-F Time
AFTM-REF	=	[double]	/	DATE-REF in ASTRO-F Time
PIMTIOBS	=	'0xXXXXXX '	/	DATE-OBS in PIM-TI (36 bits DHUTI)
PIMTIEND	=	'0xXXXXXX '	/	DATE-END in PIM-TI (36 bits DHUTI)
PIMTIREF	=	'0xXXXXXX '	/	DATE-REF in PIM-TI (36 bits DHUTI)
EQUINOX	=	2000.0000	/	Epoch of Coordinate
RA	=	320.5533	/	[degree] Target position at DATE-REF
DEC	=	-23.3325	/	[degree] Target position at DATE-REF
ROLL	=	-30.553	/	[degree] Roll Angle at DATE-REF
AA-SOL	=	90.0021	/	[degree] Solar avoidance Angle at DATE-REF
AA-EAR	=	180.2083	/	[degree] Earth avoidance Angle at DATE-REF
AA-LUN	=	210.6821	/	[degree] Lunar avoidance Angle at DATE-REF
TM-SAA	=	1829.	/	[sec] Duration since last SAA at DATE-REF
SAT-POSX	=	2903.5528	/	[km] Satellite position at DATE-REF
SAT-POSY	=	1704.3092	/	[km] Satellite position at DATE-REF
SAT-POSZ	=	1968.4286	/	[km] Satellite position at DATE-REF
DAYNIGHT	=	'DAY '	/	Day/night status at DATE-REF
STTA-NUM	=	4	/	number of tracked stars in STT-A at DATE-REF
STTB-NUM	=	4	/	number of tracked stars in STT-B at DATE-REF
STTA-MOD	=	'TRK '	/	STT-A Mode status at DATE-REF
STTB-MOD	=	'TRK '	/	STT-B Mode status at DATE-REF
COMMENT			/	Any strings
HISTORY			/	Any strings
END				

The header keywords are sorted as follows:

- FITS basic information, data size information

- SIMPLE refers to the standard FITS format
- BITPIX is the number of bits per data pixel, and equal to 16 in the case of IRC
- NAXIS is the number of axes, equal to 3 for IRC
- NAXIS1 and NAXIS2 are the image dimensions
- NAXIS3 is the number of image frames
- EXTEND refers to the presence of extensions in the FITS file
- Data type, creation and processing information
  - FMTCYPE is the type of File Format in FITS file. It can be 'ASTRO-F IMAGE IRC' or 'ASTRO-F SCAN IRC'
  - FTYPEVER is the version of the file format described in FMTCYPE
  - CNTTCYPE is the type of data content. It can be 'IRC\_NIR' or 'IRC\_MIR'
  - DATE is the file Creation Date
  - CREATOR is the data generator program name.
  - CRTRVER is the version of CREATOR. Contents TBD
  - PIPELINE is the Data Processing Pipeline name and version
  - DATASTAT is the Data status. It describes data status mainly from completeness of telemetry data. This does not tell detailed scientific quality of the data All appropriate error status are listed, otherwise GOOD is given GOOD: No problem INCOMPLETE: (Scientific data) incomplete due to telemetry loss etc. NOHK: HK Status not available NOADS: Attitude information not available STTINI: STT did not work properly. More status may be added as analysis progresses. Data other than GOOD may not be in the archive at the first stage.
- instrument information
  - ORIGIN is the organization creating FITS file
  - TELESCOP is the AKARI mission [Satellite Name]
  - INSTRUME is the Identifier of the instrument
  - DETECTOR is the detector name, either 'NIR' or 'MIR'
- observation details
  - OBSERVER is the PI Name (Observer's ID)
  - PROPOSAL is the Proposal ID
  - OBS-CAT is Observation Category, either 'LS', 'MP', 'OT', 'DT', 'CAL' or 'ENG'
  - PNTNG-ID is the Pointing ID. Usually it is identical with the Target ID, but is different for 'parallel mode' observations.
  - TARGETID is the Target ID
  - SUBID is the Target Sub ID
  - OBJECT is the Object name
  - OBJ-RA is the RA Target position in degrees recorded in the database (double precision)

- OBJ-DEC is the DEC Target position in degrees recorded in the database (double precision)
- AOT is the Observation AOT
- AOTPARAM is the AOT Parameters set
- INSTMODE is the Instrument operation mode. Contents TBD
- TIMESYS is the Time system used in this file
- DATE-OBS is the Observation start date+time, with format YYYY-MM-DDTHH:MM:SS
- DATE-END is the Observation end date+time. Same format than above
- DATE-REF is the Reference time in the Observation. Same format than above
- AFTM-OBS is the DATE-OBS in ASTRO-F Time
- AFTM-END is the DATE-END in ASTRO-F Time
- AFTM-REF is the DATE-REF in ASTRO-F Time
- PIMTIOBS is the DATE-OBS in PIM-TI (36 bits DHUTI) , format '0xXXXXXX '
- PIMTIEND is the DATE-END in PIM-TI (36 bits DHUTI), same format than above
- PIMTIREF is the DATE-REF in PIM-TI (36 bits DHUTI) , same format than above  
 ?????\_OBS and ?????\_END are identical with ?????\_REF for convenience. ?????\_REF is Reference time from TI sampled during each exposure cycle. This is due to the fact that IRC only sample time information once per exposure cycle. Note: PIMTI is the primary information directly from telemetry. AFTI- and DATE- are from the timing correction based on PIMTI.
- attitude information
  - EQUINOX is the Epoch of Coordinate
  - RA is the Target position at DATE-REF in degrees
  - DEC is the Target position at DATE-REF in degrees
  - ROLL is the Roll Angle at DATE-OBS
  - AA-SOL is the Solar avoidance Angle at DATE-REF in degrees
  - AA-EAR is the Earth avoidance Angle at DATE-REF in degrees
  - AA-LUN is the Lunar avoidance Angle at DATE-REF in degrees
  - TM-SAA is the duration in seconds since last SAA at DATE-REF. Definition of SAA is different for different detectors. SAA region is defined by the glitch rate map observed by the Star Tracker with arbitrary threshold level. IRC follows this threshold. Shifts of 30 and 60 seconds are applied to FIS SW and LW, respectively.
  - SAT-POSX is the Satellite position at DATE-REF in km
  - SAT-POSY is the Satellite position at DATE-REF in km
  - SAT-POSZ is the Satellite position at DATE-REF in km
  - DAYNIGHT is the / Day/night status at DATE-REF These fields are updated as pointing analysis goes on from On-board AOCs to G-ADS ( Pointing reconstruction for Survey mode)
  - STTA-NUM is the number of tracked stars in STT-A at DATE-REF



- STTB-NUM is the number of tracked stars in STT-B at DATE-REF
- STTA-MOD is the STT-A Mode status at DATE-REF, either 'TRK', 'ACQ', 'STB', 'INLR' or 'INLN'
- STTB-MOD is the STT-B Mode status at DATE-REF, same as above
- COMMENT: Any strings
- HISTORY: Any strings

### 3.2.3 Raw data dimensions

FITS dimension of the NIR frames is  $412 (x) \times 512 (y) \times 2$  (short+long exposure sub-frames). FITS dimension of the MIR-S and MIR-L frames is  $256 (x) \times 256 (y) \times 4$  (1 short+ 3 long exposure sub-frames). Note that, for convenience of data handling in the electronics onboard the satellite, MIR-S and MIR-L frames are attached to each other along Y axis, and form a single FITS of  $256 \times 512 \times 4$  dimensions. The lower half portion of the  $256 \times 512$  pixel images is for MIR-S, and the upper half portion is for MIR-L.

With the AOT04, one will obtain 11 or 12 sets (NIR and MIR-S/MIR-L) of frames:

- 1 set of pre-dark frame
- 8 or 9 sets of spectroscopy exposure frames
- 1 set of reference imaging exposure frame
- 1 set of post-dark frame

The dark frames will be taken, during pre- and post-satellite maneuvering period, with the shutter closed (the filter wheel at so-called "CAL" position).

The spectroscopy frames are taken with dispersers inserted along the optical path, by rotating the filter wheel.

The direct imaging frame is taken with the same ways as for the normal imaging observations (with AOT00, 02, and 03). The image taken during the spectroscopy mode (AOT04) is called as the "reference image". The N3, S9W, and L18W wide-band filters will be used as the reference images of NIR, MIR-S and MIR-L spectroscopy, respectively. Other combinations of the broad-band filters and dispersers are not available.

The satellite starts to maneuver back to the survey mode according to the timer, irrespective of the IRC operation. The last exposure should be discarded since part of the exposure could be made during the maneuver. The present FITS header does not record the status of the satellite attitude control. In the imaging data pipeline the removal of the last exposure is made automatically by checking the source intensity. Such an automatic procedure is not included in the current spectroscopy data reduction software: users need to do it by themselves (see Chapter 6). Note, however, that the automatic removal is not always perfect and users may have to do it manually in some cases even for the imaging data.

## 3.3 Quick look data

**The raw data package for both imaging and spectroscopic observations contains processed data for quick look. These files are not produced by the latest toolkit nor intended for scientific analysis. We thus strongly recommend to check the processed images in the latest public release and to run the latest toolkit if necessary.**

### 3.3.1 IRC imaging: IRC00, IRC02, IRC03, and IRC05

As explained in the README file distributed with the data in the archive, the `irc_ql` subdirectory contains, together with a set of log files, a main quick look fits image per detector, with the following naming convention. Its name is `fdmslnDwaFVVVxxxxxx-[NSL]yyy.fits`. The first prefixes refer to the performed steps during the processing: DARK correction (D), linearity (ln), distortion correction (d) and flatfielding (f). [NSL] refer to each detector.

The `irclog` file contains a brief description of each file from the data reduction pipeline.

### 3.3.2 IRC spectroscopy: IRC04

The quick look products distributed in the case of spectroscopy observations (IRC04) are the following:

- `TARGETID.SUBID.FILTER_DISPERSER.refimage.bg.fits`: dark, linearity and flatfield corrected reference image.
- `TARGETID.SUBID.FILTER_DISPERSER.specimage.bg.fits`: dark, linearity and flatfield corrected spectroscopy image. This quick look image is usable only for slit-less spectroscopy. For slit spectroscopy further processing with the spectroscopy pipeline is needed.

Auxiliary files are described in the README file distributed in the archive.

## 3.4 IRC04 image orientation and dispersion direction

Since raw NIR images are rotated for technical reasons of data handling in the IRC electronics onboard the satellite, NIR images (NP, NG and N3) will be rotated by 90 deg counterclockwise at the very first stage of the data reduction for convenience in the spectroscopy pipeline.

This is the original orientation in raw images (without rotation for NIR):

- NP: longer wavelength comes at right side (toward positive X).
- NG: longer wavelength comes at left side (toward negative X).
- SG1/2: longer wavelength comes at higher (toward positive Y).
- LG2: longer wavelength comes at lower (toward positive Y).

The IRC04 data reduction pipeline makes the rotation of the NIR images at the first step. After the NIR rotation, the dispersion directions are the same for all the dispersers in spectroscopy images. Note, however, that NP, SG1 and SG2 show positive dispersions (longer wavelength comes at higher Y), and NG and LG2 show negative dispersions (longer wavelength comes at lower Y). At the same stage, the orientation of all NIR, MIR-S and MIR-L images is also set right, i.e., the image is neither flipped nor mirrored. Thus one can match the IRC images with other WCS-correct images, such as 2MASS images, only by shifting and/or rotating the images. Since the satellite is designed to scan the sky along the ecliptic latitude on the sky, and the X axis of the IRC array is aligned perpendicular to the scan direction, the Y axis is aligned closely with the ecliptic latitude while the X axis is aligned with the ecliptic longitude.

## Chapter 4

# IRC Calibration and Accuracy

This chapter offers an overview of the main issues related to the IRC calibration and in-orbit performance. The instrument calibration is addressed in a standard way: dark level, flat-fields, linearity, point spread function, absolute flux calibration and distortion correction. Spectroscopy and imaging are addressed at the same time. Specific topics for each of them are explicitly indicated. Caveats and general concerns are also discussed.

### 4.1 Dark image

This section describes temporal variations of dark current images, which were usually taken before (pre-dark) and after (post-dark) target observations during each pointing. See §5.9.2 step 5 for how the toolkit calibrates them.

#### 4.1.1 Long-term variation

Superdark is made from the pre-dark measurements of LMC observations, **which have extensively been done at the beginning of Phase 1**. It was used by default during the automatic processing, both for imaging and spectroscopic data, after shifting its level by checking the slit area in each image. Since the number of hot pixels is increasing along the mission as shown in Figure 4.1.1, the superdark does not correct for them. Coadding (median filter) different images (IRC03/05 different observations or IRC02 different images) will filter out non corrected hot pixels.

As an alternative, selfdark created by pre-dark images can provide better results, since it corrects for hot pixels. Its S/N is lower than the superdark, especially in NIR, since each observation has only one pre-dark frame.

**In order to overcome the disadvantages of superdark and selfdark, new dark frames called “neighbor dark” are now available and set as a default in the toolkit (since pver=140001). For each pointed observation, neighbor dark frames are created by combining pre-dark frames taken within  $\pm 5$  pointed observations. Typical number of frames to be combined is 33 for MIR long exposure, which is larger than selfdark to increase the S/N and small enough to calibrate the temporal variation. Note that neighbor dark frames are available only for MIR-S and -L long exposure, since for NIR long exposure a model by Tsumura and Wada (2011) is available. For short exposure, super dark is applied.**

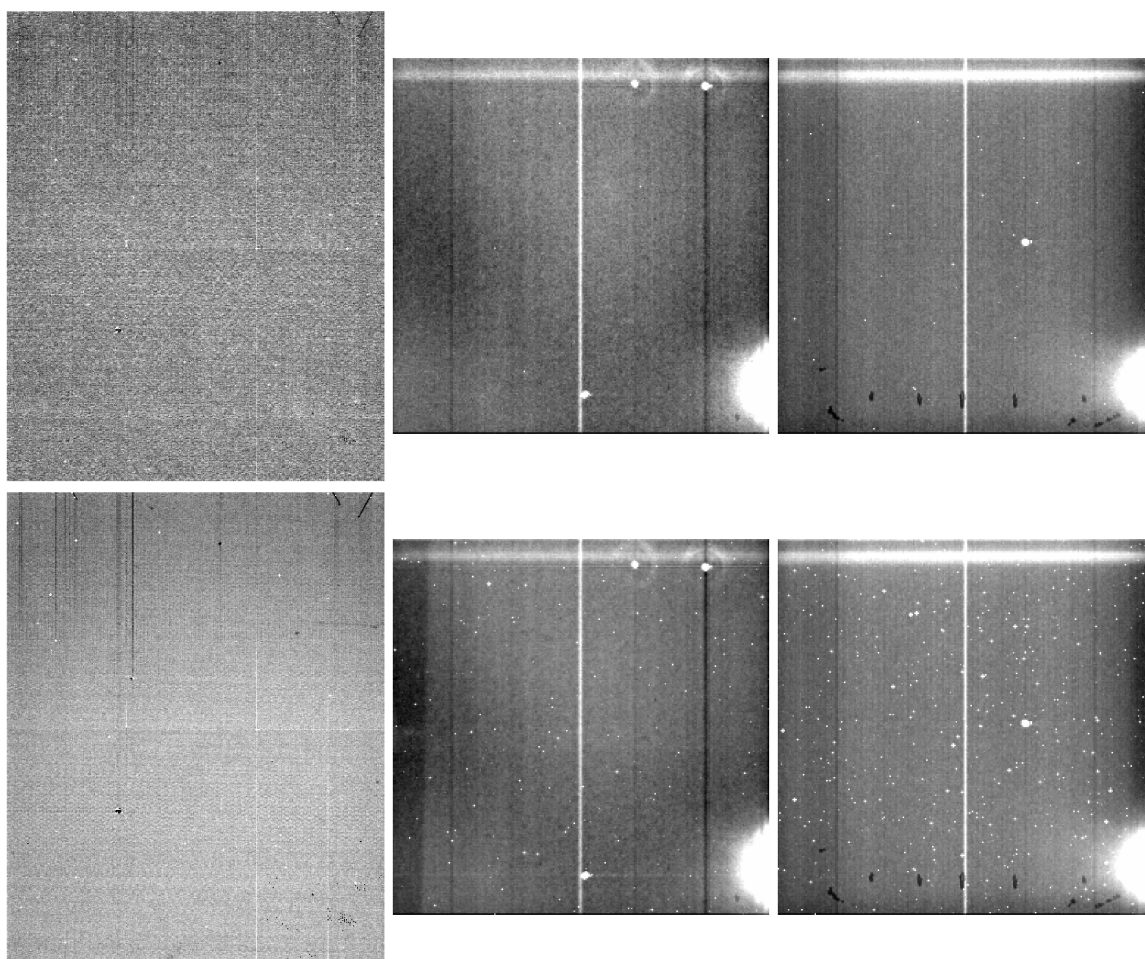


Figure 4.1.1: Dark images taken in April 2006 (top) and in August 2006 (bottom) of NIR, MIR-S, and MIR-L (from left to right), respectively. Clearly, the number of hot pixels is increasing.

### 4.1.2 Intermediate-term variation

It has been known that dark current levels increase after the passage of SAA. Tsumura and Wada (2011) provided a model for this variation of NIR long exposure and their model is used in the toolkit by default.

### 4.1.3 Short-term variation

Another problem related to the dark current arises from the IRC array operation. It is not stationary since the scan-mode clock is running for most of the time during the survey mode, and the imaging clock is running just around pointing observations. Therefore, the temperature conditions of the array could be a function of both time and pixel positions, since only a part of the entire array is used in the survey mode. The effect can be clearly seen in the pre-dark image where series of columns of higher dark current are found around the center of the Y axis in MIR-S/L, and the excess of the dark current decreases with time, and is essentially invisible in post-dark images (taken after  $\sim 20$  min from the start of the imaging mode clock operation).

In the case of spectroscopy observations, the post-dark image is taken just after finishing imaging exposures, and the image shows a memory pattern of the bright background within the slit-less area. Therefore it cannot be used as the dark image to subtract from other images.

## 4.2 Flatfield

### 4.2.1 Flatfiles for imaging data

The IRC flat frames have been made in a different way for each channel.

For MIR-S, a noticeable pattern (so-called “soramame”) in the bottom right corner was present until January 7th, 2007. Also for NIR, a similar pattern was found in the bottom left corner. Murata et al. (2013) carefully investigated its pattern in MIR-S frames and found that its shape changes during its presence. According to their study, we have defined four periods with “soramame” and made one template for each of MIR-S filters and for each period. The starting date of each period is listed in Table 4.2.1. When creating the templates, frames taken in the summer season has been excluded since the background was often severely affected by the earthshine light (§4.14). For the first period (p1), the number of frames especially for S7 is not enough to make a good flat frame, so that we have determined to provide flat frames only for the remaining three periods. This situation can be improved by further investigation. For NIR, the number of frames is not enough to make one template for each period, so that one template for the entire “soramame” period has been made for each filter. For flat frames after January 7th, 2007, one template for one filter has been created using data from the North Ecliptic Pole survey and from observations toward ecliptic plane, where the background is bright due to the zodiacal light, for NIR and MIR-S, respectively. Flat frames for NIR and MIR-S in the toolkit (flatver=140728, pipever=140002 and later) are shown in Figures 4.2.2 and 4.2.3, respectively.

In addition, the periphery of the MIR-S images is affected by scattered light. The portion affected is about 5 pixels from the left edge and 40 pixels from the bottom and right edges and no scattered light is appreciated in the top edge (Figure 4.2.4). This can be explained by the fabrication of the aperture mask. Templates of the

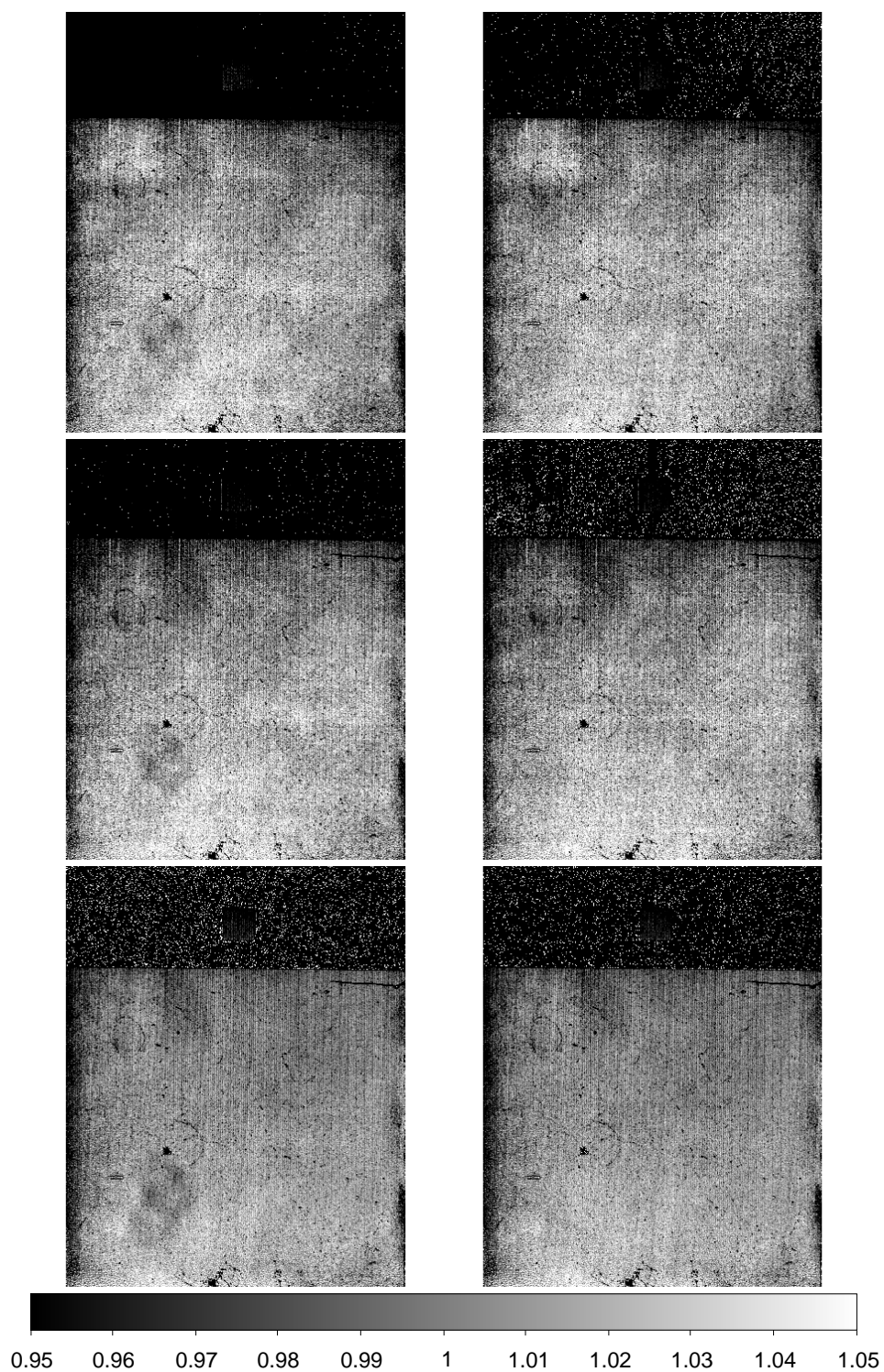


Figure 4.2.2: Flat frames for NIR bands (N2, N3, N4 from top to bottom). Left and right panels are for periods with and without soramame, respectively.

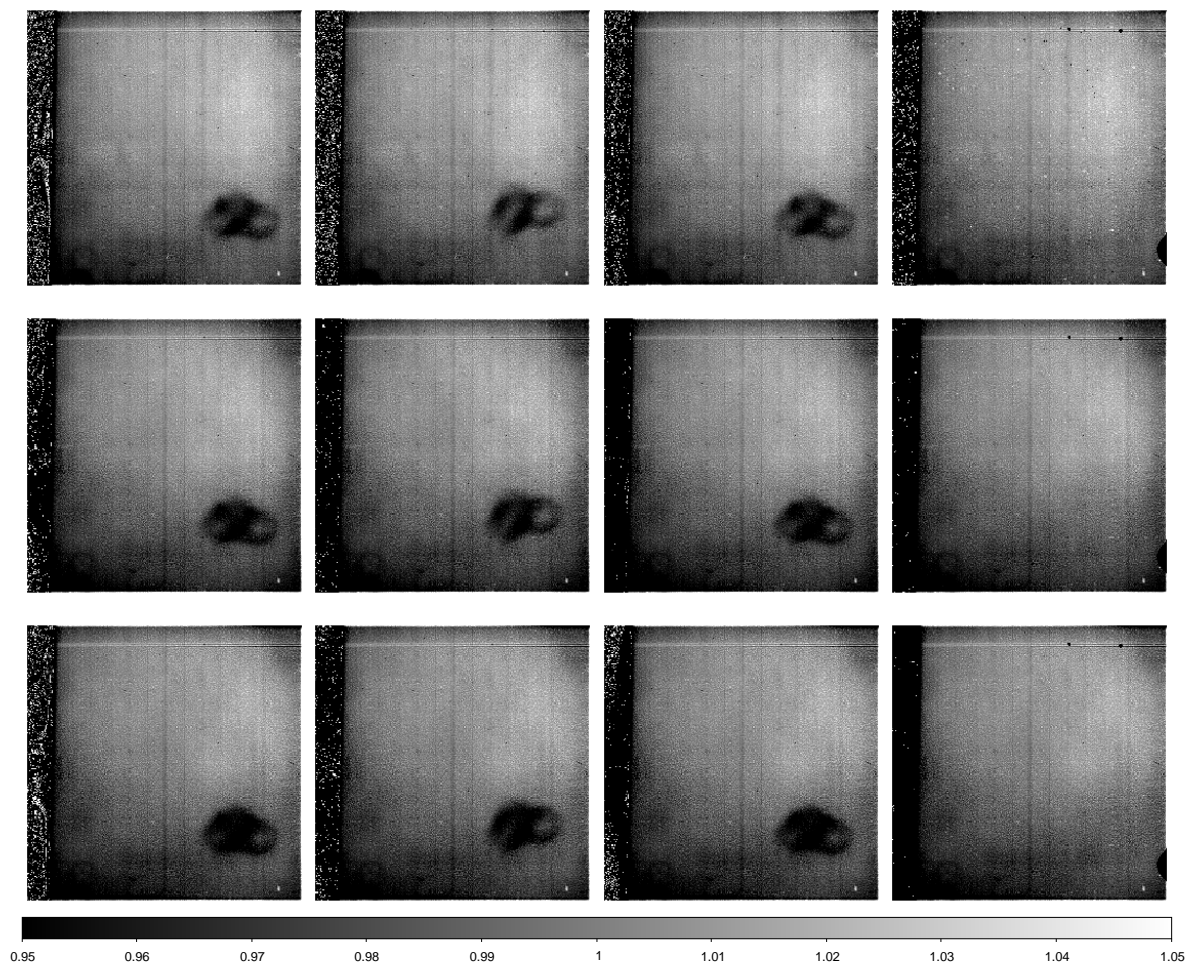


Figure 4.2.3: Flat frames for MIR-S bands (S7, S9W, S11 from top to bottom). Three columns from the left are for three periods with soramame (p23, p4, p5), and the last column is for the period without soramame (p6).

scattered light for all the MIR-S filters are now included in the toolkit and used for pipeline processing (See §5.9.2 step 6).

For MIR-L, the flat pattern in orbit is different from that in the laboratory. The cause of this pattern is now thought to be the scattering in the detector arrays and Arimatsu et al. (2011) investigated it carefully to separate this artificial pattern from a “true” flat field. The true flat field provided by Arimatsu et al. (2011) for L15 and L24 and subsequently by Murata et al. (2013) for L18W are now included in the toolkit (Figure 4.2.5). The artificial diffuse pattern can be subtracted successfully during the flat-fielding procedure.

#### 4.2.2 Flats for spectroscopy images

The spectroscopy flatfields are images made by a large number of blank sky spectroscopy images combined and normalized so that any faint object spectra are removed by clipping averaging techniques. There are five super-flats corresponding to NP, NG, SG1, SG2 and LG2. As will be

Table 4.2.1: Starting date of each period for “soramame”

Name	Date (YYYY-MM-DD)
p1	2006-04-22
p23	2006-04-29
p4	2006-12-09
p5	2006-12-15
p6	2007-01-07

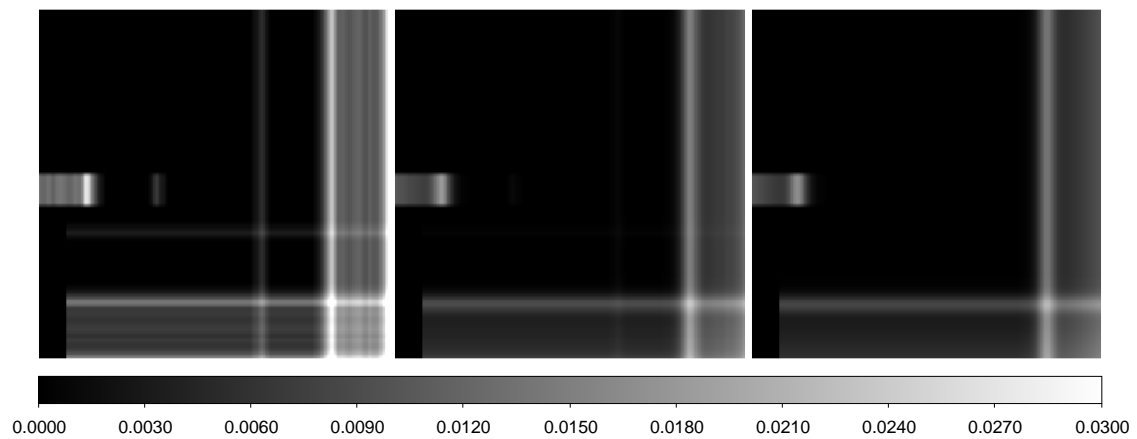


Figure 4.2.4: The modeled scattered light pattern images, from left to right, for the S7, S9W, and S11 bands.



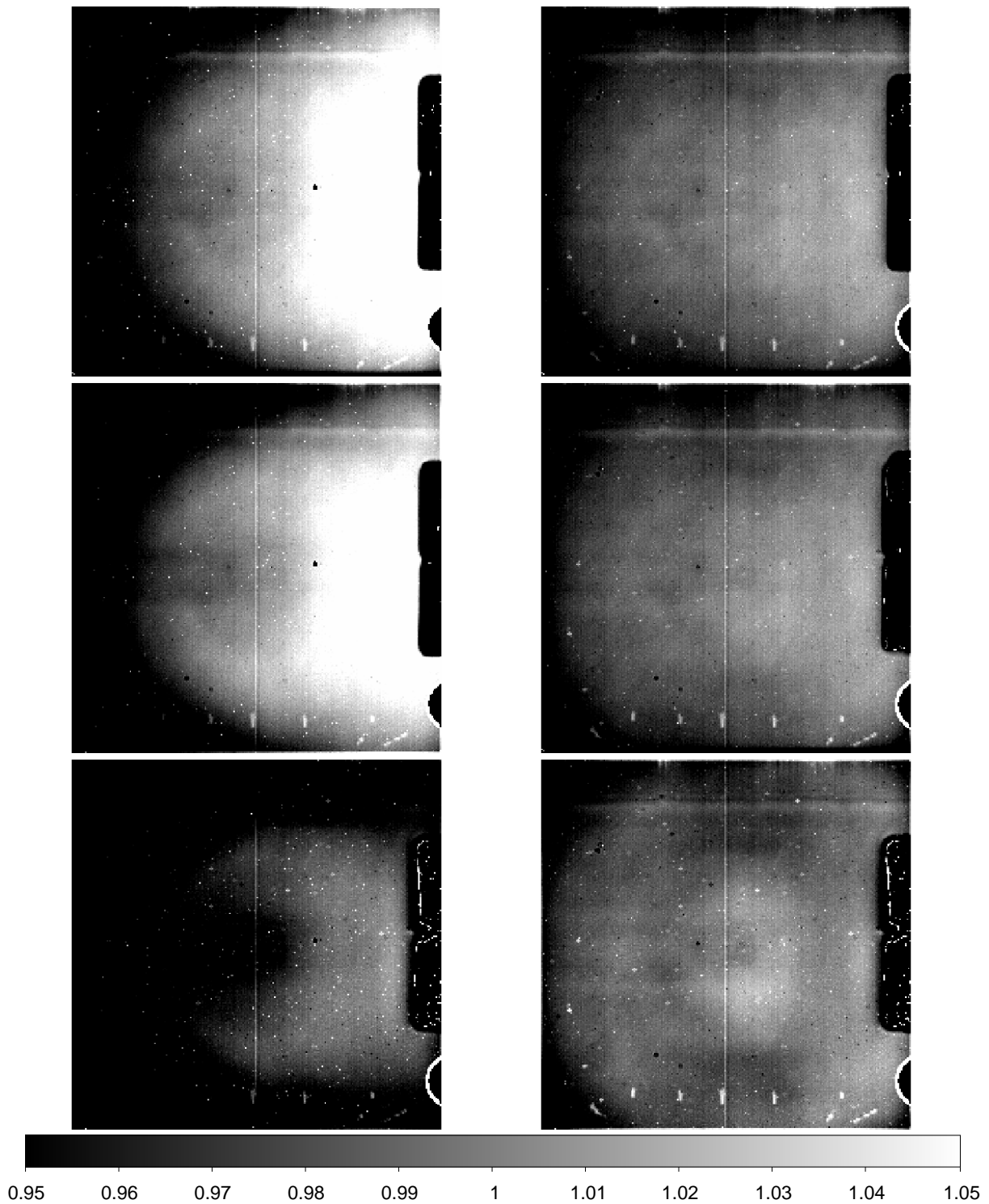


Figure 4.2.5: Flat frames for MIR-L bands (L15, L18W, L24 from top to bottom). Left and right panels are with and without the scattered light component, respectively.

described at the end of this chapter, these flats show spectral features, which are not due to the sensitivity variation. Therefore object spectra should not follow the 'flat' pattern. However, this 'super-flat' with spectral features is used in the data reduction because the color-term correction actually cancel out the spectral feature correction.

For flat fielding slit spectra, including NG with the point source aperture (Np), the super-flats are typical for conventional slit spectroscopy. These flats are also made by combining a large number of blank sky spectra. At present there are only two slit flats for NG at Np and Np at Ns. The others (NG at Nh, SG1/2 at Ns and LG2 at Ls) are in preparation.

### 4.3 Instrument linearity

Detector linearity was measured in the laboratory before launch and later in-flight. Measurements were made with a calibration lamp that illuminates the detector and an increasing range of integration times. At first it was assumed that the detector behaves linearly below 5000ADU, and was fitted with a linear curve by a least squares method. Figure 4.3.6 shows the raw signal in ADU versus the fit in ADU (signal expected if the detectors were to behave linearly) . The deviation of the raw signal from the linear expectation was then calculated and correction equations by fitting polynomials (up to 7th order) were applied. The red lines in Figure 4.3.6 represent the calculated correction equations.

Figure 4.3.7 shows how the calculated correction equations work. After the correction, the error from the ideal linear curve is better than 5% at 12000, 20000, and 20000 ADU (after irlnorm) for NIR, MIR-S, and MIR-L, respectively. Note that from Figure 4.3.6, the physical detector saturation occurs around 12500, 33000, and 33000 ADU (after irlnorm) for NIR, MIR-S, and MIR-L, respectively. No reports have been given against its reliability. Observations of very bright standard stars seem to be compatible with those of medium brightness.

### 4.4 Instrument Point Spread Function

Table 4.4.2 shows the FWHM of the in-flight PSF in the imaging mode, based on observations of standard stars, performed in May and September 2006. They are partly affected by the attitude control stability and indicate the worst cases.

Table 4.4.2: In orbit PSF (in pixels).

N2	N3	N4	S7	S9W	S11	L15	L18W	L24
2.9	2.9	2.9	2.2	2.4	2.4	2.3	2.3	2.8

The PSFs are not spherical (**See Arimatsu et al. (2011) who extensively investigated their pattern for MIR**). Therefore users are recommended to average individual images in the coadding process, if photometric accuracy is concerned. In some cases, mainly in deep survey, the median filtered image will lose some signal if the images are rotated with respect to each other. To avoid this problem users should use "average" instead of "median filter" when combining individual images.

The PSF in the spectroscopic mode is worse by one or two pixels compared to imaging data. No significant wavelength dependence is seen along dispersers.

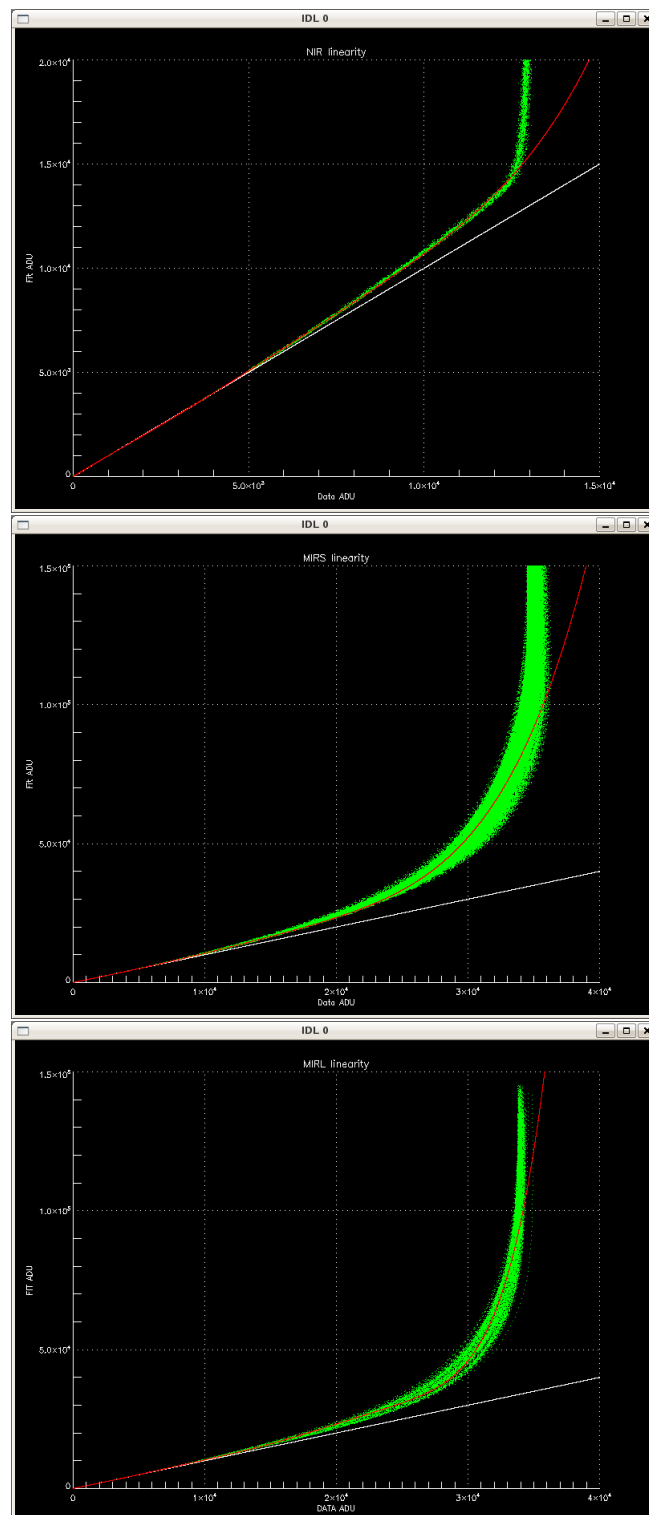


Figure 4.3.6: Raw signal versus fit (signal expected if detectors were to behave linearly). The white line shows Raw signals equals to fit, and the red line shows the calculated correction equations. Note that the physical detector saturation occurs around 12500, 33000, and 33000 ADU (after ircnorm) for NIR, MIR-S, and MIR-L, respectively.

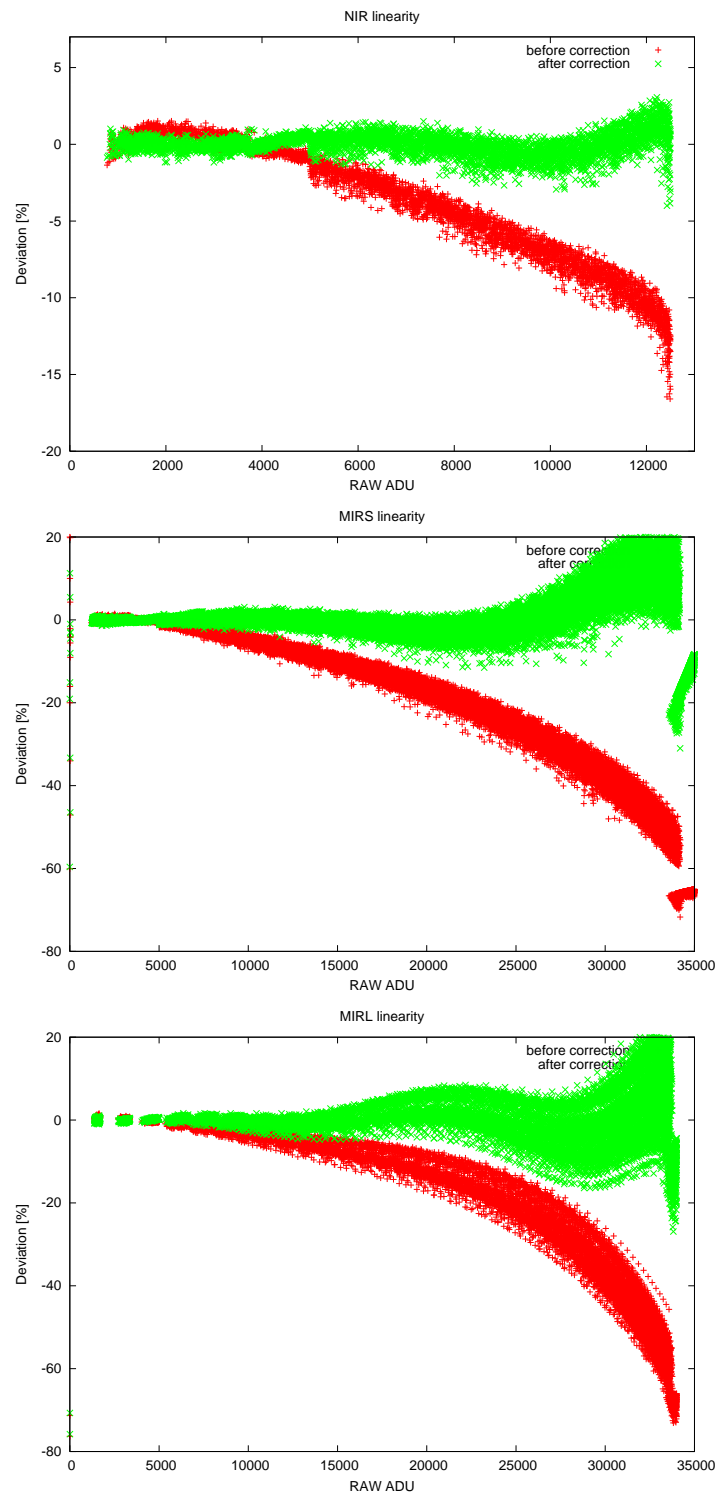


Figure 4.3.7: Raw signal versus deviation [%] from linear curve. A negative deviation means the raw signals in ADU is lower than that expected if the detector were linear. Red marks show before applying linearity correction, and the green marks represents after applying the correction.

## 4.5 RSRF

Figures 4.5.8 to 4.5.13 show the Relative Spectral Response functions (RSRF) for the different filters and dispersion elements.

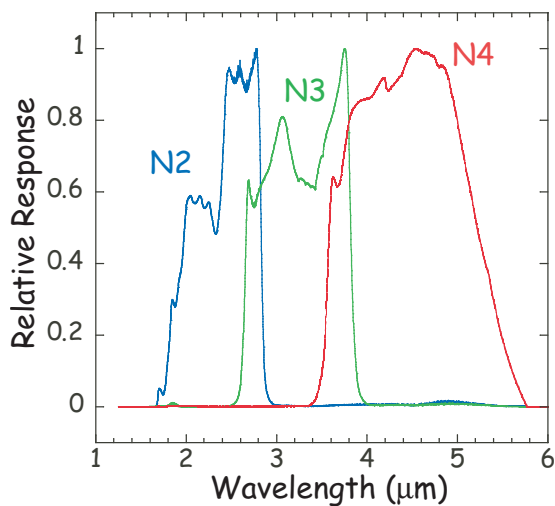


Figure 4.5.8: The Relative Spectral Response Function of the IRC/NIR Camera for  $F_\lambda$ .

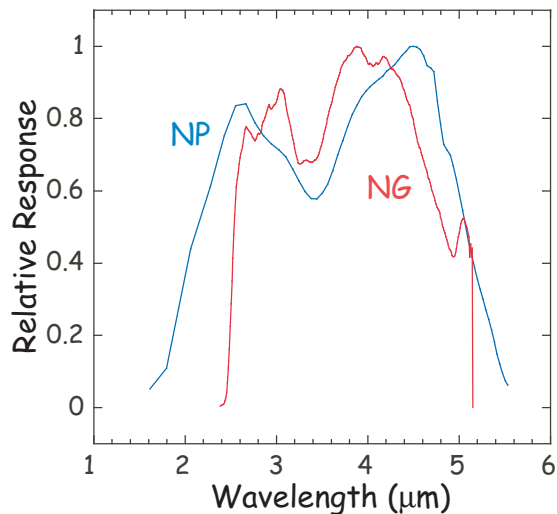


Figure 4.5.9: The Relative Spectral Response Function of the IRC/NIR dispersion elements per photon.

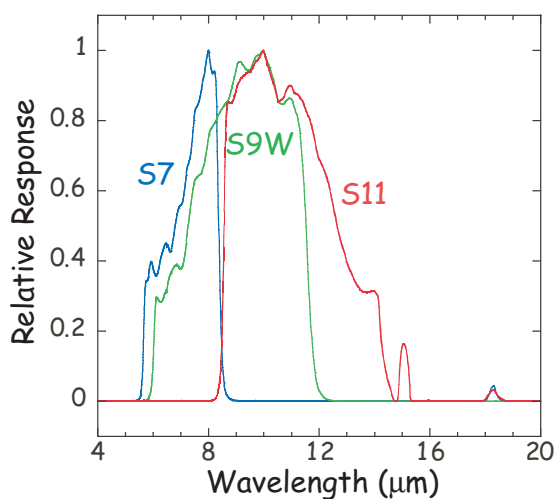


Figure 4.5.10: The Relative Spectral Response Function for  $F_\lambda$  of the IRC/MIR-S Camera.

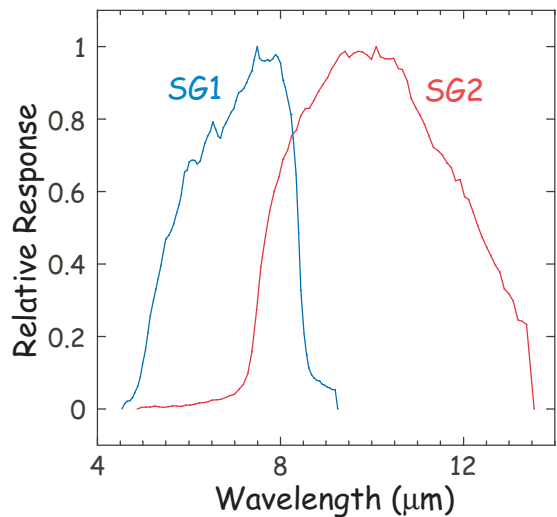


Figure 4.5.11: The Relative Spectral Response Function of the IRC/MIR-S dispersion elements per photon.

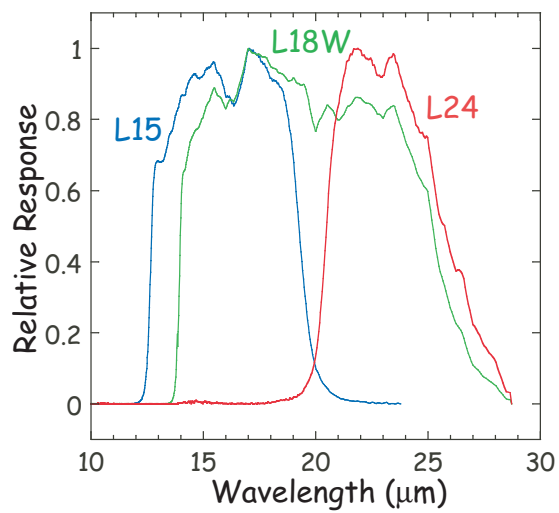


Figure 4.5.12: The Relative Spectral Response Function of the IRC/MIR-L Camera for  $F_{\lambda}$ .

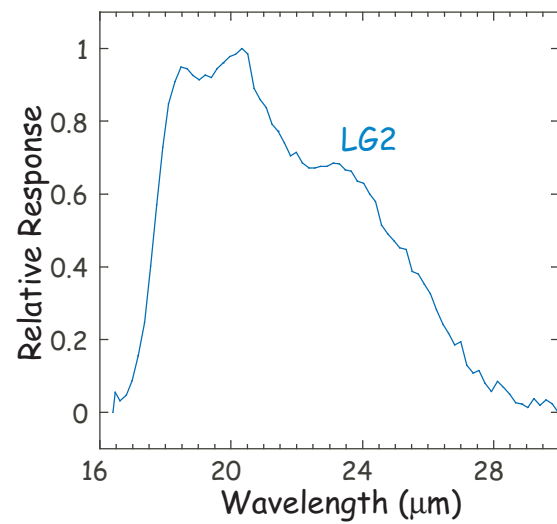


Figure 4.5.13: The Relative Spectral Response Function of the IRC/MIR-L dispersion elements per photon. LG1 will not be used for astronomical observations due to degradation. Data shown here is 2nd order light subtracted.

## 4.6 Flux calibration for point sources

### 4.6.1 Observed standards and data processing

The standard stars for the absolute flux calibration were selected in the North and South Ecliptic Pole (NEP and SEP) regions, which were established by M. Cohen originally for the calibration of the IRAC onboard *Spitzer*. We list the observed NEP and SEP standards in Table 4.6.3. The observations of these standards were carried out with IRC AOT03, which performs either imagings of all the NIR and MIR-S bands or all the MIR-L bands. In addition to these standards, we have included standard stars in the Large Magellanic Cloud. A fairly large area in the LMC have been surveyed by one of the AKARI's Large-Area Survey programs (LSLMC). The standard stars in the LMC, the so-called SAGE standards, were also established by M. Cohen for the *Spitzer* SAGE program. We list observed SAGE standards in Table 4.6.4. This survey was done with IRC AOT02 and only N3, S7, S11, L15, and L24 images are available.

Table 4.6.3: Observed NEP and SEP standard stars.

Star	2MASS ID	Sp.	$K$	Obs. Date
for NIR, MIR-S				
HD42525	06060937-6602227	A0V	5.751	2006-04-22 04:08:28
NPM1p60_0581	17245227+6025508	A1V	9.645	2007-02-13 23:48:41
1757132	17571324+6703409	A3V	11.155	2006-04-26 22:49:47
KF03T1	17574394+6626553	K0III	9.923	2006-08-03 19:30:00
KF03T2	17575147+6631034	K1.5III	8.963	2006-08-03 19:30:00
KF06T1	17575849+6652293	K1.5III	10.872	2006-04-26 19:31:48
KF06T2	17583798+6646522	K1.5III	11.149	2006-04-26 19:31:48
KF06T3	17585021+6649406	K1III	10.348	2006-04-26 19:31:48
KF06T3 2				2006-07-06 19:15:10
KF03T3	17590114+6633262	K1.5III	10.925	2006-08-11 19:08:13
KF03T4	17590395+6630593	K1III	10.091	2006-08-11 19:08:13
KF09T1	17592304+6602561	K0III	8.114	2007-04-15 02:03:34
KF09T1 2				2007-06-02 01:28:46
KF06T4	17592606+6654581	K0III	11.240	2006-07-06 19:15:10
KF01T4	18040314+6654459	K1.5III	8.067	2006-06-24 19:55:00
KF01T4 2				2007-04-15 00:24:01
KF01T4 3				2007-06-01 00:37:25
KF01T5	18040388+6655437	K1III	11.072	2006-06-24 19:55:00
KF01T5 2				2007-04-15 00:24:01
KF01T5 3				2007-06-01 00:37:25
for MIR-L				
HD42525	06060937-6602227	A0V	5.751	2006-04-22 02:03:59
NPM1p65_0451	16533704+6538175	K2III	6.524	2006-12-20 01:36:45
HD158485	17260484+5839069	A3V	6.145	2006-08-22 17:47:59
Bp66_1060	17560018+6655430	K2III	6.720	2006-11-07 16:16:54
NPM1p67_0536	17585466+6747368	K2III	6.409	2006-04-24 14:43:03
HD165459	18023073+5837381	A1V	6.584	2007-03-22 01:44:58
Bp66_1073	18030959+6628119	K1III	7.544	2006-06-28 19:41:30
KF01T4	18040314+6654459	K1.5III	8.067	2006-06-24 23:13:10

---

 HD166780      18083882+5758468    K4III      3.963    2006-09-29 19:43:33
 

---

Table 4.6.4: SAGE standard stars

Star	2MASS ID	Sp.	$K$	Obs. Date
for N3, S7, S11				
HD34461	05121801-6705415	K1III	6.927	2006-06-08 18:21:09
HD34555	05125331-6744362	A3V	9.288	2006-05-31 05:38:19
HD34943	05153759-6804070	M0III	3.970	2006-05-26 06:46:47
HD35094	05164382-6811142	A3V	8.554	2006-05-23 07:47:52
HD35094 2				2006-05-25 06:01:07
HD35183	05172303-6828190	A3V	8.754	2006-05-20 23:40:20
HD35323	05183268-6732320	M0III	5.524	2006-11-29 13:25:55
HD35461	05194979-6626353	K1III	5.683	2006-12-20 04:04:52
HD35461 2				2006-12-18 23:57:17
HD35665	05205607-6759034	K1.5III	5.887	2006-11-24 15:59:18
HD35905	05223623-6721285	K1III	6.800	2006-12-01 05:07:47
HD36207	05244398-6753507	K1III	6.451	2006-11-23 05:15:04
HD37122	05300077-6958319	K2III	5.128	2007-04-25 09:40:22
HD269704	05315890-6909392	K2III	6.760	2006-11-03 18:51:36
HD269704 2				2006-11-03 22:10:04
HD269757	05335125-6946468	K1III	8.187	2007-04-22 07:07:59
HD37722	05344387-6928187	A4V	8.640	2007-04-25 03:03:00
HD37762	05344709-7010197	K0III	5.565	2007-04-18 07:03:34
HD269788	05345367-6846395	K4III	6.331	2007-05-02 05:40:40
HD269820	05355068-6929178	K1III	7.185	2006-10-29 19:47:54
HD269820 2				2006-10-30 18:56:54
HD38861	05423256-7022555	K0III	6.780	2007-04-08 06:53:36
HD38993	05431866-7027254	K1.5III	5.478	2007-04-06 05:12:23
HD39980	05495921-6941060	K2III	5.409	2006-10-09 18:39:20
HD270186	05501123-6934296	K0III	7.774	2006-10-09 18:39:20
for L15, L24				
HD34461	05121801-6705415	K1III	6.927	2006-06-03 06:16:38
HD34461 2				2006-06-04 05:23:26
HD34489	05122388-6756520	K2III	6.169	2006-05-24 06:54:23
HD34943	05153759-6804070	M0III	3.970	2006-05-21 06:16:33
HD35323	05183268-6732320	M0III	5.524	2006-12-04 17:29:51
HD35323 2				2006-12-07 11:40:07
HD269352	05193283-6752441	K5III	6.014	2006-11-29 13:25:55
HD35461	05194979-6626353	K1III	5.683	2006-12-31 13:05:43
HD35665	05205607-6759034	K1.5III	5.887	2006-11-28 15:55:38
HD35905	05223623-6721285	K1III	6.800	2006-12-06 15:48:56
HD36207	05244398-6753507	K1III	6.451	2006-11-27 18:25:19
HD37122	05300077-6958319	K2III	5.128	2007-04-21 07:56:30
HD269704	05315890-6909392	K2III	6.760	2006-11-07 20:25:50



HD37722	05344387-6928187	A4V	8.640	2006-11-02 19:42:32
HD37722 2				2006-11-03 05:37:54
HD37762	05344709-7010197	K0III	5.565	2007-04-12 06:57:26
HD269788	05345367-6846395	K4III	6.331	2006-11-08 22:53:20
HD269820	05355068-6929178	K1III	7.185	2006-11-02 19:42:32
HD38861	05423256-7022555	K0III	6.780	2007-04-02 06:48:19
HD38993	05431866-7027254	K1.5III	5.478	2007-04-02 05:08:54
HD39980	05495921-6941060	K2III	5.409	2006-10-16 22:35:50
HD270186	05501123-6934296	K0III	7.774	2006-10-18 19:14:15

The raw data were reduced with the IRC imaging pipeline. The pipeline produces one coadded image for each band/exposure configuration, using "median" as the combine mode. Each configuration image corresponds to the exposure unit, listed in Table 4.6.5. The actual exposure time is the unit number  $\times$  the unit exposure time,  $t_{\text{unit}}$ , which is approximately 0.5844 s.

Table 4.6.5: Exposure time of each band/exposure configuration.

Band	Exposure	unit number*	
NIR	short	8	
NIR	long	76	
		112	(IRC05)
MIR	short	1	
MIR	long	28	

\*One unit time corresponds to about 0.5844 s.

An aperture photometry (IRAF/phot) was performed for each standard star. The radius of the aperture adopted is 10 pixels for NIR band and 7.5 pixels for MIR-S and MIR-L band, respectively. We determined the sky value in an annulus outside the aperture with a width of 5 pixels. A simple mean of the measured ADU values is used if the star was observed more than once.

#### 4.6.2 Estimation of the in-band flux

The in-band flux density of each band at the nominal wavelength,  $f_{\lambda}^{\text{quoted}}(\lambda_i)$ , was calculated by the following equation:

$$f_{\nu}^{\text{quoted}}(\nu_i) = \frac{\int_{\nu_{is}}^{\nu_{ie}} \frac{R_i(\nu)}{h\nu} f_{\nu}(\nu) d\nu}{\int_{\nu_{is}}^{\nu_{ie}} \left(\frac{\nu_i}{\nu}\right) \frac{R_i(\nu)}{h\nu} d\nu} \quad (4.6.1)$$

or,

$$f_{\lambda}^{\text{quoted}}(\lambda_i) = \frac{\int_{\lambda_{i_s}}^{\lambda_{i_e}} R_i(\lambda) \lambda f_{\lambda}(\lambda) d\lambda}{\int_{\lambda_{i_s}}^{\lambda_{i_e}} \left(\frac{\lambda_i}{\lambda}\right) R_i(\lambda) \lambda d\lambda} \quad (4.6.2)$$

where  $f_{\lambda}(\lambda)$  is the flux density of a standard star (Cohen template) and  $R_i(\lambda)$  is the spectral response (the transmission of the optics and the response of the detector, unit: electron photon<sup>-1</sup>) of the band  $i$ . Here  $f_{\nu} \propto \nu^{-1}$  or  $f_{\lambda} \propto \lambda^{-1}$  is assumed. The adopted normal wavelengths of each band,  $\lambda_i$ , are listed in Table 4.6.6 along with the range of the integration ( $\lambda_{i_s}$ ,  $\lambda_{i_e}$ ).

Table 4.6.6: The normal wavelength  $\lambda_i$  and the range of integration,  $\lambda_{i_s}$  and  $\lambda_{i_e}$ .

band	$\lambda_i$	$\lambda_{i_s}$	$\lambda_{i_e}$
N2	2.40	1.60	5.770
N3	3.20	1.60	5.770
N4	4.10	1.60	5.770
S7	7.00	2.50	23.860
S9W	9.00	2.50	23.510
S11	11.00	2.50	24.000
L15	15.00	2.50	23.760
L18W	18.00	2.50	28.720
L24	24.00	2.50	28.720

### 4.6.3 Absolute calibration

The observed ADUs are converted to ADU  $t_{\text{unit}}^{-1}$  according to the unit number (Table 4.6.5). We assumed that the error of the estimated flux density of the standard star is 5 %. Observational errors ranging from 5 % to 100 % were assigned according to their ADU values. A straight line was fitted to the estimated flux density vs. the *normalized* ADU (ADU  $t_{\text{unit}}^{-1}$ ). The slope of the fitted lines provides the conversion factors,  $f_0$  (ADU  $t_{\text{unit}}^{-1} \rightarrow \text{Jy}$ ), which are tabulated in Table 4.6.7. Using these factors, we calculated conversion factors,  $f_s$  (ADU to Jy for short exposure data) and  $f_l$  (ADU to Jy for long exposure data) which are tabulated in Table 4.6.8.

### 4.6.4 Overall accuracy of the flux calibration

The absolute accuracy for point sources based on observations of standard stars is less than 5% for all the bands.

The stability of the instruments are being monitored by observations of the same stars. Observations show no indications of any change in the reponsivity within 5 % for all the three channels over more than a year.

## 4.7 Flux calibration for extended sources

A correction factor should be applied to convert the point sources flux calibration into extended sources flux.

Table 4.6.7: Conversion factor (ADU  $t_{\text{unit}}^{-1}$  to Jy).

Band	$f_0$	error (%)	Nstar*
N2	$3.300 \times 10^{-5}$	2.84	19
N3	$2.580 \times 10^{-5}$	2.54	16
N4	$1.964 \times 10^{-5}$	3.35	17
S7	$2.86 \times 10^{-5}$	2.30	31
S9W	$1.596 \times 10^{-5}$	5.97	11
S11	$2.165 \times 10^{-5}$	2.36	25
L15	$4.735 \times 10^{-5}$	2.82	33
L18W	$3.210 \times 10^{-5}$	4.56	13
L24	$1.370 \times 10^{-4}$	4.72	20

\*Number of standard stars used.

Table 4.6.8: Conversion factor (ADU exposure $^{-1}$  to Jy) calculated from  $f_0$ .

Band	short exposure $f_s$	long exposure $f_l$	long exposure IRC05* $f_l$	error (%)
N2	$4.125 \times 10^{-6}$	$4.342 \times 10^{-7}$	$2.946 \times 10^{-7}$	2.84
N3	$3.225 \times 10^{-6}$	$3.394 \times 10^{-7}$	$2.303 \times 10^{-7}$	2.54
N4	$2.455 \times 10^{-6}$	$2.584 \times 10^{-7}$	$1.753 \times 10^{-7}$	3.35
S7	$2.861 \times 10^{-5}$	$1.022 \times 10^{-6}$		2.30
S9W	$1.596 \times 10^{-5}$	$5.700 \times 10^{-7}$		5.97
S11	$2.165 \times 10^{-5}$	$7.732 \times 10^{-7}$		2.36
L15	$4.735 \times 10^{-5}$	$1.691 \times 10^{-6}$		2.82
L18W	$3.210 \times 10^{-5}$	$1.146 \times 10^{-6}$		4.56
L24	$1.370 \times 10^{-4}$	$4.892 \times 10^{-6}$		4.72

\*Long exposure for IRC05

This calibration will be done using the all sky-survey data and the MSX data ( $10\mu\text{m}$ ). The  $20\mu\text{m}$  bands calibration will be more difficult because of no good reference data at these wavelengths. The absolute calibration is still being in progress with new observations and will be updated.

## 4.8 Color correction

As mentioned in previous section, the quoted values of the IRC flux calibration assume  $f_\lambda \propto \lambda^{-1}$ . For cases of other incident spectra, the color correction is required.

The quoted value at a reference frequency is given by

$$f_{\nu_i}^{\text{quoted}} = \frac{\int \frac{R_i(\nu)}{h\nu} f_\nu(\nu) d\nu}{\int \left(\frac{\nu_i}{\nu}\right) \frac{R_i(\nu)}{h\nu} d\nu},$$

where  $R$  is the response in units of electron per photon. The correction factor  $K$  is calculated as

$$f_{\nu_i}^{\text{quoted}} = \frac{\int \frac{R_i(\nu)}{h\nu}(\nu) f_\nu(\nu) d\nu}{\int \left(\frac{\nu_i}{\nu}\right) \frac{R_i(\nu)}{h\nu} d\nu} = \frac{\int \frac{R_i(\nu)}{h\nu} \frac{f_\nu(\nu)}{f_{\nu_i}^{\text{actual}}} d\nu}{\int \left(\frac{\nu_i}{\nu}\right) \frac{R_i(\nu)}{h\nu} d\nu} f_{\nu_i}^{\text{actual}} = \frac{\int \frac{R_i(\nu)}{h\nu} \frac{f_\nu(\nu)}{f_\nu(\nu_i)} d\nu}{\int \left(\frac{\nu_i}{\nu}\right) \frac{R_i(\nu)}{h\nu} d\nu} f_{\nu_i}^{\text{actual}} \equiv K(\lambda_i) f_{\nu_i}^{\text{actual}}$$

Thus,  $K$  is given by

$$K(\lambda_i) \equiv \frac{\int \frac{R_i(\nu)}{\nu} \frac{f_\nu(\nu)}{f_\nu(\nu_i)} d\nu}{\int \left(\frac{\nu_i}{\nu}\right) \frac{R_i(\nu)}{\nu} d\nu}$$

We calculate the correction factors for the following incident spectrum cases:

$$f_\nu(\lambda) = \tau_0 \left(\frac{\lambda}{\lambda_0}\right)^\alpha \left(\frac{2hc}{\lambda^3}\right) \frac{1}{\exp\left(\frac{hc}{\lambda kT}\right) - 1} \quad (4.8.3)$$

with  $\alpha = 0, -1, -2$ .

The results are shown in the following tables. The reference wavelengths are fixed as:  $\lambda_1 = 2.4\mu m$ ,  $\lambda_2 = 3.2\mu m$ ,  $\lambda_3 = 4.1\mu m$ ,  $\lambda_4 = 7.0\mu m$ ,  $\lambda_5 = 9.0\mu m$ ,  $\lambda_6 = 11.0\mu m$ ,  $\lambda_7 = 15.0\mu m$ ,  $\lambda_8 = 18.0\mu m$ ,  $\lambda_9 = 24.0\mu m$ .

Table 4.8.9: Color Correction factors for NIR channel<sup>a</sup> – Black Body ( $\alpha = 0$ )

Intrinsic Temperature (K)	NIR/N2 K(2.4 $\mu$ m)	NIR/N3 K(3.2 $\mu$ m)	NIR/N4 K(4.1 $\mu$ m)
40	–	–	–
50	–	–	–
60	–	–	–
70	–	–	–
80	–	–	–
90	–	–	396.131
100	–	–	164.506
110	–	–	81.786
120	–	873.058	46.429
130	–	297.140	29.139
140	–	121.814	19.760
150	–	58.297	14.242
160	–	31.767	10.776
170	–	19.291	8.482
180	–	12.811	6.895
190	–	9.149	5.756
200	–	6.928	4.914
210	–	5.496	4.275
220	582.603	4.526	3.778
230	316.052	3.839	3.385
240	181.324	3.336	3.069
250	109.374	2.955	2.810
300	16.057	1.952	2.024
350	5.065	1.543	1.643
400	2.631	1.333	1.428
450	1.818	1.212	1.294
500	1.463	1.136	1.204
600	1.167	1.052	1.095
700	1.051	1.012	1.033
800	0.997	0.992	0.994
900	0.970	0.982	0.969
1000	0.957	0.977	0.951
1500	0.963	0.981	0.910
2000	0.990	0.992	0.896
2500	1.013	1.001	0.890
3000	1.031	1.008	0.886
3500	1.045	1.013	0.884
4000	1.056	1.017	0.883
4500	1.064	1.020	0.882
5000	1.071	1.022	0.881
6000	1.081	1.026	0.880
7000	1.088	1.029	0.880
8000	1.094	1.031	0.879
9000	1.098	1.032	0.879
10000	1.101	1.034	0.879
20000	1.116	1.039	0.878
30000	1.121	1.041	0.877
40000	1.123	1.042	0.877
50000	1.125	1.043	0.877
60000	1.126	1.043	0.877

<sup>a</sup> Values are calculated for  $\lambda_1 = 2.4\mu m$ ,  $\lambda_2 = 3.2\mu m$ ,  $\lambda_3 = 4.1\mu m$ .

Table 4.8.10: Color Correction factors for NIR channel<sup>a</sup> – Gray Body ( $\alpha = -1$ )

Intrinsic Temperature (K)	NIR/N2 K(2.4 $\mu$ m)	NIR/N3 K(3.2 $\mu$ m)	NIR/N4 K(4.1 $\mu$ m)
40	–	–	–
50	–	–	–
60	–	–	–
70	–	–	–
80	–	–	938.233
90	–	–	305.576
100	–	–	127.958
110	–	–	64.122
120	–	541.920	36.679
130	–	187.774	23.187
140	–	78.796	15.834
150	–	38.794	11.488
160	–	21.822	8.749
170	–	13.696	6.929
180	–	9.390	5.665
190	–	6.906	4.757
200	–	5.367	4.083
210	546.949	4.356	3.571
220	280.566	3.657	3.172
230	153.521	3.154	2.856
240	89.003	2.779	2.601
250	54.374	2.492	2.393
300	8.881	1.715	1.757
350	3.276	1.390	1.449
400	1.952	1.223	1.276
450	1.477	1.127	1.168
500	1.257	1.069	1.097
600	1.064	1.007	1.011
700	0.989	0.981	0.963
800	0.957	0.971	0.934
900	0.945	0.968	0.915
1000	0.943	0.970	0.902
1500	0.982	0.992	0.875
2000	1.027	1.012	0.868
2500	1.061	1.027	0.866
3000	1.087	1.037	0.865
3500	1.106	1.045	0.865
4000	1.121	1.051	0.865
4500	1.132	1.056	0.865
5000	1.142	1.059	0.865
6000	1.156	1.065	0.866
7000	1.166	1.069	0.866
8000	1.173	1.072	0.866
9000	1.179	1.074	0.866
10000	1.183	1.076	0.867
20000	1.203	1.084	0.868
30000	1.210	1.087	0.868
40000	1.213	1.089	0.868
50000	1.215	1.089	0.868
60000	1.216	1.090	0.868

<sup>a</sup> Values are calculated for  $\lambda_1 = 2.4\mu m$ ,  $\lambda_2 = 3.2\mu m$ ,  $\lambda_3 = 4.1\mu m$ .

Table 4.8.11: Color Correction factors for NIR channel<sup>a</sup> – Gray Body ( $\alpha = -2$ )

Intrinsic Temperature (K)	NIR/N2 K(2.4 $\mu$ m)	NIR/N3 K(3.2 $\mu$ m)	NIR/N4 K(4.1 $\mu$ m)
40	–	–	–
50	–	–	–
60	–	–	–
70	–	–	–
80	–	–	719.020
90	–	–	236.320
100	–	–	99.825
110	–	–	50.445
120	–	339.050	29.088
130	–	120.115	18.531
140	–	51.864	12.748
150	–	26.407	9.316
160	–	15.397	7.143
170	–	10.012	5.694
180	–	7.092	4.686
190	–	5.367	3.959
200	549.483	4.275	3.418
210	264.183	3.541	3.006
220	136.893	3.025	2.685
230	75.855	2.647	2.430
240	44.673	2.361	2.224
250	27.825	2.140	2.055
300	5.291	1.528	1.541
350	2.329	1.268	1.293
400	1.566	1.135	1.154
450	1.270	1.061	1.068
500	1.125	1.017	1.012
600	0.996	0.976	0.946
700	0.949	0.963	0.910
800	0.935	0.962	0.889
900	0.936	0.968	0.876
1000	0.945	0.975	0.868
1500	1.019	1.016	0.855
2000	1.084	1.047	0.855
2500	1.132	1.068	0.857
3000	1.166	1.084	0.860
3500	1.192	1.095	0.862
4000	1.212	1.103	0.864
4500	1.227	1.110	0.866
5000	1.239	1.115	0.867
6000	1.258	1.123	0.869
7000	1.271	1.129	0.871
8000	1.281	1.133	0.873
9000	1.288	1.137	0.874
10000	1.294	1.139	0.874
20000	1.320	1.151	0.879
30000	1.329	1.155	0.880
40000	1.333	1.157	0.881
50000	1.335	1.158	0.881
60000	1.337	1.159	0.881

<sup>a</sup> Values are calculated for  $\lambda_1 = 2.4\mu m$ ,  $\lambda_2 = 3.2\mu m$ ,  $\lambda_3 = 4.1\mu m$ .

Table 4.8.12: Color Correction factors for MIR channel<sup>a</sup> – Black Body ( $\alpha = 0$ )

Intrinsic Temperature (K)	MIR-S/S7 K(7.0 $\mu$ m)	MIR-S/S9W K(9.0 $\mu$ m)	MIR-S/S11 K(11.0 $\mu$ m)	MIR-L/L15 K(15.0 $\mu$ m)	MIR-L/L20W K(18.0 $\mu$ m)	MIR-L/L24 K(24.0 $\mu$ m)
40	–	–	204.598	14.514	14.825	0.942
50	–	373.308	21.615	5.989	5.661	0.882
60	–	31.533	6.632	3.516	3.178	0.870
70	–	9.722	3.371	2.492	2.198	0.875
80	619.872	5.209	2.217	1.971	1.720	0.887
90	110.313	3.493	1.685	1.670	1.454	0.902
100	29.730	2.629	1.399	1.480	1.292	0.917
110	11.350	2.124	1.230	1.352	1.187	0.931
120	5.796	1.803	1.123	1.262	1.116	0.945
130	3.691	1.585	1.053	1.196	1.066	0.958
140	2.731	1.430	1.006	1.147	1.031	0.969
150	2.221	1.318	0.973	1.109	1.005	0.980
160	1.917	1.233	0.952	1.079	0.986	0.990
170	1.717	1.168	0.937	1.055	0.972	0.999
180	1.577	1.118	0.927	1.035	0.961	1.007
190	1.474	1.078	0.921	1.019	0.953	1.015
200	1.395	1.047	0.918	1.006	0.947	1.022
210	1.332	1.022	0.917	0.995	0.942	1.029
220	1.282	1.002	0.918	0.986	0.939	1.035
230	1.240	0.986	0.919	0.978	0.937	1.040
240	1.206	0.974	0.922	0.972	0.935	1.046
250	1.176	0.964	0.925	0.966	0.934	1.050
300	1.081	0.939	0.947	0.947	0.933	1.070
350	1.032	0.938	0.970	0.937	0.936	1.085
400	1.004	0.946	0.992	0.931	0.940	1.096
450	0.987	0.958	1.011	0.928	0.944	1.104
500	0.977	0.972	1.028	0.925	0.947	1.111
600	0.967	0.998	1.056	0.923	0.954	1.122
700	0.963	1.021	1.076	0.922	0.959	1.130
800	0.961	1.040	1.092	0.922	0.963	1.135
900	0.961	1.057	1.105	0.921	0.966	1.140
1000	0.962	1.070	1.115	0.921	0.969	1.144
1500	0.966	1.113	1.146	0.922	0.977	1.155
2000	0.969	1.136	1.162	0.922	0.981	1.161
2500	0.971	1.149	1.171	0.923	0.984	1.165
3000	0.972	1.158	1.177	0.923	0.985	1.167
3500	0.973	1.165	1.181	0.923	0.987	1.169
4000	0.974	1.169	1.184	0.923	0.987	1.170
4500	0.975	1.173	1.186	0.924	0.988	1.172
5000	0.975	1.176	1.188	0.924	0.989	1.172
6000	0.976	1.180	1.191	0.924	0.990	1.174
7000	0.977	1.184	1.193	0.924	0.990	1.175
8000	0.977	1.186	1.195	0.924	0.991	1.175
9000	0.977	1.188	1.196	0.924	0.991	1.176
10000	0.978	1.189	1.197	0.924	0.991	1.176
20000	0.979	1.196	1.201	0.924	0.993	1.178
30000	0.979	1.198	1.202	0.924	0.993	1.179
40000	0.979	1.199	1.203	0.924	0.993	1.179
50000	0.979	1.199	1.204	0.925	0.994	1.180
60000	0.980	1.200	1.204	0.925	0.994	1.180

<sup>a</sup> Values are calculated for  $\lambda_4 = 7.0\mu\text{m}$ ,  $\lambda_5 = 9.0\mu\text{m}$ ,  $\lambda_6 = 11.0\mu\text{m}$ ,  $\lambda_7 = 15.0\mu\text{m}$ ,  $\lambda_8 = 18.0\mu\text{m}$ ,  $\lambda_9 = 24.0\mu\text{m}$ .



Table 4.8.13: Color Correction factors for MIR channel<sup>a</sup> – Gray Body ( $\alpha = -1$ )

Intrinsic Temperature (K)	MIR-S/S7 K(7.0 $\mu$ m)	MIR-S/S9W K(9.0 $\mu$ m)	MIR-S/S11 K(11.0 $\mu$ m)	MIR-L/L15 K(15.0 $\mu$ m)	MIR-L/L20W K(18.0 $\mu$ m)	MIR-L/L24 K(24.0 $\mu$ m)
40	–	–	126.883	11.699	11.085	0.913
50	–	175.833	15.078	4.943	4.371	0.870
60	–	19.630	5.044	2.961	2.528	0.869
70	–	7.299	2.712	2.135	1.798	0.883
80	239.889	4.200	1.855	1.715	1.443	0.902
90	44.874	2.906	1.452	1.472	1.247	0.922
100	13.402	2.228	1.235	1.320	1.130	0.942
110	5.953	1.826	1.107	1.218	1.056	0.960
120	3.563	1.568	1.029	1.147	1.008	0.977
130	2.580	1.393	0.979	1.096	0.976	0.993
140	2.088	1.270	0.947	1.057	0.954	1.007
150	1.801	1.181	0.928	1.028	0.940	1.021
160	1.615	1.115	0.916	1.006	0.930	1.033
170	1.485	1.065	0.910	0.988	0.924	1.044
180	1.389	1.027	0.908	0.974	0.920	1.054
190	1.316	0.999	0.909	0.963	0.918	1.063
200	1.258	0.977	0.912	0.954	0.917	1.072
210	1.212	0.960	0.916	0.946	0.917	1.080
220	1.174	0.948	0.922	0.940	0.918	1.088
230	1.143	0.939	0.928	0.935	0.919	1.094
240	1.116	0.933	0.935	0.931	0.921	1.101
250	1.094	0.928	0.942	0.927	0.923	1.107
300	1.023	0.927	0.979	0.917	0.934	1.131
350	0.988	0.944	1.014	0.913	0.946	1.150
400	0.969	0.967	1.045	0.911	0.956	1.164
450	0.960	0.992	1.072	0.911	0.965	1.176
500	0.955	1.016	1.095	0.912	0.973	1.185
600	0.953	1.059	1.132	0.913	0.985	1.200
700	0.955	1.094	1.160	0.915	0.995	1.211
800	0.958	1.124	1.181	0.917	1.002	1.220
900	0.961	1.148	1.198	0.919	1.008	1.227
1000	0.964	1.168	1.212	0.920	1.013	1.233
1500	0.975	1.232	1.253	0.924	1.027	1.254
2000	0.982	1.264	1.273	0.927	1.035	1.267
2500	0.986	1.284	1.285	0.929	1.040	1.275
3000	0.988	1.297	1.293	0.930	1.043	1.281
3500	0.990	1.306	1.298	0.931	1.046	1.285
4000	0.992	1.313	1.303	0.931	1.047	1.288
4500	0.993	1.318	1.306	0.932	1.049	1.291
5000	0.994	1.322	1.308	0.932	1.050	1.293
6000	0.995	1.328	1.312	0.933	1.051	1.297
7000	0.996	1.333	1.315	0.933	1.053	1.299
8000	0.997	1.336	1.317	0.933	1.053	1.301
9000	0.997	1.339	1.318	0.934	1.054	1.302
10000	0.998	1.341	1.320	0.934	1.055	1.303
20000	1.000	1.350	1.325	0.935	1.057	1.309
30000	1.001	1.353	1.327	0.935	1.058	1.311
40000	1.001	1.355	1.328	0.935	1.058	1.312
50000	1.001	1.356	1.329	0.935	1.059	1.312
60000	1.001	1.356	1.329	0.935	1.059	1.313

<sup>a</sup> Values are calculated for  $\lambda_4 = 7.0\mu\text{m}$ ,  $\lambda_5 = 9.0\mu\text{m}$ ,  $\lambda_6 = 11.0\mu\text{m}$ ,  $\lambda_7 = 15.0\mu\text{m}$ ,  $\lambda_8 = 18.0\mu\text{m}$ ,  $\lambda_9 = 24.0\mu\text{m}$ .

Table 4.8.14: Color Correction factors for MIR channel<sup>a</sup> – Gray Body ( $\alpha = -2$ )

Intrinsic Temperature (K)	MIR-S/S7 K(7.0 $\mu$ m)	MIR-S/S9W K(9.0 $\mu$ m)	MIR-S/S11 K(11.0 $\mu$ m)	MIR-L/L15 K(15.0 $\mu$ m)	MIR-L/L20W K(18.0 $\mu$ m)	MIR-L/L24 K(24.0 $\mu$ m)
40	–	–	80.578	9.482	8.362	0.890
50	–	88.714	10.821	4.108	3.417	0.864
60	–	13.417	3.932	2.513	2.044	0.875
70	866.347	5.731	2.228	1.847	1.500	0.897
80	95.149	3.460	1.582	1.508	1.238	0.923
90	19.552	2.451	1.275	1.313	1.097	0.949
100	6.900	1.909	1.110	1.192	1.015	0.974
110	3.696	1.586	1.016	1.112	0.966	0.996
120	2.559	1.379	0.961	1.057	0.936	1.017
130	2.034	1.240	0.928	1.017	0.919	1.037
140	1.740	1.142	0.910	0.989	0.909	1.054
150	1.553	1.073	0.901	0.968	0.904	1.070
160	1.424	1.023	0.899	0.952	0.903	1.085
170	1.330	0.987	0.901	0.939	0.903	1.099
180	1.258	0.961	0.907	0.930	0.906	1.111
190	1.202	0.942	0.914	0.923	0.909	1.123
200	1.158	0.929	0.923	0.917	0.913	1.133
210	1.122	0.921	0.933	0.913	0.918	1.143
220	1.093	0.915	0.943	0.910	0.923	1.152
230	1.068	0.913	0.954	0.907	0.928	1.161
240	1.048	0.913	0.965	0.905	0.933	1.169
250	1.032	0.914	0.976	0.904	0.938	1.177
300	0.980	0.939	1.031	0.902	0.962	1.208
350	0.957	0.976	1.079	0.904	0.983	1.233
400	0.948	1.016	1.121	0.907	1.000	1.253
450	0.946	1.055	1.157	0.910	1.015	1.269
500	0.947	1.092	1.187	0.914	1.028	1.284
600	0.953	1.156	1.235	0.920	1.048	1.309
700	0.960	1.209	1.272	0.926	1.063	1.329
800	0.967	1.251	1.300	0.930	1.076	1.348
900	0.974	1.286	1.322	0.934	1.086	1.364
1000	0.980	1.315	1.340	0.937	1.094	1.379
1500	0.999	1.404	1.394	0.948	1.120	1.439
2000	1.009	1.450	1.421	0.953	1.135	1.483
2500	1.015	1.478	1.436	0.957	1.144	1.514
3000	1.019	1.496	1.447	0.959	1.151	1.538
3500	1.022	1.509	1.454	0.961	1.155	1.557
4000	1.025	1.519	1.460	0.963	1.159	1.571
4500	1.026	1.526	1.464	0.964	1.162	1.583
5000	1.028	1.532	1.468	0.964	1.164	1.593
6000	1.030	1.541	1.473	0.966	1.167	1.608
7000	1.031	1.548	1.476	0.967	1.170	1.620
8000	1.032	1.552	1.479	0.967	1.172	1.628
9000	1.033	1.556	1.481	0.968	1.173	1.635
10000	1.034	1.559	1.483	0.968	1.174	1.641
20000	1.037	1.572	1.490	0.970	1.180	1.667
30000	1.038	1.576	1.493	0.971	1.182	1.676
40000	1.038	1.578	1.494	0.971	1.183	1.681
50000	1.039	1.580	1.495	0.971	1.183	1.683
60000	1.039	1.581	1.495	0.972	1.183	1.685

<sup>a</sup> Values are calculated for  $\lambda_4 = 7.0\mu\text{m}$ ,  $\lambda_5 = 9.0\mu\text{m}$ ,  $\lambda_6 = 11.0\mu\text{m}$ ,  $\lambda_7 = 15.0\mu\text{m}$ ,  $\lambda_8 = 18.0\mu\text{m}$ ,  $\lambda_9 = 24.0\mu\text{m}$ .

## 4.9 Distortion

Because of geometric distortion in the IRC images, the original detector pixel solid angle varies over the field of view. We observed globular clusters and Galactic center with the IRC, where many stars are expected to be detected. Then we matched their 2MASS coordinates with the detector xy coordinates by fitting polynomials. In the fitting, we fixed the pixel field of view to be 1.46, 2.38, and 2.40 arcsec/pix for the NIR, MIR-S, and MIR-L, respectively. The deviation from an ideal grid square are up to 2, 0.6 and 16 pixels at the edge for NIR, MIR-S and MIR-L, respectively. There is little difference with filters. Figure 4.9.14 shows the distortion vector for N2, S7, and L24, respectively.

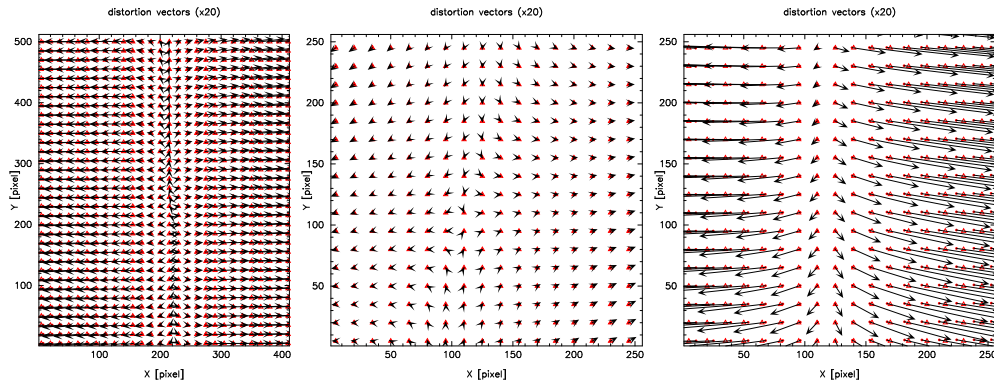


Figure 4.9.14: Distortion from ideal grid square for N2, S7, and L24 (from left to right), respectively. For clarity, the length of distortion vectors are multiplied by 20.

Table 4.9.15 shows the accuracy of the distortion correction. In summary, except for L24, the accuracy is about 0.1 pixel (N4 may be slightly worse). The bad value of L24 comes mostly from scarcity of good bright sources and the matter of statistics. With the accumulation of the data, it could be improved.

Table 4.9.15: Accuracy of the distortion correction in units of pixels.

	$X_{rms}$	$Y_{rms}$
N2_distortion_database.dat:	0.090	0.111
N3_distortion_database.dat:	0.103	0.128
N4_distortion_database.dat:	0.093	0.153
S7_distortion_database.dat:	0.091	0.069
S9W_distortion_database.dat:	0.050	0.059
S11_distortion_database.dat:	0.072	0.067
L15_distortion_database.dat:	0.056	0.052
L18W_distortion_database.dat:	0.063	0.054
L24_distortion_database.dat:	0.520	0.340

As described in §5.10.2 step 2, only linear terms of calculated distortion factors are adopted in the toolkit and non-linear terms are neglected.

## 4.10 Memory effects caused by bright source observations

MIR-S and MIR-L channels show an anomalous sign after they observe bright sources. Examples are shown in Figures 4.10.15 and 4.10.16. The former is the case when a bright source was observed in a pointed observation, while the latter is the case when such a source was in the field of view during all-sky and slow-scan observations.

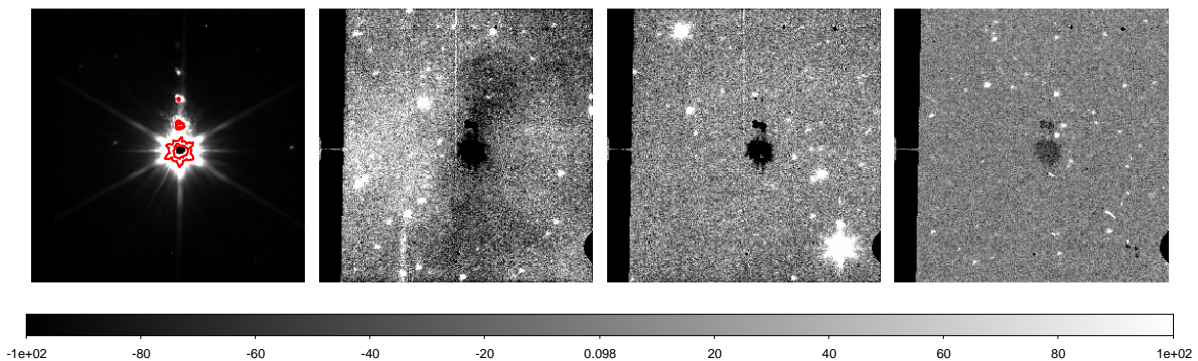


Figure 4.10.15: Memory effects seen in MIR-S S11 frames after observing a bright source (CRL618 in the left panel) during a pointed observation. Time since observing the bright source are  $\sim 1, 2, 4$  hours from left to right, respectively. Frames after flat fielding are shown in all the panels and note that the color scale is different for the left panel. The red contours indicate a plausible threshold level for the memory effect.

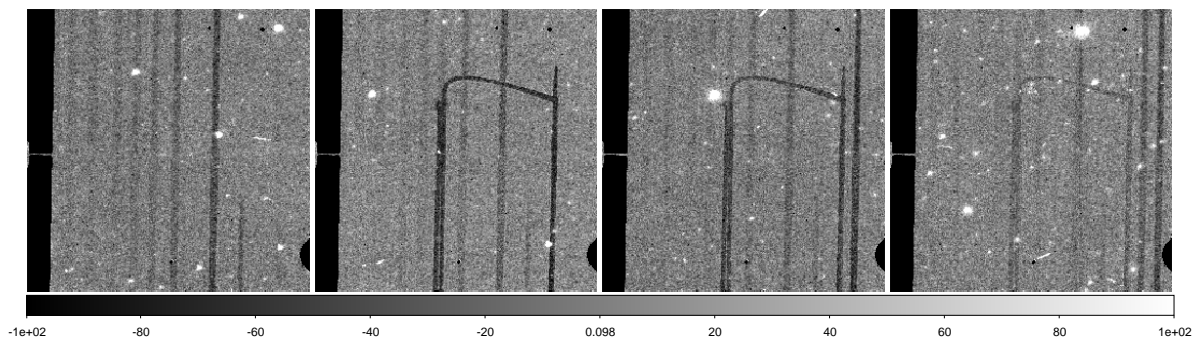


Figure 4.10.16: Example of memory effect after observing a bright source in all-sky survey and in slow-scan observation. The former appears as the dark stripes, which increase toward right. A causing source of these stripes is most likely \* P Dor. The latter appears as the arc- or bow-like shape, delineating the slow-scan pattern. The time interval between the frames are 100 [min], 100 [min], 160 [min], from left to right. S11 frames after flat calibration are presented.

This effect appears as a decrease of the sensitivity. Although the amount is a few % at most, it could severely affect the detection of faint sources because of the high background level at MIR. For long-exposure frames taken in pointed observations, we have estimated the threshold brightness of the causing source and duration

of this effect to be  $\sim 10^5$  [ADU] and  $\sim 400$  [min], respectively, for MIR-S. For MIR-L, the threshold is estimated to be  $\sim 10^6$  [ADU]. Since the number of data is not enough, the duration is not clear but perhaps is shorter than the MIR-S case. Furthermore, the duration and strength of this effect can be dependent on the source brightness, but again the data sample was not enough to determine the dependency.

At this moment, a technique to fully recover this effect has not been established. Instead, we offer a scheme to mask the affected pixels using the mask information of the bright source. We have confirmed that this scheme works at least for several cases.

## 4.11 Astrometry

A corrected and final astrometry can be achieved at the end of the pipeline by cross-correlating with the 2MASS or WISE catalogue. This option is turned off by default. This is because the software to retrieve the catalog may be platform-dependent. To enable this option, “curl” has to be installed in the system. The instructions for it are beyond this manual. Ask your computer administrator for the installation.

The current pipeline has a capability to first include the pointing information from the attitude and orbital control system (AOCS) directly in the WCS format. If matching with the catalog is successful, then the pointing information will be replaced by the matching data. The parameter “WCSROOT” in the FITS header indicates which information (AOCS/2MASS/WISE) is used to determine the coordinates. **The parameters “WCSNSTAR” and “WCSERROR” indicate the number of stars used for matching and the error in the coordinate fitting.**

## 4.12 Arrays anomalies

### 4.12.1 NIR array

NIR anomalies (Muxbleed, Muxstripes, Column pulldown, Banding) are shown in Figures 4.12.17 and 4.12.18. Most of them also affects the Spitzer IRAC instrument. **When the telescope passed through the auroral area, i.e. around the North and South poles, trapped positrons and electrons hit the detectors. This temporary increases the number of hot pixels and its effect is most notable in the NIR.**

A robust way to calibrate all of these anomalies is not yet established,

### 4.12.2 MIR arrays

There is a problem in the short-exposure frame data taken with IRC00, IRC04 and IRC05. The phenomenon is only seen in the short frames immediately following the frames without any operations (such as filter wheel operation and dithering). Therefore the very first short frame in all modes and the short frame after the image frame in IRC04 should be fine since they follow the filter operation. These short exposure frames can be used for checking the saturation, but should not be used for scientific purpose.

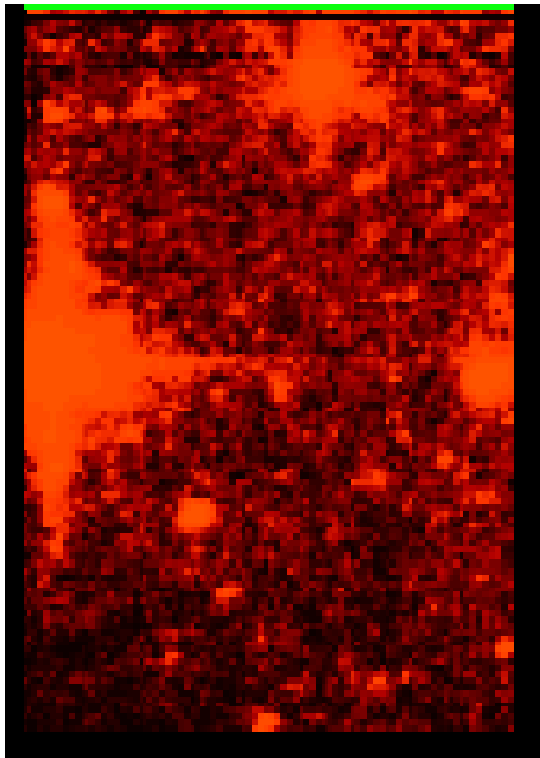


Figure 4.12.17: Banding in NIR array

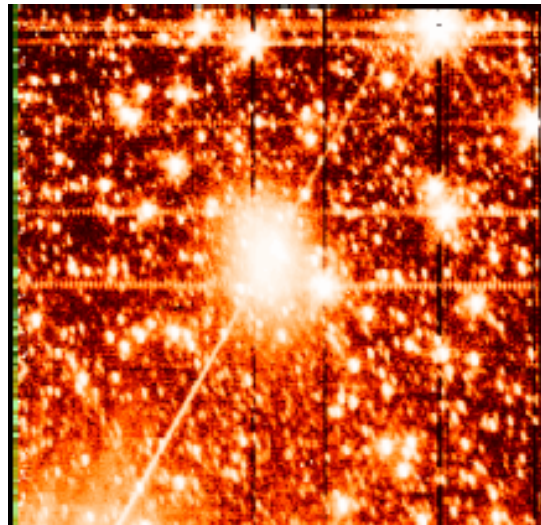


Figure 4.12.18: NIR array anomalies: Muxbleed, Muxstripes and column pull-down

## 4.13 Ghosts

Ghosts appear in all three channels. NIR and MIR-S ghosts originate from the beam splitter, while those in the MIR-L arise from the lenses.

### 4.13.1 Arcmin-scale ghosts

For MIR-S and -L ghosts, Arimatsu et al. (2011) examined their locations and brightness relative to the parent source in detail. For MIR-S, point-like ghosts appear at interval of  $\sim 24$  pixels ( $\sim 1'$ ) in the scan (or Y-axis) direction from a real source. This interval may also be dependent on the source position. For MIR-L, at least three (one compact and two extended) ghosts are known. The extended ghosts are thought to be the cause of the artificial pattern seen in the MIR-L flat (§4.2.1). Meanwhile, Murata et al. (2013) identified three different ghosts for NIR.

The intensity of the ghosts is estimated to be a few % of the parent source for NIR,  $\lesssim 4\%$  for S11 and  $\lesssim 1\%$  for the other MIR-S filters, and  $\sim 10\%$  for MIR-L. Their relative brightness may also depend on the source color.

### 4.13.2 Degree-scale ghosts

An arc-like pattern is found when a bright source is at  $\sim 1.5^\circ$  away from the FoV. A similar pattern is also recognized in the all-sky survey data. Although the position and shape have not been characterized yet, there is an indication that shapes in NIR and MIR-S differ. An example of this arc-like ghosts in an N3 frame is shown in Figure 4.13.19.

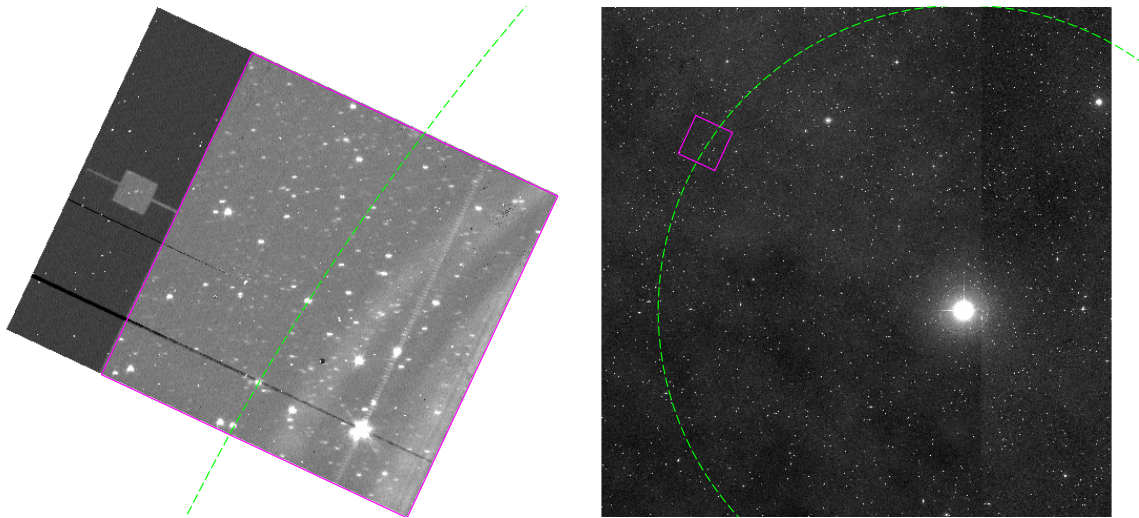


Figure 4.13.19: Arc-like artifacts seen in an N3 frame (left) and a causing bright source from the DSS IR image (right). The magenta box indicates the N3 FoV and the dashed green circle is centered on the bright source (\* psi Peg,  $K_{\text{mag}} = -0.06$  in 2MASS PSC) with radius of  $1.2^\circ$ .

#### 4.14 The earthshine light (EL)

The background level changes during some pointed observations. As it is due to the Earth shine reflection, it depends on the angle between satellite and Earth and the epoch of the observation. The effect from the Earthshine Light (EL) is the worst around the north ecliptic pole during June, July & August. The background level is different at the beginning and at the end of the observation (see Figure 4.14.20), at different pointings (see Figure 4.14.21) and in different seasons (strongest in solstices).

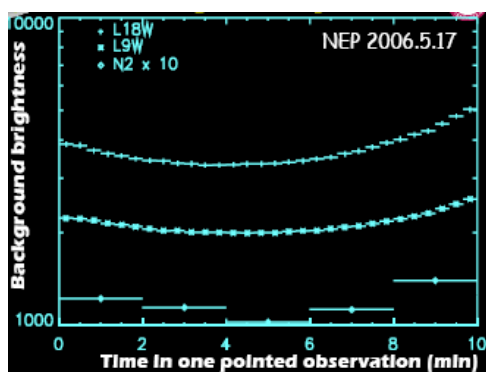


Figure 4.14.20: Change in the background level in a pointed observation.

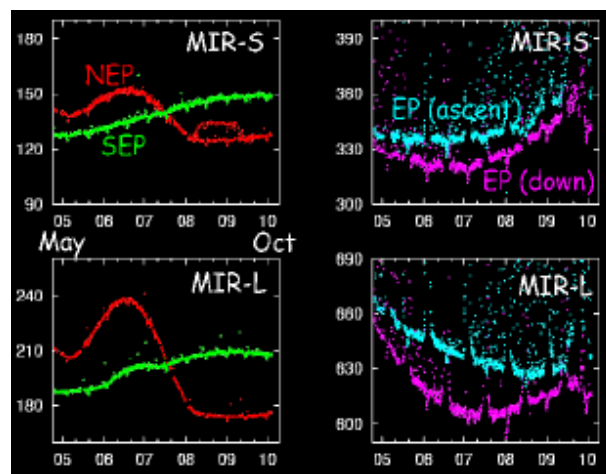


Figure 4.14.21: Variation of background levels from May to October 2006.

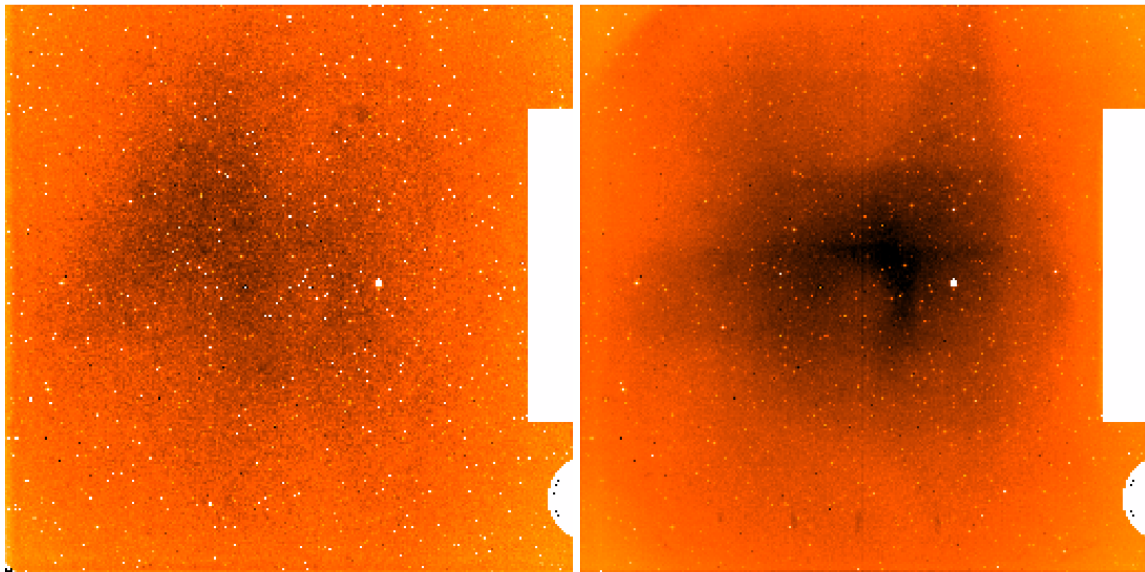


Figure 4.14.22: EL templates for L15 (left) and L24 (right) created from images taken in PID=1402624.1 (obsdate: 2007-06-13) and 1800706.1 (obsdate: 2007-06-15). AOTPARAM=a;N (i.e. the target source not in the MIR-L field) for both pointings.

A template of EL for a pointed observation can be made by combining images from neighbor pointed observations in which observing dates and target positions are close to those of interest (e.g., Egusa et al., 2013; Murata et al., 2013). Example templates for L15 and L24 are shown in Figure 4.14.22.

## 4.15 Relative shift values

Shift in x- and y-axis direction and rotation angle relative to the first frame are calculated by `bluebox.calcshift` (§5.11) for each filter and each pointed observation. For observations with dithering (i.e. AOT = IRC02 or IRC03), mean, median, and standard deviation of shift values are calculated for each exposure cycle (or *ndither*) and no significant difference has been found between the AOTs. For observations with AOT of IRC00 or IRC05, these values are calculated from all the frames since no dithering was performed. Histograms of shift in x- and y-axis direction in the case of MIR-S frames are presented in Figures 4.15.23 (for IRC02 and IRC03) and 4.15.24 (for IRC00 and IRC05). Since these values are calculated for double-sized images, 2.0 pixels correspond to the original 1.0 pixel. Distribution of rotation angle is investigated without taking account into the exposure cycle, since a rotation of field of view was not performed explicitly for each pointed observation. Histograms of rotation angle are presented in Figure 4.15.25. A gaussian profile is fitted to each histogram.

We find that the deviation from the gaussian profile is larger for the shift in x-direction. In other words, the histograms show wings in the left panels of Figures 4.15.23 and 4.15.24. A miss-matching of sources in the shift calculation is one cause, but it does not explain the difference between x- and y-directions. Another possibility is slewing or drifting of the telescope. The telescope FoV is controlled



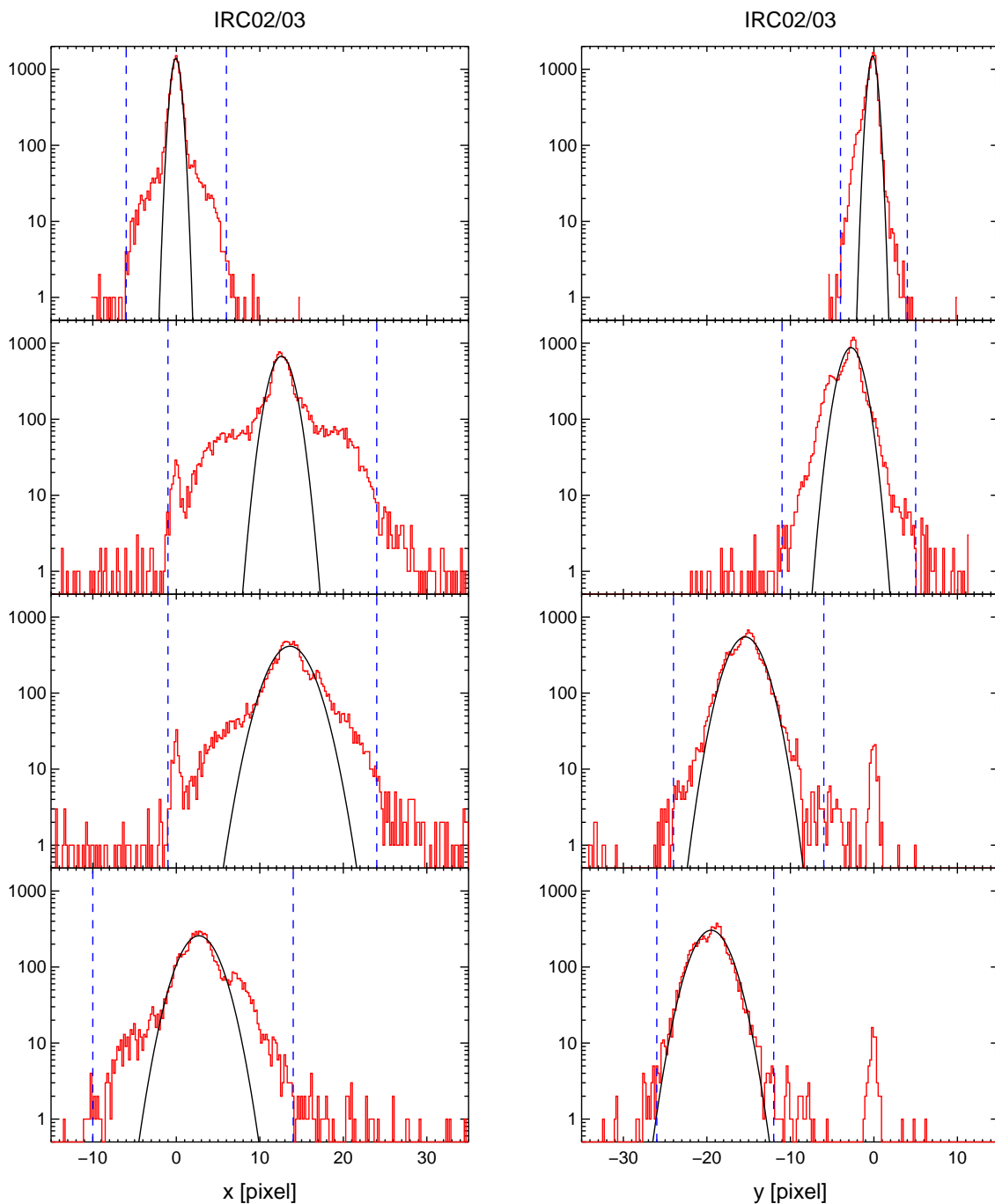


Figure 4.15.23: Histogram of shift in x- (left) and y-axis (right) for AOT of IRC02 and IRC03.  $ndither = 1$  to 4 from top to bottom. Note that pixel values are for double-sized images. Black curves are fitted gaussian profiles to the histogram.

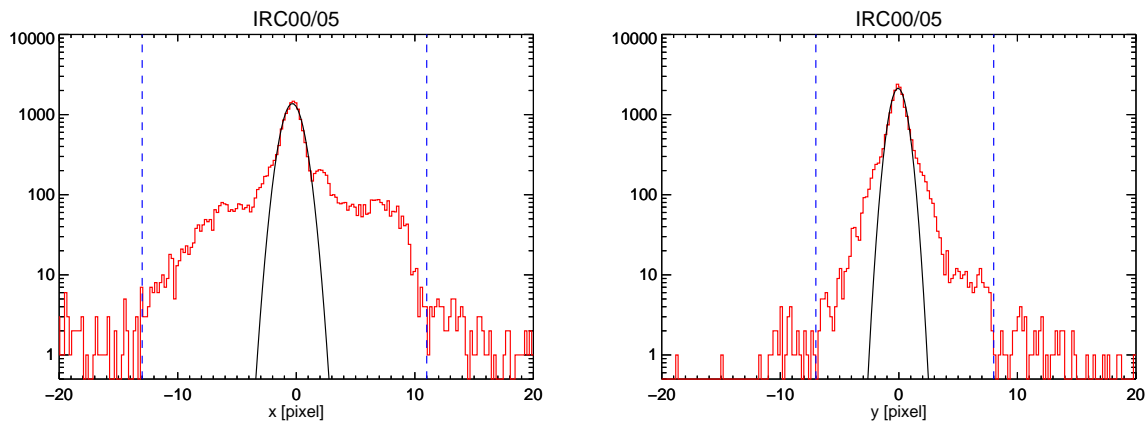


Figure 4.15.24: Same as Figure 4.15.23 but for AOT of IRC00 and IRC05.

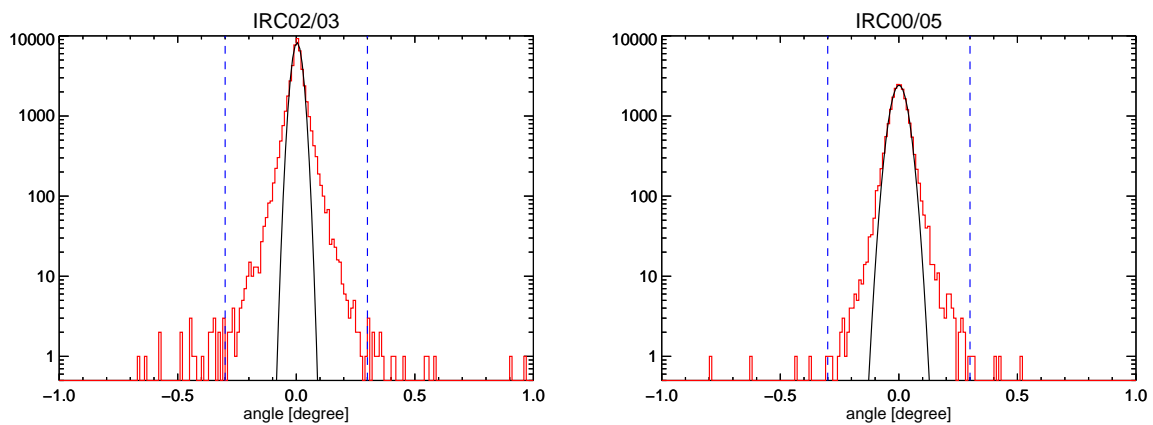


Figure 4.15.25: Histogram of rotation angle [degree] for AOT of IRC02 and IRC03 (left) and of IRC00 and IRC05 (right). Black curves are fitted gaussian profiles to the histogram.

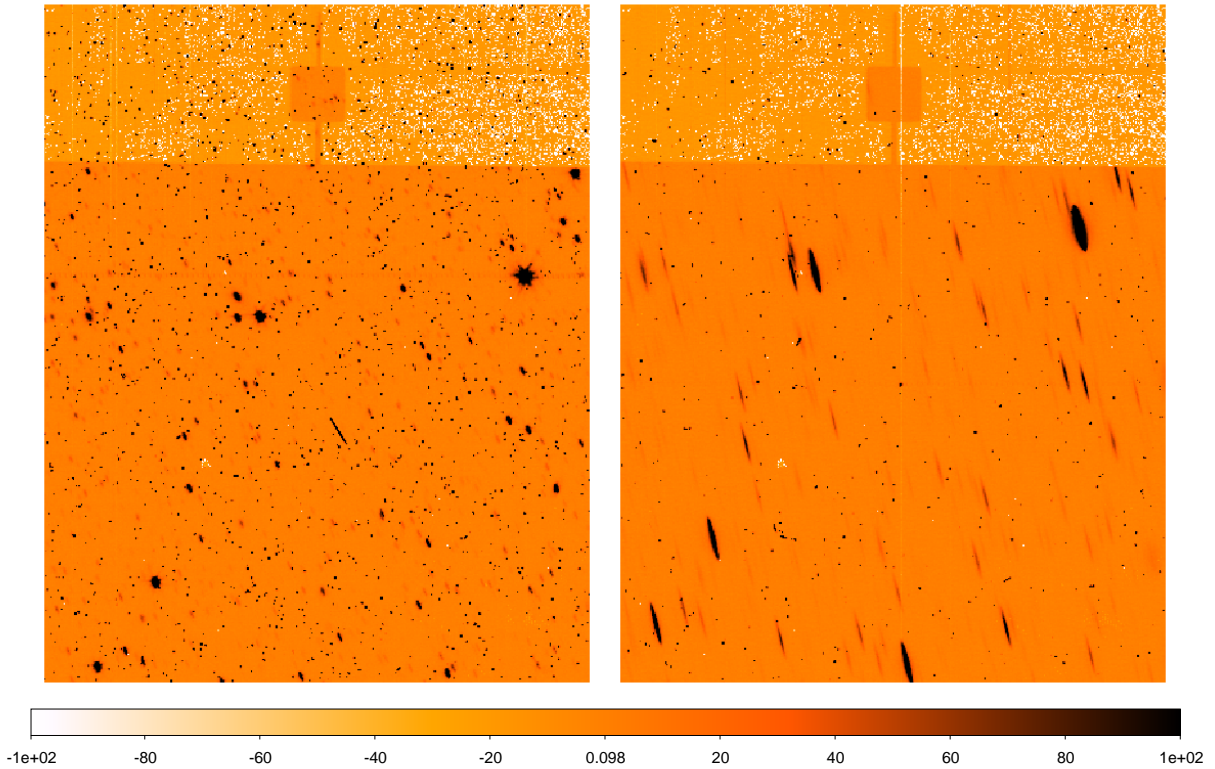


Figure 4.15.26: N3 frames after flat calibration from ObsID=1320235\_001 (left) and 003 (right). The field of views coincide but the right frame suffers from drifting.

by the two optical star trackers and the relative positions of their FoVs should be fixed during observations. However, due to a setting of heaters of the star trackers, they were not completely fixed and thus the telescope FoV sometimes drifted away from where it should be. Not only the shift values but also the PSFs, especially in NIR long-exposure frames, are affected by this drifting. The x-direction of MIR-S corresponds to the y-direction of NIR. In the worst cases, NIR PSFs became very elongated as shown in Figure 4.15.26.

#### 4.16 Difference between MIR-S and -L shift values

Since MIR-S and -L frames were obtained simultaneously, their shift values should in principle be consistent. In Figure 4.16.27, the difference of shift values for MIR-S and -L frames ( $RSV_{L-S}$ ) is presented for each AOT. These values are from the data sets released on 31 March 2015, which are produced by the toolkit ver.150331. Pixel numbers are after sub-pixel sampling (i.e. twice the original pixel numbers).

From these histograms, it is clear that large difference ( $\sim 10$  pixels) appears in IRC02 and IRC03 cases, i.e. observations with dithering. The absence of large difference for IRC00 and IRC05 is at least partly due to the limit values (blue dashed lines in Figure 4.15.24). The large difference is likely due to incorrect calculations of shift values either or both of MIR-S and -L frames. However, it is hard to identify which calculation is incorrect. Thus a warning ‘Wusv’ for

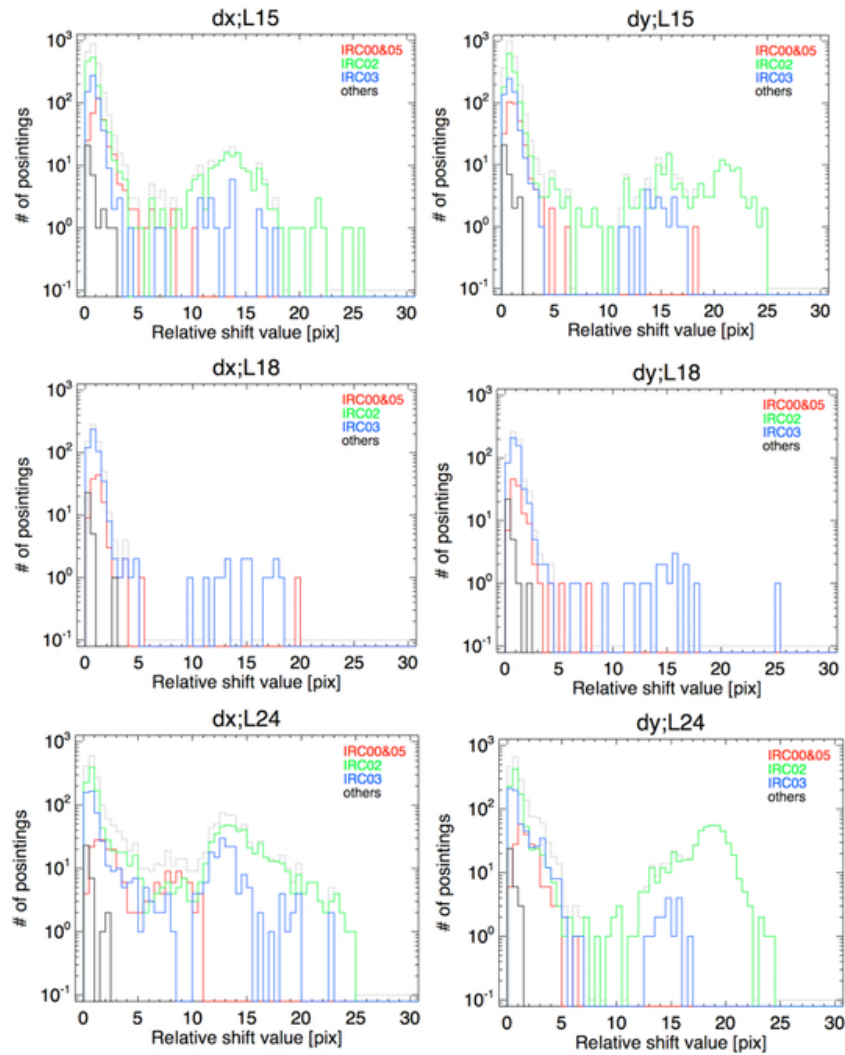


Figure 4.16.27: The difference of the shift values between simultaneously observed frames of MIR-S and MIR-L.

MIR stacked images with ‘uncertain shift values’ is introduced. This warning is applied when any one of frames has the difference that exceeds half of the geometrically averaged FWHM of the PSFs ( $5''.8$ ,  $6''.2$ , and  $6''.9$  for L15, L18W, and L24, respectively).

In the data sets released on 30 March 2015 (produced by the toolkit ver. 150331), this warning is applied to 8%, 3%, and 30% of L15, L18W, and L24 stacked images, respectively. The large difference in shift values and thus this warning percentage may be improved by a future version of the toolkit.

## 4.17 General concerns on slit-less spectroscopy data

This section is dealing mainly with problems related to the slit-less spectroscopy data.

- **Wavelength reference point:** In the slit-less spectroscopy mode, the wavelength reference point depends on the location of objects within the FOV. Therefore, the determination of the source positions on the reference image is very important. Errors in the source positions leads to errors in the assigned wavelengths and, hence the flux calibration.
- **Contamination by nearby sources:** Spectra of more than two objects aligned along with the Y axis could overlap on the same pixels with different wavelengths. It is impossible to separate the spectral overlap on the observed image, without knowing the spectrum of each object.
- **Contamination by zero-th/2nd order light:** For the gratings, images of the zero-th and the 2nd order light can be seen as well as the 1st order image (our prime target for data reduction), although the efficiency for the zero-th and the 2nd order light is very low. All these images contaminate other spectra aligned along with the columns of pixels where the objects exit. These contaminations can be ignored in most cases, and cautions are needed actually only around very bright sources. For the NG spectroscopy with point source aperture ( $N_p$ ), there is little chance for this kind of contamination to occur since the aperture size is much smaller than the size of the dispersed spectroscopy image along the Y or the dispersion direction.
- **Spectral smearing for extended sources:** In the slit-less spectroscopy mode, the spectral resolution is determined by the size of the sources (or the PSF structure plus satellite attitude drift). Thus the spectral resolution is lower for extended objects. If an extended object shows resolved structures, the interpretation of the 2D spectra becomes very difficult because of the convolution of the spectrum over the object spatial structure.
- **Background spectral features:** Although the background sky is essentially "flat" in the imaging mode, it is not true for spectroscopy images.

Note that these features would not be observed with the point source aperture ( $N_p$ ) and other narrow slits, since the aperture size is much smaller than the size of the dispersed spectroscopy image along the Y or the dispersion direction.

- **Faint background areas near the  $Y=0$  or  $Y=Y_{\max}$  edge of FOV:** For the slit area, the background is dominated by the zodiacal light. The spectral-response curve shows a simple pattern with the decreasing sensitivity at the highest and lowest wavelength ends of the disperser's spectral coverage. Thus one will see a background pattern which becomes faint at the top and bottom of the image in units of ADU. For the slit-less area, both the wavelength and the spatial axis Y go along with the same direction (Y), and thus the observed background image is a spatially convolved background spectrum. Since the length of the spectrum along Y (50-70 pix) is much smaller than the aperture size (256 or 412 pix), the resultant background spectrum is almost constant across Y after being convolved spatially by the large aperture. The regions around  $Y=0$  and  $Y=Y_{\max}$  are exceptions, where the edge of the aperture prevents full convolution of the background spectrum along the Y direction and, hence, the background signal becomes faint near  $Y=0$  and  $Y=Y_{\max}$  is seen. Note that this kind of pattern at the very Y edge of the FOV does occur only for the background light, but not for object spectra.

- Jump of the background (ridge) near the center of FOV: Another background feature is a ridge seen near the Y center, stretching along the X axis, seen in grism spectroscopy images. This is caused by the zero-th order light of the gratings. Since the zero-th order light image forms at an offset position from the reference image, only about a half of the FOV suffers from its contamination. This jump of the background flux level (in ADU) is about 2–3% of the total background for SG1, SG2 and LG2.
- Satellite attitude stability/instability: Position shifts among sub-frames are frequently observed due to the satellite attitude drift in the pointing attitude control mode. The drift is as large as several pixels in the worst cases. To correct the drift, one needs to register images among spectroscopy sub-frames and between spectroscopy and reference images. The second correction is very important to determine the wavelength reference point. Note that it takes about 30 sec to switch the spectroscopy mode to/from the imaging mode for the filter wheel rotation. Thus the time interval between the last spectroscopy sub-frame and the first imaging sub-frame is longer by this period than the interval between taking spectroscopy sub-frames. To measure the image drift among spectroscopy images, we use cross-correlation image matching technique. To measure the image drift between spectroscopy and reference images, we could use the same cross-correlation technique. In this cross-correlation we use a template spectrum that was extracted from the data with negligible drifts. Then by comparing the template with spectra extracted from the spectroscopy data in question, we estimate the relative drift.

Since all the channels operate simultaneously, any image drifts along the X and Y directions found in NIR or MIR-S should be seen in MIR-L with the different pixel scale.

For spectra of diffuse sources at the narrow slits (Nh, Ns, and Ls), we do not have to take account of the satellite attitude stability, if the size of the drift is much smaller than that of the objects.

- Ghosts in Np observations: Ghosts relating the Np slit have also been recognized. Left panel of Figure 4.17.28 shows an example of the imaging data. There are sources seen on the slit mask region, which must be ghosts from the sources in the Np slit. Right panel of Fig 4.17.28 shows the corresponding spectral data, in which ghost spectra overlap with the source spectrum.

A similar ghost is also reported for SG2, in which the effect of the ghost should not be significant, since the ghost spectrum appears at much shorter wavelengths (lower part of the image) and does not overlap the source spectrum. No definite origin for these ghosts have been elucidated and thus no clear recipe has been prepared to correct for them.

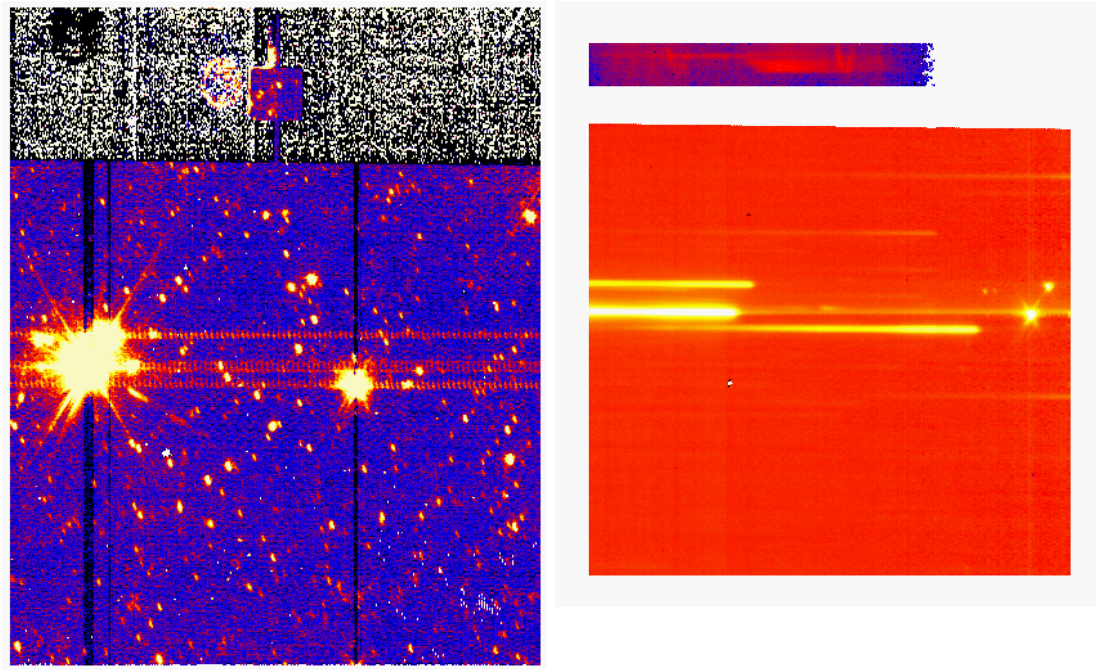


Figure 4.17.28: Ghosts generated in Np observations. Left panel: Imaging data. Right panel: spectroscopic data

## Chapter 5

# Imaging toolkit cookbook

### 5.1 Introduction

The IRC imaging data reduction toolkit is developed to address and correct any IRC instrument features, such as linearity, flat fielding, distortion etc., and converts the raw ADU signal to physically meaningful units (i.e. flux). **The WCS information can be added by matching sources in 2MASS or WISE catalogs.**

The toolkit (including the entire source code) will be released, and be progressively updated reflecting the user’s feedback. **The raw data, calibrated and stacked images, and intermediate files created by the toolkit will be archived.** The user may customize the toolkit at his/her own risk.

The goal for the toolkit is to achieve an absolute flux accuracy of better than 30%, 25% and 25% at the 5 sigma detection limit for NIR, MIR-S and MIR-L channels, respectively. However, these goals are at present the optimal values, and we do not guarantee the numbers.

**In this chapter, §5.4 and 5.5 describe procedures to install and update the toolkit, §5.7–5.11 explain each of pipeline processes, and §5.14 lists limitations and caveats of the toolkit.**

### 5.2 General overview of the toolkit processing

The toolkit runs on IRAF and consists of three main steps, prepipeline, pipeline1, and pipeline2. While prepipeline corresponds to Red Box, pipeline1 and 2 do not correspond to Green and Blue Boxes each other.

- Pre-pipeline Processor (Red Box) : Produces *Basic Data*
  - redbox.ircslice: header formatting, slice IRC 3D images into usual 2D ones
  - redbox.mkirclog: making the observing log file “irclog”
- Pipeline (Green Box) : Produces *Basic Science Data*
  - greenbox.wraparound: wrap around correction
  - greenbox.ircnorm: normalize sampling and compression bit shift
  - greenbox.linearity: correct linearity of the detector response
  - greenbox.dark: subtract dark current



- greenbox.scatt\_light: subtract the MIR-S scattered light pattern
- greenbox.cosmic\_ray: remove cosmic rays
- greenbox.flat: flat pattern correction
- greenbox.maskall: mask bad/dead/hot pixels, saturated pixels, and the slit area on the detector
- greenbox.aspect\_ratio: distortion correction (aspect ratio resampling)
- Post-Pipeline Processor (Blue Box):
  - bluebox.coadd: to form a co-added image (called from pipeline2 processor by default)
    - \* source\_extract, source\_extract2: perform source extraction
    - \* calcshift: calculate shift & rotation between images
    - \* adjust\_sky: adjust sky level before stacking
    - \* irc\_stack: stack individual frames to form a co-added image
  - blubox.putwcs: update WCS information

The pipeline can be run automatically or interactively step by step.

**Additional modules to help improving the resultant images by the above processes are stored in IRC\_TOOL and described in §5.13.**

### 5.3 Expected Data Processing Rate (minimum expectation)

- NIR =  $412 \times 512 [\text{pixels}] \times 16 [\text{bit/pixel}] / 8 [\text{bit/byte}] = 412 \text{ Kbyte/frame}$ 
  - 1 NIR fits =  $412 \text{ Kbyte/frame} \times 2 \text{ frame/fits} = 824 \text{ Kbyte/fits file}$
- MIR =  $256 \times 512 [\text{pixels}] \times 16 [\text{bit/pixel}] / 8 [\text{bit/byte}] = 256 \text{ Kbyte/frame}$ 
  - 1 MIR fits =  $256 \text{ Kbyte/frame} \times 4 \text{ frame/fits} = 1024 \text{ Kbyte/fits file}$
- AOT02:  $6 \text{ exposure cycles/pointing} \times (1 \text{ NIR fits} + 1 \text{ MIR fits})/\text{exposure cycle} \sim 10.8 \text{ Mbyte/pointing}$
- AOT03:  $6 \text{ exposure cycles/pointing} \times (1 \text{ NIR fits} + 1 \text{ MIR fits})/\text{exposure cycle} \sim 10.8 \text{ Mbyte/pointing}$
- AOT05:  $9 \text{ exposure cycles/pointing} \times (1 \text{ NIR fits} + 1 \text{ MIR fits})/\text{exposure cycle} \sim 16.2 \text{ Mbyte/pointing}$

The toolkit requires 3 or 4 times of disk space compared to the raw data.

## 5.4 How to install the IRC imaging Toolkit

### 5.4.1 Requirements

The toolkit is developed in a Linux PC environment and has also been successfully run in the Mac OSX Unix environment. The toolkit requires the following environment for its full function:

- unix (Solaris, MacOS X, Linux, BSD)

- IRAF 2.12.2 or later
- gcc 3.2 or later
- perl
- curl (for WCS calculation on Solaris machines)

#### 5.4.2 Install IRAF

- see <http://iraf.noao.edu/> or <http://iraf.net/>

#### 5.4.3 Download IRC imaging data reduction software package

The latest version of the toolkit with installation and operating instructions can be obtained from the AKARI Observer's web site (see section 1.3).

#### 5.4.4 Unpack irc.tgz

- `mv ircYYMMDD.tgz /where/you/want/to/install`
- `cd /where/you/want/to/install`
- `tar xvzf ircYYMMDD.tgz`

#### 5.4.5 Make irc binaries

- `cd /where/you/want/to/install/irc/src`
- `make`

This will create binary files in `/where/you/want/to/install/irc/bin/`

#### 5.4.6 Run "setpath.pl"

- `cd /where/you/want/to/install/irc/lib`
- `perl setpath.pl`

This will rewrite the "setpath.dat". Please check the following line in "setpath.dat" is the following format

```
set irchome = "/where/you/want/to/install/irc/"
```

This line should indicate the location where you installed the irc package.

#### 5.4.7 Perl path

Typing **which perl** in the unix environment indicates where the perl is installed in your system. The toolkit assumes that the perl is installed in `/usr/local/bin/perl`

Therefore, those who have the perl binary elsewhere, should do as follows:

- If you know the root password, please create a symbolic link in `/usr/local/bin` by typing:
  - `cd /usr/local/bin`

- `ln -s 'which perl' perl`

It will create a symbolic link **perl** in `/usr/local/bin`.

- If you don't know the root password, please modify the first line of every perl script file in `/where/you/want/to/install/irc/perl`. For example, if you have perl in `/usr/bin/perl`, please modify it as;

- `#!/usr/local/bin/perl → #!/usr/bin/perl`

As long as you have perl in `/usr/bin/perl`, you can also achieve the same result by running a script

- `cd /where/you/want/to/install/irc/perl`
- `perlpath.sh`

which will create a directory **temp** containing perl files whose first lines are modified as above. Then you can overwrite these new perl files by typing;

- `mv ./temp/*.pl .`

Those who do not have perl in `/usr/bin/perl`, please modify **perlpath.sh** and indicate the location of your perl.

#### 5.4.8 Add IRC entry to IRAF

- If you use **IRAF v2.15 or later** and installed the **IRC toolkit ver.20131202 or later** under “`iraf$extern`” directory, the toolkit should be automatically recognized by IRAF without following steps.

- If you know root password and you installed IRAF package into for example `/iraf`,

- `cd /iraf/iraf/unix/hlib/`
- edit the file `extern.pkg`

Please add the following 2 lines to A `/iraf/iraf/unix/hlib/extern.pkg`,

```
reset irc = /where/you/want/to/install/irc/
```

```
task $irc.pkg = irc$irc.cl
```

DO NOT FORGET THE "\$" BEFORE THE IRC.PKG!! DO NOT FORGET THE LAST SLASH!!

- If you don't know root password then you should launch iraf from your home directory everytime you want to use irc package

- `cd` (change directory to your home directory)
- `mkiraf` (only when using IRAF for the very first time)

This will create the “`login.cl`” file in your home directory. Then edit “`login.cl`” and add 2 lines:

```
reset irc = /where/you/want/to/install/irc/
```

```
task $irc.pkg = irc$irc.cl
```

DO NOT FORGET THE "\$" BEFORE THE IRC.PKG!! DO NOT FORGET THE LAST SLASH!!

The toolkit is now installed and is ready to be run !!

## 5.5 How to UPGRADE the version of IRC imaging toolkit

Upgrades to the IRC imaging toolkit is a progressive and ongoing process and new versions of the toolkit will be available to users throughout the course of the mission. On receiving a new version of toolkit package (e.g., ircYYMMDD.tgz), the following commands are required to be input;

- mv ircYYMMDD.tgz /where/you/installed/previous/version/
- cd /where/you/installed/previous/version/
- tar xvzf ircYYMMDD.tgz

These commands will OVERWRITE any old files/directories. Then, follow the original procedure described in §5.4.5 and 5.4.7. Finally, please type following commands when you use a new version of the toolkit for the first time.

- launch IRAF
- load the ircpackage by typing “irc”
- type “unlearn\_all”
- load the irc\_tool package by typing “irc\_tool”
- type “unlearn coaddLusingS” (and other tasks if previously used)

## 5.6 Setting up your toolkit environment and running the pipeline

The steps to reduce the raw data are outlined below.

### 5.6.1 Creating the directory structure

The toolkit assumes the following directory structure (see Figure 5.6.1);

```
~/anyname +
——rawdata (must be this name)
——anyname (your working directory)
```

e.g.

```
~/data/rawdata/
~/data/working/
```

The toolkit should be run in the working directory. Thus you may create sets of these directory structures for different sets of IRC data.

### 5.6.2 Launch IRAF

Launch IRAF in your home directory and check that you have an entry for the irc package in the list of IRAF packages (see Figure 5.6.2).

Then you can move to your working directory before starting to run the different tools by typing:

- cd to\_your\_working\_directory

where to\_your\_working\_directory should follow the rules explained in Section 5.6.1.

```

xterm
polaire:yita % pwd
/home/yita
polaire:yita % tar xzf sample_data.tgz
polaire:yita % cd sample_data
polaire:yita % mkdir yita
polaire:yita % ls
sample_data/ yita/
polaire:yita % █

```

Figure 5.6.1: Example directory structure for IRC toolkit.

```

xgterm
NOAO PC-IRAF Revision 2.12.2-EXPORT Sun Jan 25 16:09:03 MST 2004
This is the EXPORT version of PC-IRAF V2.12 supporting most PC systems.

Welcome to IRAF. To list the available commands, type ? or ?? . To get
detailed information about a command, type 'help command'. To run a
command or load a package, type its name. Type 'bye' to exit a
package, or 'logout' to get out of the CL. Type 'news' to find out
what is new in the version of the system you are using. The following
commands or packages are currently defined:

color.      images.      noao.        softtools.   utilities.
ctio.       inc.          obsolete.    southafrica.
dataio.     language.    plot.        stsdas.
dbms.       lists.       proto.       system.
finder.     rmisc.       sirius.     tables.

c1> █

```

Here

Figure 5.6.2: Start up screen for IRAF showing the IRC package visible in the list of IRAF packages.

### 5.6.3 Load the IRC package

The irc package can be loaded by typing “irc”. You should then see the IRC pipeline splash screen (welcome message) and a list of the available IRC packages (see Figure 5.6.3). The screen shows the version of toolkit, super-flat, super-dark, linearity, and distortion. Please let us know these numbers if you send any email to the help desk [iris\\_help@ir.isas.jaxa.jp](mailto:iris_help@ir.isas.jaxa.jp) to inquire any trouble with the toolkit.

```

dataio.  irc.    lists.  plot.   stsdas.  utilities.
dbms.   irc_p3. noao.   proto.  system.  vo.
images.  language. obsolete. softools. tables.

vocl> irc

+-----+
|           AKARI IRC imaging data reduction pipeline           |
|           pipeline  version: 150331                          |
|           flat      version: 140728                          |
|           dark      version: 101116                          |
|           linearity version: 061121                          |
|                                                                 |
|           Copyright (C) 2005                                  |
|           Institute of Space and Astronautical Science,      |
|           Japan Aerospace Exploration Agency                  |
|                                                                 |
|           For help, send email to iris_help@ir.isas.jaxa.jp  |
+-----+

bluebox.  irc_tool.  pipeline2  redbox.
greenbox. pipeline1  prepipeline unlearn_all

irc.>

```

Figure 5.6.3: Start up screen for the IRC package showing the available modules and tools. The start up splash screen gives the current version of the toolkit, and current versions of flat, dark, linearity, distortion files etc.

## 5.7 The pre-pipeline processor (Red-Box)

Note that prepipeline processor is a one-time-only process. **If the script finds the file “irclog” (output of prepipeline), it recognizes that prepipeline has already been run and stops. In addition, if there are no valid rawdata, prepipeline stops as well.**

### 5.7.1 Configuration

Before running prepipeline, you can configure the parameters for prepipeline by typing “epar prepipeline”. This displays the parameter edit screen as shown in Figure 5.7.4.

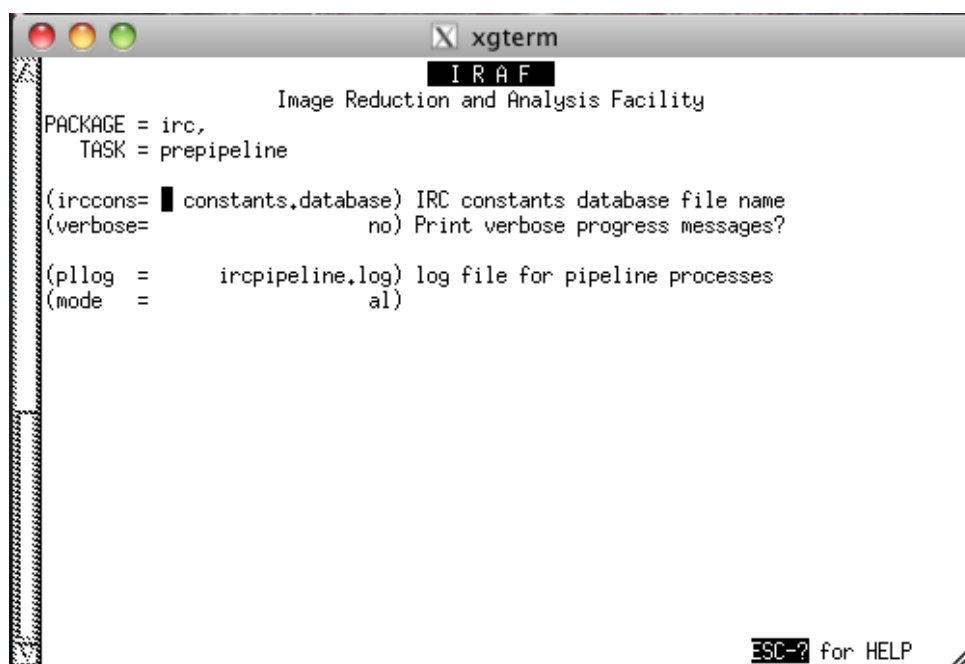


Figure 5.7.4: Parameter edit screen for prepipeline showing the available parameters.

The parameters of prepipeline are listed below.

- **ircconst** (string, default=“ircconstants.database”):  
NEVER CHANGE THIS. This is the irc constant file name.
- **verbose** (boolean, default=no):  
Activate if you want to print vrebiose progress messages.
- **pllog** (string, default=“ircpipeline.log”):  
A log file for pipeline processes. Recommended to leave as default.

### 5.7.2 Running the prepipeline processor

The prepipeline processor consists of the following two functions.

- **redbox.ircslice**: slice IRC 3D images into usual 2D ones
- **redbox.mkirclog**: make the observing log file “irclog”

The prepipeline processor is run by entering “prepipeline” at the IRAF command prompt. Alternatively, the individual Red-Box modules can be run by entering “redbox” at the IRAF command prompt. The present configuration of the pre-pipeline modules is shown in Figure 5.7.5:

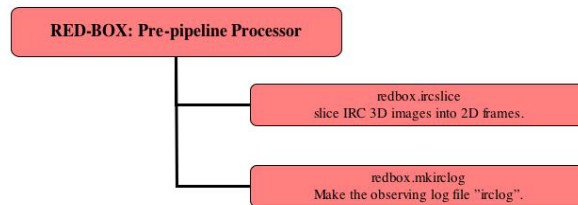


Figure 5.7.5: Present configuration of the Red-Box prepipeline modules.

### 1. **redbox.ircslice**

The number of FITS files produced for any given single pointed observation depends on the AOT. Each AOT comprises a combination of Exposure Cycles (EC), Filter Wheel changes (W), and Dither Maneuvers (M) (see Figure 2.2.6). The IRC FITS data are not a usual 2D one. A raw data FITS file is created for each Exposure Cycle during a pointing for the NIR and combined MIR-S/MIR-L channels (i.e. 1 NIR FITS file and 1 MIR FITS file = 2 FITS files per Exposure Cycle). The filename format is given as F\*\*\*\*\*\_N.fits or F\*\*\*\*\*\_M.fits, where \*\*\*\*\* is a distinct incremental reference number. A NIR raw FITS data file is a data cube containing 2 frames within it, corresponding to one short and one long exposure. Each MIR raw FITS file contains 4 frames within it (one short and three long exposures) for both the MIR-S and MIR-L channels respectively making a total of 8 frames per MIR FITS file per Exposure Cycle (see Figure 5.7.6).

In addition to the Exposure Cycles, dark frames were taken at the beginning and the end of the operation for both the NIR and MIR channels (i.e. extra 2 raw FITS files for both NIR and MIR). Therefore, as shown in Figure 2.2.6 for AOT IRC02, the maximum number of raw FITS data files is  $(1 \text{ NIR} + 1 \text{ MIR FITS})/\text{EC} \times 7(\text{EC}) + 4(\text{Dark}) = 18$  for one pointed observation. Meanwhile, for AOT IRC03, the raw data files comprise of  $(1 \text{ NIR} + 1 \text{ MIR FITS})/\text{EC} \times 8(\text{EC}) + 4(\text{Dark}) = 20$  FITS files for one pointed observation. In addition to the raw FITS files, a text file is also included giving details of the original target list for the observation.

The “redbox.ircslice” module slices each raw FITS file into the individual frames (separates all individual IRC frames for one Exposure Cycle). Thus for every NIR raw FITS file (including the Dark), redbox.ircslice creates 2 FITS files (corresponding to the short and long exposure). For every MIR raw FITS file (including the Dark), redbox.ircslice creates 8 FITS files (corresponding to single short and three long exposures for both the MIR-S and MIR-L channels). Therefore after running “redbox.ircslice” on a single pointed observation with AOT IRC03, you expect to see as many as 100 individual FITS files. The filename format takes the original format with an extension defining the channel (N,S,L) and frame number (001-004). For example, an original raw FITS file for the MIR channel F23340\_M.fits is sliced into 8 separate FITS files F23340\_L001.fits, F23340\_L002.fits, F23340\_L003.fits, F23340\_L004.fits, F23340\_S001.fits, F23340\_S002.fits, F23340\_S003.fits, F23340\_S004.fits.



Figure 5.7.7 shows the images of IRC raw data for the NIR and MIR bands. The orientation of the images are such that the NIR is rotated by 90 degrees relative to MIR-S/L. The dark area in each image is masked for the slit spectroscopic observations and thus should not receive any light during imaging observations, so that we are able to monitor dark current level variation during a pointed observation. Hereafter, we refer to this dark area as the “slit area” and the other as the “imaging area”.

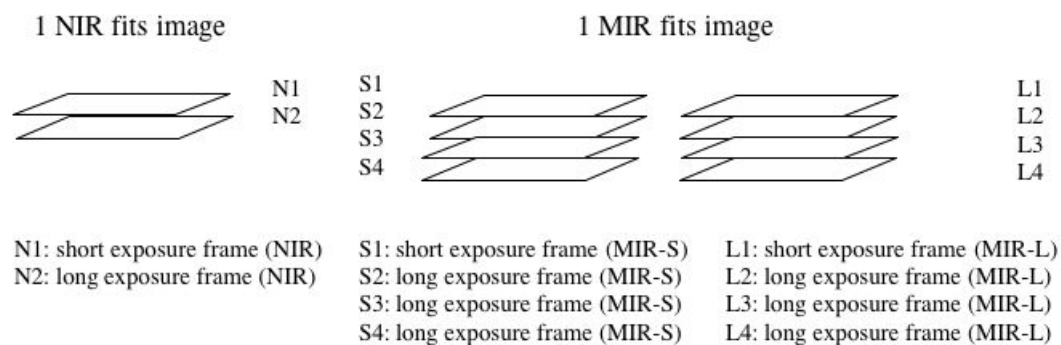


Figure 5.7.6: IRC raw FITS file data structure for NIR and MIR images.

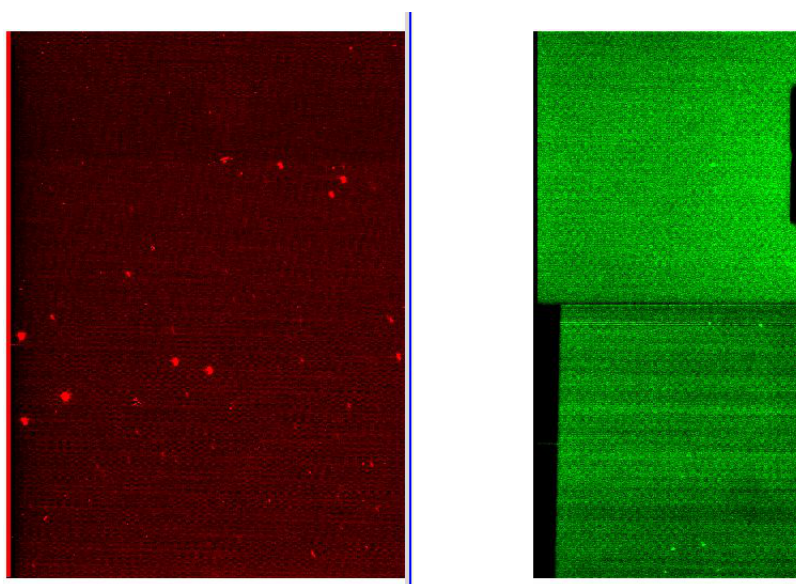


Figure 5.7.7: Image of IRC raw data NIR and MIR bands. The NIR raw FITS file (left) is 2 frames deep (corresponding to 1 short and 1 long exposure). The MIR raw FITS file (right) is 2 frames wide and 4 frames deep (corresponding to 1 short and 3 long exposures each for MIR-S and MIR-L).

## 2. redbox.mkirclog

The “redbox.mkirclog” creates the observing log file “irclog”. This is a text file with contents shown in Table 5.7.1. The contents of the irclog file summarize the nature of the processed files in the working directory. The table entries correspond to;

- FRAME: The filename corresponding to the “sliced frame” (e.g. following the format such as F23340.L001.fits as described above) without “.fits” extension
- OBJECT: Target name taken from the original target list (space is replaced by \_)
- NAXIS: Number of pixels in the cross-scan direction (256 for MIR and 412 for NIR)
- FILTER: Filter name (i.e. N2, N3, N4, S7, ..., L24 or DARK)
- RA-SET: Right ascension coordinates
- DEC-SET: Declination coordinates
- AOT: AOT type (e.g. IRC02, IRC03 etc.)
- EXPID: Sequential frame number during an exposure cycle (e.g. 1 or 2 for NIR and 1, 2, 3 or 4 for MIR-S and MIR-L images)
- IDNUM: Pointing ID
- SUBID: Sub-Pointing ID (greater than 1 for multi-pointing observations)

Table 5.7.1: Sample of the “irclog” file

FRAME	OBJECT	NAXIS1	FILTER	RA-SET	DEC-SET	AOT	EXPID	IDNUM	SUBID
#F004160544.L001	"LMC-FIELD218"	256	DARK	80.54688	-68.17107	IRC02	1	2210218	1
#F004160544.L002	"LMC-FIELD218"	256	DARK	80.54688	-68.17107	IRC02	2	2210218	1
#F004160544.L003	"LMC-FIELD218"	256	DARK	80.54688	-68.17107	IRC02	3	2210218	1
#F004160544.L004	"LMC-FIELD218"	256	DARK	80.54688	-68.17107	IRC02	4	2210218	1
#F004160544.S001	"LMC-FIELD218"	256	DARK	80.54688	-68.17107	IRC02	1	2210218	1
#F004160544.S002	"LMC-FIELD218"	256	DARK	80.54688	-68.17107	IRC02	2	2210218	1
#F004160544.S003	"LMC-FIELD218"	256	DARK	80.54688	-68.17107	IRC02	3	2210218	1
#F004160544.S004	"LMC-FIELD218"	256	DARK	80.54688	-68.17107	IRC02	4	2210218	1
#F004160545.N001	"LMC-FIELD218"	412	DARK	80.54688	-68.17107	IRC02	1	2210218	1
#F004160545.N002	"LMC-FIELD218"	412	DARK	80.54688	-68.17107	IRC02	2	2210218	1
F004160546.L001	"LMC-FIELD218"	256	L15	80.54688	-68.17107	IRC02	1	2210218	1
F004160546.L002	"LMC-FIELD218"	256	L15	80.54688	-68.17107	IRC02	2	2210218	1
F004160546.L003	"LMC-FIELD218"	256	L15	80.54688	-68.17107	IRC02	3	2210218	1
F004160546.L004	"LMC-FIELD218"	256	L15	80.54688	-68.17107	IRC02	4	2210218	1
F004160546.S001	"LMC-FIELD218"	256	S7	80.54688	-68.17107	IRC02	1	2210218	1
F004160546.S002	"LMC-FIELD218"	256	S7	80.54688	-68.17107	IRC02	2	2210218	1
F004160546.S003	"LMC-FIELD218"	256	S7	80.54688	-68.17107	IRC02	3	2210218	1
F004160546.S004	"LMC-FIELD218"	256	S7	80.54688	-68.17107	IRC02	4	2210218	1
#F004160547.N001	"LMC-FIELD218"	412	NP	80.54688	-68.17107	IRC02	1	2210218	1
#F004160547.N002	"LMC-FIELD218"	412	NP	80.54688	-68.17107	IRC02	2	2210218	1
.....	.....	.....	.....	.....	.....	.....	.....	.....	.....
F004160558.L001	"LMC-FIELD218"	256	L24	80.53135	-68.17282	IRC02	1	2210218	1
F004160558.L002	"LMC-FIELD218"	256	L24	80.53135	-68.17282	IRC02	2	2210218	1
F004160558.L003	"LMC-FIELD218"	256	L24	80.53135	-68.17282	IRC02	3	2210218	1
F004160558.L004	"LMC-FIELD218"	256	L24	80.53135	-68.17282	IRC02	4	2210218	1
F004160558.S001	"LMC-FIELD218"	256	S11	80.53135	-68.17282	IRC02	1	2210218	1
F004160558.S002	"LMC-FIELD218"	256	S11	80.53135	-68.17282	IRC02	2	2210218	1
F004160558.S003	"LMC-FIELD218"	256	S11	80.53135	-68.17282	IRC02	3	2210218	1
F004160558.S004	"LMC-FIELD218"	256	S11	80.53135	-68.17282	IRC02	4	2210218	1
F004160559.N001	"LMC-FIELD218"	412	N3	80.53135	-68.17282	IRC02	1	2210218	1
F004160559.N002	"LMC-FIELD218"	412	N3	80.53135	-68.17282	IRC02	2	2210218	1
#F004160560.L001	"LMC-FIELD218"	256	UNDEF	80.53135	-68.17282	IRC02	1	2210218	1
#F004160560.L002	"LMC-FIELD218"	256	UNDEF	80.53135	-68.17282	IRC02	2	2210218	1
#F004160560.L003	"LMC-FIELD218"	256	UNDEF	80.53135	-68.17282	IRC02	3	2210218	1
#F004160560.L004	"LMC-FIELD218"	256	UNDEF	80.53135	-68.17282	IRC02	4	2210218	1
#F004160560.S001	"LMC-FIELD218"	256	UNDEF	80.53135	-68.17282	IRC02	1	2210218	1
#F004160560.S002	"LMC-FIELD218"	256	UNDEF	80.53135	-68.17282	IRC02	2	2210218	1
#F004160560.S003	"LMC-FIELD218"	256	UNDEF	80.53135	-68.17282	IRC02	3	2210218	1
#F004160560.S004	"LMC-FIELD218"	256	UNDEF	80.53135	-68.17282	IRC02	4	2210218	1
#F004160561.N001	"LMC-FIELD218"	412	UNDEF	80.53135	-68.17282	IRC02	1	2210218	1
#F004160561.N002	"LMC-FIELD218"	412	UNDEF	80.53135	-68.17282	IRC02	2	2210218	1
#F004160562.L001	"LMC-FIELD218"	256	DARK	359.7475	-59.3225	IRC02	1	2210218	1
#F004160562.L002	"LMC-FIELD218"	256	DARK	359.7475	-59.3225	IRC02	2	2210218	1
#F004160562.L003	"LMC-FIELD218"	256	DARK	359.7475	-59.3225	IRC02	3	2210218	1
#F004160562.L004	"LMC-FIELD218"	256	DARK	359.7475	-59.3225	IRC02	4	2210218	1
#F004160562.S001	"LMC-FIELD218"	256	DARK	359.7475	-59.3225	IRC02	1	2210218	1
#F004160562.S002	"LMC-FIELD218"	256	DARK	359.7475	-59.3225	IRC02	2	2210218	1
#F004160562.S003	"LMC-FIELD218"	256	DARK	359.7475	-59.3225	IRC02	3	2210218	1
#F004160562.S004	"LMC-FIELD218"	256	DARK	359.7475	-59.3225	IRC02	4	2210218	1
#F004160563.N001	"LMC-FIELD218"	412	DARK	359.7475	-59.3225	IRC02	1	2210218	1
#F004160563.N002	"LMC-FIELD218"	412	DARK	359.7475	-59.3225	IRC02	2	2210218	1

## 5.8 Before running the pipeline processor

After running “prepipeline”, the following three text files should be created in the working directory.

- **irclog**

The irclog file is used to select the data to be reduced by the following pipelines. If you find the pipeline crashes due to bad frames, removing (or commenting out by #) such frames may solve the problem.

Note that dark frames and any grism/prism images are automatically commented out by the prepipeline. The data frame taken during the maneuver should also be automatically discarded.

- **darklist.before**

In a pointed observation, dark frames are taken at the beginning and the end of the operation for both the NIR and MIR channels. This file “darklist.before” contains the name of dark frames taken at the beginning of the operation. Dark frames taken at the end of the operation may be affected by latent, so they are excluded from the list. Those who want to use these “pre-dark” images should set **darktype="se"** (see §5.9.2 for detail), then the pipeline processor will read the darklist.before file and will make a dark image by averaging over 3 images of MIR-S and MIR-L long exposure dark frames. However, super-dark will be used for all short frames even if **darktype="se"**, since only one pre-dark frame is available for short exposure.

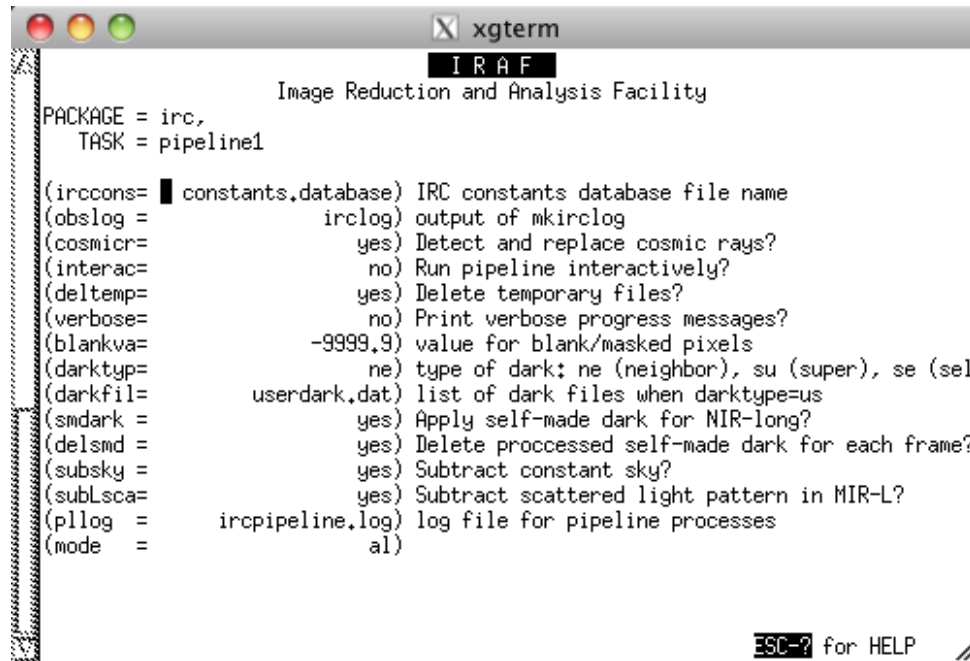
- **ircpipeline.log**

**A log file for pipeline processing. By default, logs from pipeline1 and pipeline2 will be appended to this file as well.**

## 5.9 The pipeline1 processor (Green-Box)

### 5.9.1 Parameter configuration

Before running the pipeline1, you can configure the parameters for the pipeline1 by typing “epar pipeline1”.



```

xterm
IRAF
Image Reduction and Analysis Facility
PACKAGE = irc,
TASK = pipeline1

(ircconsts= constants.database) IRC constants database file name
(obslog =      irclog) output of mkirclog
(cosmicr=     yes) Detect and replace cosmic rays?
(interac=     no) Run pipeline interactively?
(deltemp=     yes) Delete temporary files?
(verbose=     no) Print verbose progress messages?
(blankva=    -9999.9) value for blank/masked pixels
(darktyp=     ne) type of dark: ne (neighbor), su (super), se (sel
(darkfil=     userdark.dat) list of dark files when darktype=us
(smdark =     yes) Apply self-made dark for NIR-long?
(delsmd =     yes) Delete processed self-made dark for each frame?
(subsky =     yes) Subtract constant sky?
(sublsca=     yes) Subtract scattered light pattern in MIR-L?
(pllog =      ircpipeline.log) log file for pipeline processes
(mode =       al)
ESC-? for HELP

```

Figure 5.9.8: Screen for parameter configuration for pipeline1.

The parameters of pipeline1 are listed below. For details, see §5.9.2.

- `ircconst` (string, default=“constants.database”):  
**NEVER CHANGE THIS.** This is the irc constant file name.
- `obslog` (string, default=“irclog”):  
**NEVER CHANGE THIS.** Output filename of redbox.mkirclog.
- `cosmicray` (boolean, yes or no, default=no):  
Detect and replace cosmic rays in MIR images. Cosmic ray events in each image are detected and replaced by the average of the four nearest neighbors. Type “help cosmicrays” inside IRAF’s shell for details. **The IRAF task “cosmicrays” may not work properly with IRAF v2.15 or v2.16. This problem can be solved by updating “x\_crutil.e” in “noao\$bin.\*”. See README file of toolkit ver.20131202 for more detailed instruction. Or, updating IRAF to v2.16.1 should also fix the problem.**
- `interactive` (boolean, yes or no, default=no):  
With this option selected, the pipeline can be run step by step, e.g. as  
`Greenbox.anomalous_pix`  
`Greenbox.dark`, etc  
or alternatively by typing `Greenbox` then running from inside the Green-Box as  
`anomalous_pix`  
`dark`, etc.

- `deltemp` (boolean, yes or no, default=yes):  
Set to no if you do not want to delete any temporary created file.
- `verbose` (boolean, yes or no, default=no):  
Activate if you want to print verbose progress messages
- `blankvalue` (real,  $\leq -1000.$ , default=-9999.9):  
Specify a value for blank/masked pixels.
- **`darktype` (string, “ne”/“su”/“se”/“us”, default=“ne”):**  
**Select dark type for reduction. Four options are available; “ne” for neighbor dark, “su” for super dark; “se” for self dark; “us” for user dark.**
- `darkfile` (string, default=“usedark.dat”):  
Specify a file containing list of dark files, if you want to use your own dark with `darktype=“us”` option.
- `smdark` (boolean, yes/no, default=yes):  
Set yes if you want to apply the “self-made” dark to NIR long exposure frames.
- `delsmd` (boolean, yes/no, default=yes):  
Set yes if you want to delete processed self-made dark frames.
- `subsky` (boolean, yes/no, default=yes):  
Set yes if you want to subtract a constant as a sky background from each frame.
- `subLscat` (boolean, yes/no, default=yes):  
Set yes if you want to subtract a scattered light pattern seen in MIR-L frames.
- **`plog` (string, default=“ircpipeline.log”):**  
**A log file for pipeline processes. Recommended to leave as default.**

### 5.9.2 Execution

Type `pipeline1` at the IRAF command prompt to start `pipeline1` processing.

Alternatively, the individual modules can be run interactively by 3 possible methods;

- By setting the `interac` parameter in the parameter list
- By running the `pipeline1` with the command `pipeline1 interactive=yes`
- By running the `pipeline1` with the command `pipeline1 interactive+`

When running the `pipeline1` interactively, individual steps may be entered as

`Greenbox.wraparound`

`Greenbox.dark`, etc.

or alternatively by typing `Greenbox` then running from inside the Green-Box as

`wraparound`

`dark`, etc.

When running interactively, there are options to perform/skip/stop for each process. The present configuration of the `pipeline1` modules are shown in Figure 5.9.9.

Each module is described below in the order of processing in the `pipeline1` script. After each step of processes, a prefix is added to the original filename. The prefixes and corresponding modules are listed in Table 5.9.2.

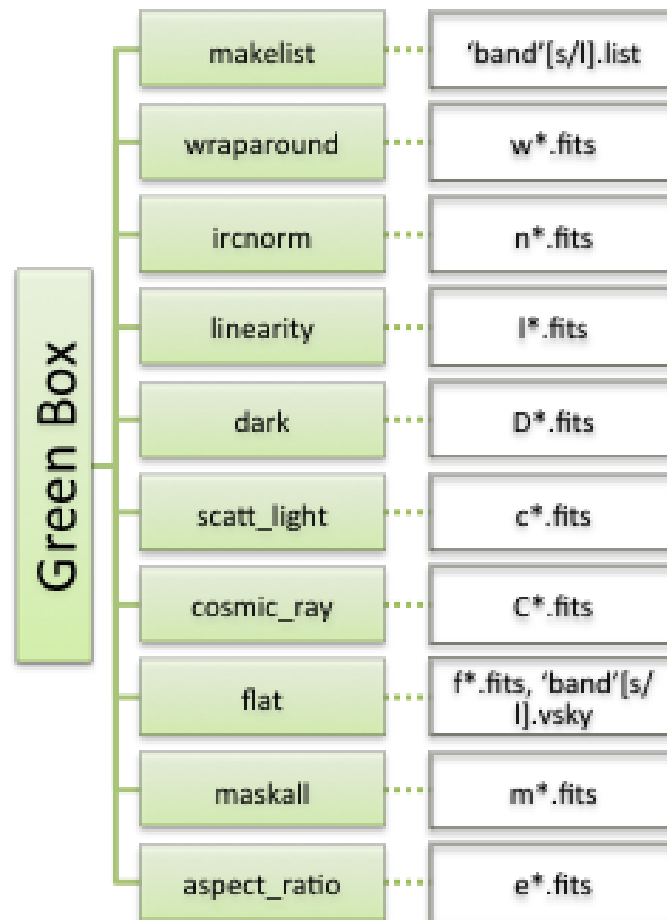


Figure 5.9.9: Present configuration of the Green Box. The white boxes connected with dotted lines indicate output files created by each module. Note that the last two modules (i.e., maskall and aspect\_ratio) are called by pipeline2, while the others are called by pipeline1.

Table 5.9.2: Prefixes added during Pipeline1 processing

prefix	module	action
w	greenbox.wraparound	Wraparound Correction
n	greenbox.ircnorm	Normalization
l	greenbox.linearity	Linearity Correction
D	greenbox.dark	Dark Subtraction
c	greenbox.scatt_light	Subtract Scattered Light Pattern
C	greenbox.cosmic_ray	Detect and Replace Cosmic Rays
f	greenbox.flat	Flat Fielding

### 1. Make Lists: (`greenbox.makelist`)

Relevant options: none.

This module creates a list for each band and each exposure. For example, the list for L15 long exposure frames is “L15l.list”.

### 2. Wraparound Correction: (`greenbox.wraparound`)

Relevant options: none. This should be applied to all the frames.

Due to data volume constraints the IRC compresses the data when it is transmitted to the ground by discarding the data sign bit. This will cause obvious ambiguities in the corresponding flux values. Since the IRC data structure uses the 2’s complement method to represent negative numbers, discarding the sign bit (most significant bit) will result in apparently extremely large positive numbers for negative values. Thus pixels suffering from this effect may appear as hot or dead in the image plane. However, these values are designed to be smaller than the saturation limit of the detectors, such that values higher than the maximum saturation levels must in fact be (*wrapped*) negative numbers. This correction is made by

$$A_{\text{corrected}} = A_{\text{uncorrected}} + 2^{16} \quad (5.9.1)$$

for any pixels that have a pixel value smaller than  $-11953$ .

After the wraparound processing is completed, a prefix `w` is added to the processed filename such that `F23342_S004.fits` becomes `wF23342_S004.fits`

### 3. Normalization: (`greenbox.ircnorm`)

Relevant options: none. This should be applied to all the frames.

To reduce the readout noise of the detectors the IRC data are read with the Fowler sampling method; non-destructively reading and summing the array multiple times (determined by the Fowler number) then dividing this resulting sum by the Fowler number. However, when the data are transmitted to the ground, for the purpose of data compression, the least significant bit is dropped. This normalization process accounts for this bit loss by correcting the data value by

$$A_{\text{corrected}} = \frac{A_{\text{uncorrected}} \times 2^{\text{bitshift}}}{\text{Fowler number}}, \quad (5.9.2)$$

where “bitshift” represents the number of bit shifts employed.

The normalization factor (i.e.  $2^{\text{bitshift}}/\text{Fowler number}$ ) is

- 4.0 for NIR short exposure frames with IRC05,
- 0.25 for NIR long exposure frames and MIR short exposure frames,
- 1.0 for the remaining (i.e. NIR short with AOT other than IRC05 and MIR long frames).

After the normalization process a prefix `n` is added such that `wF23342_S004.fits` becomes `nwF23342_S004.fits`

### 4. Linearity Correction: (`greenbox.linearity`)

Relevant options: none. This should be applied to all the frames.

The linearity correction is made as explained in §4.3. After the linearity correction, a prefix `l` is added such that `nwF23342_S004.fits` becomes `lnwF23342_S004.fits`.

## 5. Dark Subtraction: (greenbox.dark)

Relevant options: `darktype`, `darkfile`, `smdark`, `delsmd`

Choice of dark types are:

- **neighbor dark:** Neighbor dark frames for MIR-S and -L are stored in `dark/` directory in the distributed data package for each pointed observation. As described in §4.1.1, neighbor dark frames for each pointed observation are created by combining pre-dark frames of neighboring observations. This is the default for pipeline processing.
- **super dark:** Super dark frames are stored in `/where/you/installed/irc/lib/dark`. There are at least two known flaws in the current super dark.
  - (a) It does not correct for the increased dark signal due to the IRC all-sky survey observations in MIR-S/L. This effect corresponds to the belt-like pattern in the horizontal direction.
  - (b) It does not accommodate the increasing number of hot pixels.
- **self dark:**

In a pointed observation, dark frames are taken at the beginning (pre-dark) and the end of the operation for both the NIR and MIR channels. Those who want to use these pre-dark images in preference to the super-dark images should set `darktype="se"`. Then the pipeline processor will make dark images by averaging over the 3 images of MIR-S and MIR-L long exposure dark frames. Hereafter, we refer to these dark images as the selfdark image. However, the super-dark is still used for all short exposure frames and also the NIR long exposure frames even if `darktype="se"`.
- **user dark:**

If you have a dark frame more appropriate to your data set, you can use it by setting `darktype="us"`. In that case, dark frames should be in the working directory and listed in a file specified by the option `darkfile` in the same format as the “irc-const.database” file.
- **smdark:**

**For NIR long exposures, the dark level variation due to the passage of SAA region is well modeled by Tsumura and Wada (2011). Set `smdark=yes` to apply this model. This option supersedes the above selection of `darktype`, i.e. when `smdark=yes`, the model dark is *always* used for NIR long frames. If you want to inspect each created dark frame for each object frame, set `delsmd=no` to keep all the temporary files.**

Since wraparound, normalization, and linearity corrections were already performed to object frames, the same processes are applied to dark frames before subtraction.

Due to various reasons (the 1st frame effect, and so on), the dark level may vary during a pointed observation. We monitor the slit-area as a reference of the dark level, and adjust dark levels by adding/subtracting a constant to dark frames. The adjusted dark frame is then subtracted from each object frame to account for the changes in the dark level.

After the dark subtraction, a prefix D will be added such that `lnwF23342_S004.fits` becomes `DlnwF23342_S004.fits`. The FITS parameter “DRKTYPE” indicates which of above dark frames is used for dark subtraction and “DRKSHIFT” indicates the amount of adjustment in dark level described above.



## 6. Scattered Light Pattern Subtraction: (greenbox.scatt.light)

Relevant options: none. This should be applied to all the frames.

Due to the scattering of light from the edges of the detectors, lattice-shaped sky patterns are present in the imaging area. The patterns are especially prominent in the MIR-S images, and the intensity of the pattern is proportional to the sky background level. Therefore, the scattered light pattern has been modeled and template images for the three MIR-S filters are stored in `/where/you/installed/irc/lib/scatt`. Figure 4.2.4 in §4.2 shows the modeled scattered light template images. These template images are multiplied by the mode of the sky background level, which is then subtracted from each image to eliminate the pattern.

After the `scatt.light` process a prefix `c` will be added such that `DlnwF23342_S004.fits` becomes `cDlnwF23342_S004.fits`.

## 7. Cosmic Ray Rejection: (greenbox.cosmic\_ray)

Relevant options: `cosmicray`.

This module is to detect and replace cosmic rays in the MIR images, by using the IRAF task `cosmicrays`, which may not work properly with IRAF v2.15 and 2.16. Updating “`x_crutil.e`” in “`noao$bin.*`” may solve the problem. See README file of the IRC toolkit ver.20131202 for more detailed instruction.

After the cosmic ray rejection, a prefix `C` will be added such that `cDlnwF23342_S004.fits` becomes `CcDlnwF23342_S004.fits`.

## 8. Flat Fielding: (greenbox.flat)

Relevant options: `subsky`, `subLscat`.

The flat fielding is made using the imaging super flats, described in §4.2. A sensitivity variation within the detector array (i.e. true flat) and scatter pattern due to internal reflection in MIR-L are well separated by Arimatsu et al. (2011). If `subLscat=yes`, this artificial pattern is removed before flat fielding for MIR-L frames. Since this procedure includes the background sky subtraction, the sky level after this process should be around 0. If you do not prefer having negative values in the data sets, set `subsky=no`. Then an average sky level is calculated and added back to the processed frames. On the other hand, if you want to subtract sky backgrounds from NIR and MIR-S frames, set `subsky=yes`.

In any case, the variation of sky levels is calculated during this process. If this variation is large, an additional procedure (most probably the earth shine light correction) might be needed. In such a case, a message is shown in the terminal and frames before flat fielding are not deleted even if `deltemp=yes`.

Note that there was a noticeable pattern in the lower right corner of MIR-S flat images. A similar pattern also appeared in NIR flat images. However, these patterns suddenly disappeared on January 7th, 2007. In addition, the shape of the pattern has been found to change depending on the date (Murata et al., 2013). Thus, the pipeline now incorporates two sets of flat frames for each NIR filter and four for MIR-S (Figures 4.2.2 and 4.2.3).

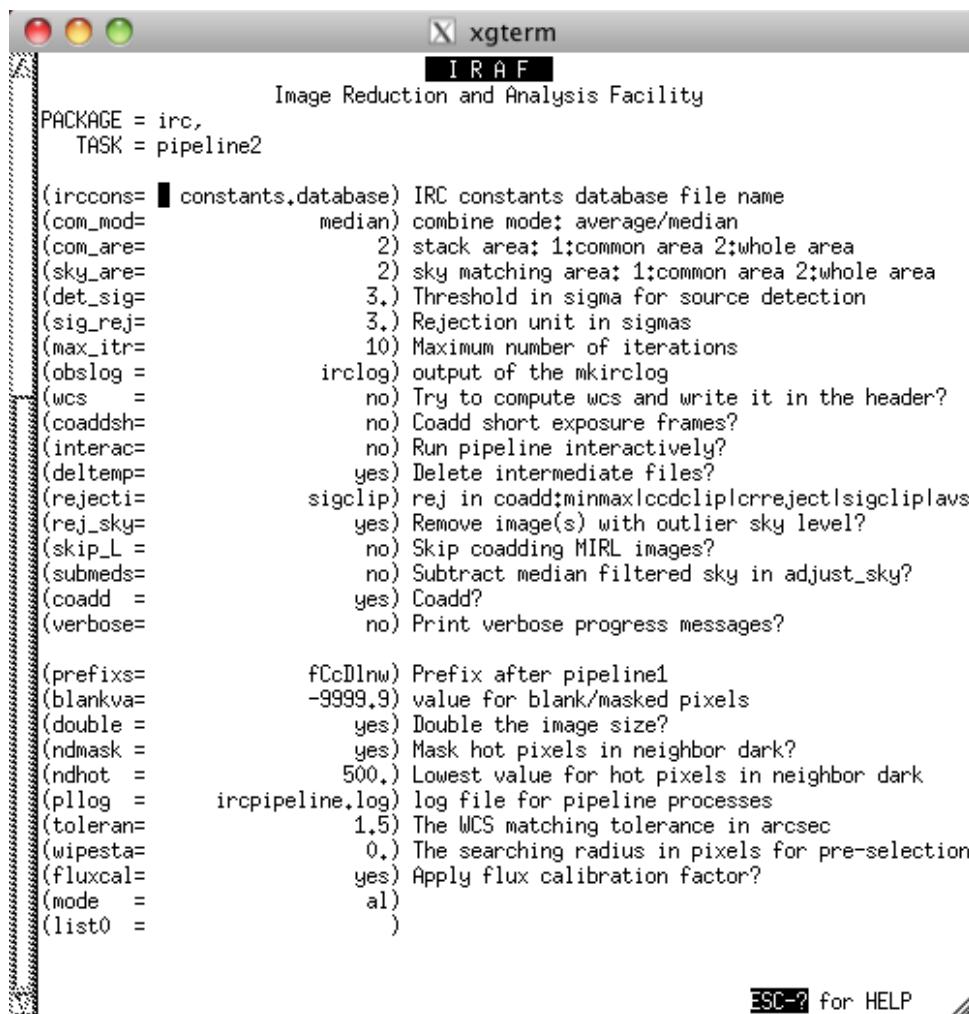
After the flat fielding process, a prefix `f` will be added such that `CcDlnwF23342_S004.fits` becomes `fCcDlnwF23342_S004.fits`.

At the end of pipeline1, fully calibrated frame files should have a prefix `fCcDlnw` to the original file name.

## 5.10 The pipeline2 processor (Green-Box & Blue-Box)

### 5.10.1 Parameter configuration

Before running the pipeline2, you can configure the parameters for the pipeline2 by typing “epar pipeline2”.



```

PACKAGE = irc,
TASK = pipeline2

(irconst= constants.database) IRC constants database file name
(com_mod= median) combine mode: average/median
(com_area= 2) stack area: 1;common area 2;whole area
(sky_area= 2) sky matching area: 1;common area 2;whole area
(det_sig= 3.) Threshold in sigma for source detection
(sig_rej= 3.) Rejection unit in sigmas
(max_itr= 10) Maximum number of iterations
(obslog = irclog) output of the mkirclog
(wcs = no) Try to compute wcs and write it in the header?
(coaddsh= no) Coadd short exposure frames?
(interac= no) Run pipeline interactively?
(deltmp= yes) Delete intermediate files?
(rejecti= sigclip) rej in coadd;minmax|ccdclip|crreject|sigclip|pavs
(rej_sky= yes) Remove image(s) with outlier sky level?
(skip_L = no) Skip coadding MIRA images?
(submeds= no) Subtract median filtered sky in adjust_sky?
(coadd = yes) Coadd?
(verbose= no) Print verbose progress messages?

(prefix= fCcdInw) Prefix after pipeline1
(blankva= -9999.9) value for blank/masked pixels
(double = yes) Double the image size?
(ndmask = yes) Mask hot pixels in neighbor dark?
(ndhot = 500.) Lowest value for hot pixels in neighbor dark
(pllog = ircpipeline.log) log file for pipeline processes
(toleran= 1.5) The WCS matching tolerance in arcsec
(wipesta= 0.) The searching radius in pixels for pre-selection
(fluxcal= yes) Apply flux calibration factor?
(mode = al)
(list0 = )

```

ESC-? for HELP

Figure 5.10.10: Screen for parameter configuration for pipeline2.

The parameters of pipeline2 are listed below. For more details, see §5.10.2.

- `irconst` (string, default=“constants.database”):  
**NEVER CHANGE THIS.** This is the irc constant file name.
- `com_mod` (string, average/median, default=“median”):  
Method of combining of frame images.
- `com_area` (int, 1 or 2, default=2):  
Coadded image area of stacked frames used for extraction (see Figure 5.10.11).

– **THIS PARAMETER IS NOT SUPPORTED YET, AND YOU WILL**

**GET THE WHOLE AREA IMAGE EVEN IF YOU CHOOSE 1 TO GET THE COMMON AREA.**

- 1: Only the common area (red region) is extracted.
  - 2: The whole area (areas within green dashed line) is extracted.
- sky\_area (int, 1 or 2, default=2):  
Area of sky to be used for statistics to adjust sky level before coadding frames.
    - 1: Only the common area is used.
    - 2: The whole area is used.
  - det\_sig (real, min=1.0, max=1000.0, default=4.0):  
Source detection threshold in sigmas.
  - sig\_rej (real, min=0.0, max=100.0, default=3.0):  
Rejection unit in sigmas.
  - max\_itr (int, min=1, max=10, default=10):  
Maximum number of iterations in statistical process.
  - obslog (string, default="irclog"):  
**NEVER CHANGE THIS.** Output filename of redbox.mkirclog.
  - wcs (boolean, yes or no, default=no):  
Try to match the 2MASS or **WISE** sources to calculate wcs? To use this function, you should have internet connection to automatically download the catalog. This process will not be executed as default. Note; although the toolkit was checked on Solaris machines also, **Solaris does not have curl in the original applications. You need to install it to run putwcs.**
  - coaddshort (boolean, yes or no, default=no):  
Coadd short exposure frames as well as long ones?
  - interactive (boolean, yes or no, default=no):  
Option to run the pipeline interactively
  - deltemp (boolean, yes or no, default=yes):  
Set to no if you do not want to delete any temporary created file.
  - rejection (string, none||minmax||ccdclip||crreject||sigclip||avsigclip||pclip, default=sigclip):  
Type of rejection operation performed in coadding.
    - none : No rejection
    - minmax : Reject the nlow and nhigh pixels
    - ccdclip : Reject pixels using CCD noise parameters
    - crreject : Reject only positive pixels using CCD noise parameters
    - sigclip : Reject pixels using a sigma clipping algorithm
    - avsigclip : Reject pixels using an averaged sigma clipping algorithm
    - pclip : Reject pixels using sigma based on percentiles

- **rej\_sky** (boolean, yes or no, default=yes):  
Activate if you want to reject any images which have outlier sky level from the coaddition process. Some frames may be taken during maneuver, and the pipeline will detect such frames by watching their sky level.
- **skip\_L** (boolean, yes or no, default=no):  
Activate if you want to skip the process of coadding MIR-L images. It will save you great time and you can use a tool to coadd the MIR-L images after the pipeline2 has finished.
- **submedsky** (boolean, yes or no, default=no):  
Activate if you want to make a median filtered sky image and subtract it from each image before coadding. This option is useful if you are interested in unresolved sources such as stars.
- **coadd** (boolean, yes or no, default=yes):  
De-activate if you do not want to try to coadd images. This option is useful for users who have their own coaddition strategy and software.
- **verbose** (boolean, yes or no, default=no):  
Activate if you want to print verbose progress messages.
- **prefixs** (string, default="fCcDlnw"):  
Prefix after pipeline1.
- **blankvalue** (real,  $\leq -1000.$ , default=-9999.9):  
Specify a value for blank/masked pixels.
- **double** (boolean, default=yes):  
Set to no for skipping subsampling. If yes, a single pixel is divided to  $2 \times 2$  pixels.
- **ndmask** (boolean, default=yes):  
Set to no for skipping mask hot pixels defined by neighbor dark frames.
- **ndhot** (real, default=500.):  
Definition of "hot pixels" in neighbor dark frames.
- **pllog** (string, default="ircpipeline.log"):  
A log file for pipeline processes. Recommended to leave as default.
- **tolerance** (real, default=1.5):  
Tolerance for the WCS fitting in the unit of arcsec.
- **wipestar** (real, default=0.0):  
The searching radius in pixels for pre-selection of sources in putwcs.
- **fluxcal** (boolean, default=yes):  
Set to no if you do not want to apply the flux calibration factor.

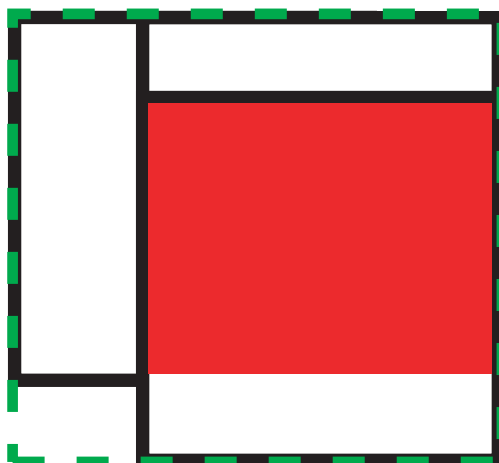


Figure 5.10.11: Area utilized for the Co-added images depends upon the parameter `com_area`. The 2 options are common area (red region) and whole area (within green dashed region).

Table 5.10.3: Prefixes added during Pipeline2 processing

prefix	module	action
m	greenbox.maskall	Mask
e	greenbox.aspect_ratio	Aspect Ratio Resampling
S	bluebox.source_extract	Pad blank around
R	blubox.calcshift	Shift & rotate
A	bluebox.adjust_sky	Adjust sky levels

## 5.10.2 Execution

Type `pipeline2` at the IRAF command prompt to start pipeline2 processing.

Each module is described below in the order of processing in the pipeline2 script. After each step of processes, a prefix is added to the original filename. The prefixes and corresponding modules are listed in Table 5.10.3.

### 1. Mask: (greenbox.maskall)

Relevant options: `blankvalue`, `ndmask`, `ndhot`

This module apply mask for:

- **anomalous pixels:**  
Bad or dead pixels were identified by using pre-flight laboratory data. Mask files are stored in `ircroot/lib/anomalous_pix` and shown in Figure 5.10.12.
- **hot pixels:**  
**If `ndmask=yes`, pixels above the level of `ndhot` in neighbor dark frames are defined as “hot pixels” and masked in the corresponding object frames. This is performed only for MIR-S and -L long exposure frames.**
- **saturated pixels:**  
Physical detector saturation occurs around 12500, 33000, and 33000 ADU (after `ircnorm`) for NIR, MIR-S, and MIR-L, respectively (§4.3). Therefore, any pixels with

values greater than the “scaled values” in the short exposure frame are picked out and the corresponding pixels in the long exposure frames will be masked. The “scaled values” in the exposure frames are calculated by

$$S_{\text{short exposure in ADU}} = S_{\text{physical saturation in ADU}} \times \frac{\text{Exposure Time}_{\text{short frame}}}{\text{Exposure Time}_{\text{long frame}}}. \quad (5.10.3)$$

This is done because the IRC uses Correlated Double Sampling and with the current IRC operating clock, we cannot determine which pixels are saturated by long exposure frames alone.

- **slit area:**  
The area defined as “slit area” is masked. The definition files are stored in **irc-root/lib/slit\_mask**.

For these pixels, the value is replaced by blankvalue.

After the masking, a prefix **m** will be added such that **fCcDlnwF23342\_S004.fits** becomes **mfCcDlnwF23342\_S004.fits**.



Figure 5.10.12: Mask files for NIR, MIR-S, and MIR-L (from left to right). Outlier pixels to be masked have a value of 0 (white) and others 1 (black).

## 2. Aspect Ratio Resampling: (**greenbox.aspect\_ratio**)

Relevant options: **double**. This should be applied to all the frames.

This is a distortion correction. The module corrects aspect ratios of pixels to be square, i.e. the aspect ratio is corrected to 1 to 1 by resampling the image. Thus the toolkit corrects the linear distortion only. Non-linear distortion is not corrected for at present since it is assumed to be negligible (§4.9).

**If double=yes, a single pixel is divided into  $2 \times 2$  pixels. This sub-pixel sampling is expected to increase the accuracy of relative shift calculation and WCS matching during the coadd process and to be suitable for applying the PSF correction described in Arimatsu et al. (2011).**

After the resampling, a prefix **e** will be added such that **mfCcDlnwF23342\_S004.fits** becomes **emfCcDlnwF23342\_S004.fits**.

## 3. Coadd: (**bluebox.coadd**)

Relevant options: many.

This is a wrapper module for coadding individual frames. Procedures in this module are described in §5.11 in detail.

#### 4. Flux Calibration: (bluebox.calflux)

Relevant options: fluxcal

This applies the flux calibration factors derived by Tanabé et al. (2008) to coadded images created by the coadd module. The unit of output images is  $\mu\text{Jy}/\text{pix}^1$ . Note that these factors are based on aperture photometry of point sources with radius of 10 and 7.5 pixels for NIR and MIR, respectively. For other aperture sizes, the aperture correction may be necessary. Separate calibration factors for extended sources are not currently available.

After the flux calibration, the file name will be changed such that from `NGC2403_S7_long.fits` to `NGC2403_S7_long.f.fits`.

---

<sup>1</sup>Conversion factors to MJy/sr ( $F/[\text{MJy}/\text{sr}] = a \times F/[\mu\text{Jy}/\text{pix}]$ ) are  $a = 8.1\text{e-}2$ ,  $3.1\text{e-}2$ , and  $3.0\text{e-}2$ , for NIR, MIR-S, and MIR-L, respectively in the case of `double=yes`.

## 5.11 The coadding processor (Blue-Box)

### 5.11.1 The Blue-Box Co-Add Wrapper

The green box produces the basic processed data for individual frames. Before stacking these frames, a relative shift and rotation due to

1. jitter – a slight positional movement resulted by pointing uncertainty
2. dither – an intentional positional offset in order to eliminate pixel oriented artifacts

need to be corrected. This positional matching and successive stacking are called coadding and carried out by the modules in the Blue-Box. Note that this process is performed automatically at the end of pipeline2 if `coadd=yes`.

In order to coadd frames, bright sources (stars) are extracted from each frame. The list of extracted sources is then used to calculate the shift and rotation for each frame looking at a particular field of view on the sky using the first frame as a reference.

The present configuration of the Blue-Box modules is shown in Figure 5.11.13.

The starting point for the Blue-Box Co-Add wrapper are the files created from the final step in the Green-Box Processor, i.e. `emfCcDlnwF23342_S004.fits`. The Co-Add wrapper (i.e. `bluebox.coadd`) then performs the following tasks:

1. **Extract bright reference sources: (`bluebox.source_extract`)**

Relevant options: `det_sig`, `sig_rej`

This module extracts individual bright sources from each frame. Before extraction, original images are pasted to larger images to prepare for the shift and rotation. **Note that the size of larger images has changed since ver. 140000. Previous sizes were  $1024 \times 1024$  and  $512 \times 512$  for NIR and MIR, respectively, while new images are created by adding 128 pixels to the all four sides.** These larger images are identified by an additional prefix S.

Then, bright sources (stars) are extracted from each frame. **The parameter `det_sig` defines the lower detection limit in sigma, while `sig_rej` is the rejection threshold in sigma when calculating image statistics. A text file with the extension of `.coo.1` containing the list of extracted sources is created for each frame.**

2. **Calculate Shift & Rotation to match frames: (`bluebox.calcshift`)**

Relevant options: `sig_rej`, `max_itr`

Lists of the bright reference star (`*.coo.1`) are used to calculate the relative shift and rotation values between individual image frames, by looking at a particular field of view on the sky using the first frame as a reference. **The parameters `sig_rej` and `max_itr` are used for this calculation. The file name, shift in x and y, rotation values, and the number of stars finally used for shift calculation are recorded in a log file (`*.shift`) for each band.** After this shift and rotation process, the original frame file names will receive an additional R prefix such that `SemfCcDlnwF23342_S004.fits` becomes `RSemfCcDlnwF23342_S004.fits`.

**If there are not enough stars for matching two frames, a warning messages is given and the corresponding file name will be added to a log file `coadd.failure`.** Another log file `calcshift.log` is also produced listing the number of matched stars and the fitting rms for x and y direction. Note that especially for the long wavelength



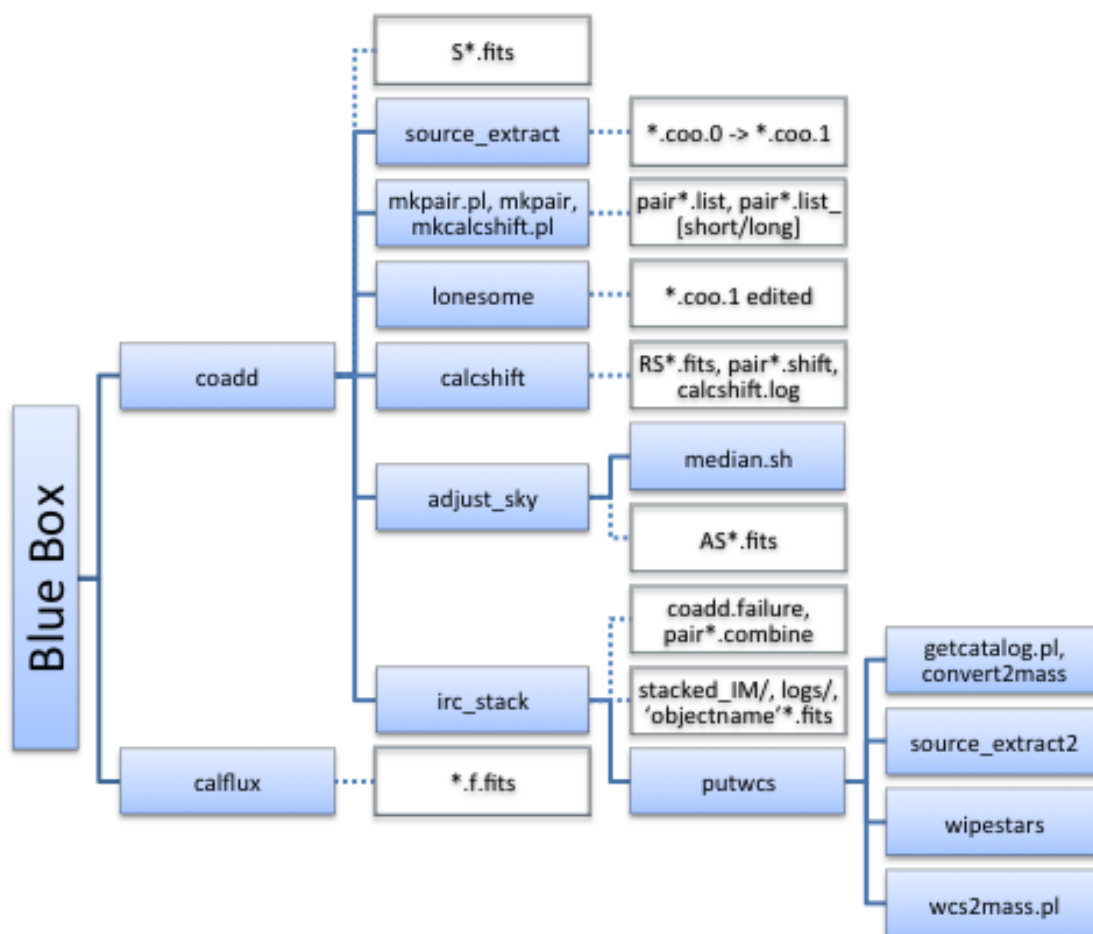


Figure 5.11.13: Present configuration of the Blue Box. The white boxes connected with dotted lines indicate output files created by each module.

channels (MIR-L) there may be occasions when there are not enough guide stars for matching. Alternative procedures which utilizes the MIR-S shift & rotation for the MIR-L channel (`coaddLusingS`) or cross correlation between frames (`coadd2`) are also provided in `IRC_TOOL` (See §5.13 for detail).

**In addition, results from statistics of shift and rotation values (§4.15) are used to exclude frames with wrong or doubtful shift values. When shift and rotation values derived by this module do not fall between pre-defined lower and upper limits, that frame will be excluded and will also be put into `coadd.failure`. Parameters needed for this procedure are stored in `lib/constants.database`.**

### 3. Adjust Sky Level: (`bluebox.adjust_sky`)

Relevant options: `submedsky`

The `bluebox.adjust_sky` module collects all frames looking at a given area on the sky and calculates the median sky from each image. Each calculated median value is then subtracted from each corresponding frame. From these median values an average sky brightness is calculated that is then re-added to all the frames. A log file is produced during this process with a name `skypair0002_N2.list.long` or similar. This file lists the frames looking at a given area on the sky with the corresponding mean, median and mode sky brightness and  $1\sigma$  standard deviation. Those who want to subtract median box car filtered image instead of adjusting sky level should configure the following parameters by typing “`epar adjust_sky`” **before running pipeline2**.

- `submedsky` (boolean, yes or no, default=no):  
Subtract median filtered sky?
- `rmmedsk` (boolean, yes or no, default=yes):  
Remove median filtered image? Those who want to check box car median filtered image, set this parameter no.
- `x_box`: (integer, min=1, max=100, default=21):  
x box car size
- `y_box`: (integer, min=1, max=100, default=21):  
y box car size

The parameters `x_box` and `y_box` change the size of the median kernel.

After adjusting the sky level, the `R` prefix is *replaced by* `A`, such that `RSemfCcDlnwF23342_S004.fits` becomes `ASemfCcDlnwF23342_S004.fits`.

### 4. Image Stacking (Co-adding): (`bluebox.irc_stack`)

Relevant options: `coadd`

Once object frames have been correctly matched and the sky brightness adjusted, they are stacked to produce the final co-added image. The FITS images and files created from the stacking process can be found in a new directory `stacked_IM`. The stacking process creates 3 files for any given filter position on the sky;

- A co-added image file (e.g. `1757132_N2.long.fits`).
- A noise map (e.g. `sigma1757132_N2.long.fits`)
- Summary File (e.g. `p11757132_N2.long.fits.pl`)

## 5. Update WCS: (`bluebox.putwcs`)

Relevant options: `wcs`, `tolerance`, `wipestars`

After the Co-add wrapper has been completed, this module updates WCS information to the stacked FITS images by matching with 2MASS or WISE catalog coordinates using the following procedures;

- (a) download 2MASS or WISE (**depending on the filter**) catalog for the observed area
- (b) convert the catalog RA DEC to the x'y' image coordinates
- (c) source extraction of stars from the IRC image (`source_extract2`)
- (d) **wipe stars if requested (i.e., if `wipestars` > 0)**
- (e) match the catalog x'y' coordinates with image xy coordinates

At this point there will be a list for extracted IRC stars corresponding to

```
star1 x1' y2' ra1 dec1 x1 y2
star2 x2' y3' ra2 dec2 x2 y2
.... .... ....
starN xN' yN' raN decN xN yN
```

for the matched stars. The module then calculates a transformation matrix (Nth-order polynomial) that will convert xy to RA and DEC. The module attempts to find the best fitting solution by increasing the order of polynomial from 2 to 4. Usually, the best result should be 2nd order, as long as the image has been corrected for distortion.

**The fitting results (arcsec/pix and position angle) are compared with expected values, and those significantly different from expectations are rejected. In addition, the results are rejected if the fitting rms is larger than the parameter tolerance. In such cases, the fitting will be performed again with fewer stars.**

- (f) (if matched) update the following keywords in the header
  - **WCSROOT:** AOCS/2MASS/WISE
  - **WCSNSTAR:** the number of stars used for WCS fitting
  - **WCSORDER:** the order of WCS fitting
  - **WCSERROR:** the rms of WCS fitting [arcsec]
  - **WIPERAD:** the radius for wipestars [pixel]

The final result is the basic science grade images (see Figure 5.11.14).

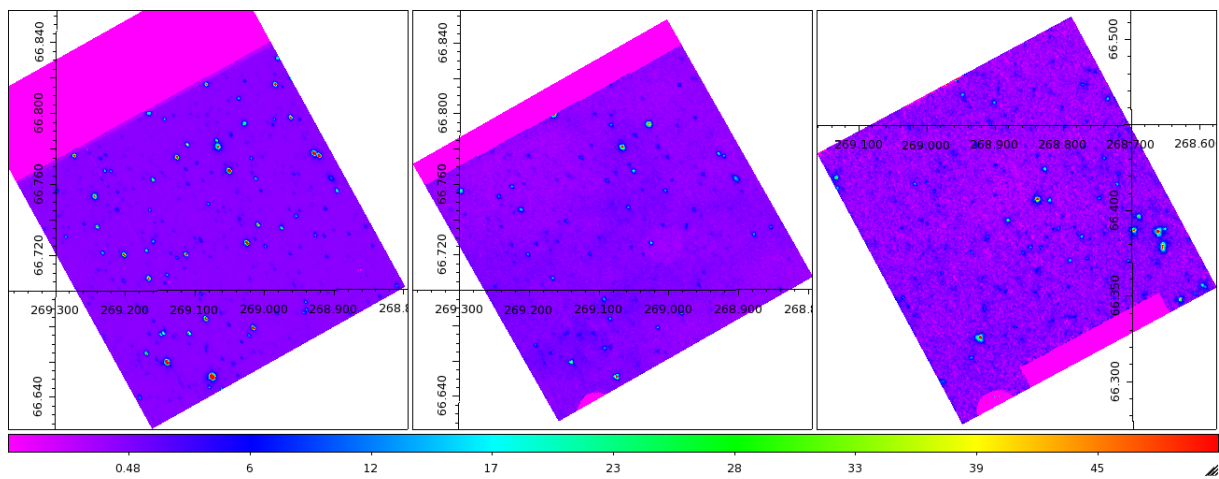


Figure 5.11.14: Example of final science grade data produced by the Green-Box and Blue-Box Co-Add Wrapper. Filters are N2, S9W, and L18W from left to right. Coordinates are in (R.A., Dec.) [J2000]. Pixel units are [ $\mu\text{Jy}/\text{pix}$ ].

## 5.12 Log files produced from the toolkit

Here we summarize various log files produced by the standard pipeline processing, i.e. prepipeline, pipeline1, and pipeline2, in the toolkit. Some of these log files are save in a directory logs.

### 5.12.1 prepipeline

During the process of prepipeline, following files are created. Detailed descriptions are in §5.8.

- **irclog**: list of all the sliced frames
- **darklist.before**: list of pre-dark frames
- **ircpipeline.log**: log for pipeline processes. will be used for pipeline1 & 2 as well.

### 5.12.2 pipeline1

- **bandname[l or s].list**: list of frames for each band and exposure
- **bandname[l or s].vsky**:  
This file is created by flat if the background levels vary significantly.

### 5.12.3 pipeline2

- **.coo**:  
The .coo files (e.g. SemfCcDlnwF23343\_N002.fits.coo.1) are the results for robust source extraction that extracts  $x$  and  $y$  coordinates & robust photometry. One .coo file is created for each individual exposure frame. These files can then be used to calculate the shift and rotation of frames that are being co-added by matching bright stars in the extracted source lists.
- **Pair Files**  
The *pair* files collect together and list all (long and short) frames that point the same area of sky.

Taking the N3 band as an example the following files may be seen,

```
pair0001_N3.list
pair0001_N3.list_short
pair0001_N3.list_long
pair0001_N3.list_long.shift
pair0001_N3.list_long.shift.0
pair0001_N3.list_long.combine
```

The pair0001\_N3.list file lists all (long and short) frames that point at the same area of sky. The contents of the file are the original frame names (e.g. F23343\_N001), IRC channel and the coordinates. The files pair0001\_N3.list\_short & pair0001\_N3.list\_long are extracted and segregated from F23343\_N001 on the basis of the exposure time (long or short exposure frames). The file pair0001\_N3.list\_long.shift lists the result of the coordinate matching before coadding. Each line entry in the file consists of a filename, x-shift (pix), y-shift (pix), rotation (deg) and the number of stars used for the shift & rotation angle calculation. For example;

```
SemfCcDlnwF003182658_N002.fits.coo.1 0.0 0.0 0.0 126
SemfCcDlnwF003182664_N002.fits.coo.1 -5.506 -4.934 -0.00017 51
```

The values are calculated relative to the first frame listed in the file, such that the first entry is always `filename 0.0 0.0 0.0 *`. **If the last column (i.e. the number of stars) is negative, it means that this frame is rejected by `bluebox.calcshift` because the number of stars is not enough or shift and/or rotation values are far from their mean. Such frames should also be listed in `coadd.failure`.**

- `exp.input` files

These files contain a list of all the pair files for all filters pointing at one position on the sky. There may be files for both the long `long_exp.input` and short `short_exp.input` exposure frames.

- Skypair Files

These log file can be found inside the separate directory `logs`. This log file is produced during the adjustment of the sky level between frames (`bluebox.adjust_sky`) with a name `skypair0002_N2.list_long` or similar. This file lists the frames looking at a given area on the sky with the corresponding mean, median and mode sky brightness and  $1\sigma$  standard deviation.

- `calcshift.log`:

This log file can be found inside the separate directory `logs`. The `calcshift.log` file is the log file for the calculation of shift and rotation in the `bluebox.calcshift` process. Relative to the first frame in the pair file described above the log file gives the number of stars matched between 2 `.coo` files and the corresponding  $x$  &  $y$  offset for these frames. The `calcshift.log` file will also record any matching failures.

- `coadd.failure`:

If the `coadd` wrapper fails to `coadd` one or more frames, this file is created containing the name of such frames.

### 5.13 The IRC TOOL (`irc_tool`)

Additional tools which may improve the pipeline results are stored here. The present configuration of the IRC TOOL is shown in Figure 5.13.15.

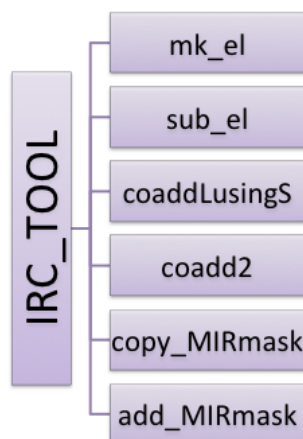


Figure 5.13.15: Present configuration of IRC TOOL.

- **Make a template for EL pattern: (`irc_tool.mk_el`)**  
 Using this module, a template for the EL pattern can be created. The input should be
  - `filelist` (string, no default): list of files before flat fielding
 and the output EL template is “filelist”.EL.fits. The input frames should be for the same filter and exposure, and should not contain extended sources. In addition, the observing dates and coordinates should be close to the target observations. For other parameters and outputs, see `irc/pkg/irc_tool/mk_el.cl`.
- **Subtract the EL pattern: (`irc_tool.sub_el`)**  
 This module fits and subtracts the EL pattern from object frames. The input parameters are
  - `filelist` (string, no default): list of files before flat fielding
  - `ELfits` (string, no default): EL pattern created by `mk_el`
  - `maskfits` (string, no default): mask file created by `mk_el`
 The EL pattern is fit and subtracted from files listed in “filelist” and then the flux calibration is applied. The prefix `f` is added to the output files so that they are consistent with other frames without EL subtraction and ready for pipeline2. For other parameters and outputs, see `irc/pkg/irc_tool/sub_el.cl`.
- **Coadd L frames using S shifts: (`irc_tool.coaddLusingS`)**  
 An alternative procedure which utilizes the MIR-S shift & rotation for the MIR-L channel. This function is especially useful when `bluebox.calcshift` fails to calculate the xy shift and rotation angle for the MIR-L channel, because there are few reference stars detected. The `coaddLusingS` has several parameters, but they are identical to those in `pipeline2`, except the `s_list`.

- `s_list` (string, default=`pair0005_S9W.list_long`):

The name of MIR-S pair list, for which the `calcshift` has successfully matched frames.

**Other parameters should basically be set to the same values as was in pipeline2. Given these parameters properly set, this procedure calls `bluebox.adjust_sky` and `bluebox.irc_stack` in order to coadd corresponding MIR-L images and move the stacked image to the `stacked_IM` directory. The header parameter `SHIFT-TYP` is set to be “`LusingS`” in order to indicate that the image is created by this module.**

**Note:** One needs to make sure that the correct corresponding MIR-S file is used with the desired MIR-L file. As an example:

In the `irclog`, the appropriate corresponding filter pair can be selected using the the same file number F40813. As raw data, all these files are packed into a single fits file. Pre-pipeline slices the MIR fits file into the 8 (4 MIR-S + 4 MIR-L) files.

```
F40813_L001 "NGC104" 256 L18W 5.293348 -72.44307 IRC03 1 5020012 1
F40813_L002 "NGC104" 256 L18W 5.293348 -72.44307 IRC03 2 5020012 1
F40813_L003 "NGC104" 256 L18W 5.293348 -72.44307 IRC03 3 5020012 1
F40813_L004 "NGC104" 256 L18W 5.293348 -72.44307 IRC03 4 5020012 1
F40813_S001 "NGC104" 256 S7 5.293348 -72.44307 IRC03 1 5020012 1
F40813_S002 "NGC104" 256 S7 5.293348 -72.44307 IRC03 2 5020012 1
F40813_S003 "NGC104" 256 S7 5.293348 -72.44307 IRC03 3 5020012 1
F40813_S004 "NGC104" 256 S7 5.293348 -72.44307 IRC03 4 5020012 1
```

In this case, using “`pair0002_S7.list_long`” for the reference, the `coaddLusingS` function will make the `L18W_long` image.

Please note that running this function will overwrite **relevant files previously created by `coadd`** (e.g. `[R/A]*L*.fits`, `coadd.failure`, `stacked_IM/*L.fits`). If you want to keep the previous results, rename these files or copy the current working directory. In addition to these files, this module creates several list files with the names of `*_forL*`. In the case of above example, “`pair0002_S7.list_long_forL`”, “`pair0002_S7.list_long_forL.shift`” “`pair0002_S7.list_long_forL.combine`”. They are basically the same as the usual `coadd` results except that the contents are for the MIR-L (L18W in this case) frames.

Also note that this function does not apply the flux calibration factor to the output image. If needed, `bluebox.calflux` should be applied separately. See §5.10.2 step 4 for detail and consult `ircpipeline.log` for parameters used in `pipeline2`.

- **Coadd using `xregister`: (`irc_tool.coadd2`)**

This module calculates the cross correlation between two frames by shifting in `x` and `y` directions and find the best-fit values where the cross correlation is the largest. As a consequence, a rotation between the frames is not supported. The input parameters are

- `inputlist` (string, no default): list of files to be coadded
- `prefixs` (string, default=`“emfCcDlnw”`):



- `adj_sky` (boolean, default=yes): adjust sky before stacking?
- `double` (boolean, default=no): set yes for double-sized frames

Note that the prefixes will be added to filename listed in `inputlist`.

A stacked image is moved to `stacked_IM` and the naming rule is the same as standard `coadd`. The header parameter `SHIFTTYP` is “xregister” after this process, since it uses the IRAF task `xregister`.

- Copy mask of MIR-S or -L frames: (`irc_tool.copy_MIRmask`)  
This module copies the masked area of MIR-S or -L frames to `MIR[S/L]mask.fits`. The input parameter is
  - `channel` (string, no default): specify ‘S’ or ‘L’

As is obvious, `prepipeline`, `pipeline1`, and `maskall` in `pipeline2` should be run before running this module.

- Add mask to MIR-S or -L frames: (`irc_tool.add_MIRmask`)  
This module adds the mask created by `copy_MIRmask` to MIR-S or -L frames, which suffer from the memory effect. Since the masked area is mostly from the saturated pixels and the saturation level is lower than the memory effect threshold, this module may “over-mask” the affected pixels. The input parameter is
  - `channel` (string, no default): specify ‘S’ or ‘L’

Note that this module is designed to add the mask to the output of `maskall` in `pipeline2` (i.e. `m*F*.fits`). In addition, the mask file `MIR[S/L]mask.fits` should be in the current working directory. While running this module, the original files are renamed to `mm*F*.fits` and new `m*F*.fits` files with the additional mask are created so that they can be used in `pipeline2`.

After running this module, run `pipeline2` in the interactive mode to skip `maskall` with specifying the prefix after `maskall`. For example,

```
irc_tool> prepipeline
irc_tool> pipeline1
irc_tool> maskall (leave all the parameters as default)
irc_tool> ! cp somewhere/MIRSmask.fits ./
irc_tool> add_MIRmask S
irc_tool> pipeline2 deltemp- interac+ prefix='mfCcDlnw' (skip maskall)
```

## 5.14 Limitations of the functionalities in the current version of the imaging toolkit

- **First frame effect:** The first frame of the dark current prior to the pointing observation shows larger values than others, particularly for MIR-S and MIR-L detectors. This effect could be related to the detector temperature.
- **Dark current variation:** As described in §4.1, the increase of hot pixels, the variation of NIR dark current due to the SAA passage, and level shift during a pointing should be calibrated well by the latest toolkit.
- **Memory effects:** A decrease in the sensitivity has been found in MIR images, if a bright source is in the field of view of a previous pointing. More detailed information is given in §4.10. To mask the affected pixels, use [copy/add]\_MIRmask modules in IRC\_TOOL (§5.13). A list of ObsIDs which may cause the memory effect is in the README file for each pointed observation.
- **Effects of high energy particle hits:** The toolkit does not perform any deglitching. Glitches should disappear when coadding individual images (median filter). Even so, their effect on the responsivity are not yet well investigated. Future versions of the toolkit will involve a more careful treatment of cosmic ray hits.
- **Ghosts:** See §4.13 for a detailed description of the ghosts.

The maskall called by pipeline2 prints a warning message if pixel(s) exceeding a limit (currently 10000 ADU) are found in MIR-S long exposure frames.

- **Earthshine in imaging observations:** Data taken in May, June and July may suffer from the Earthshine problem as described in §4.14. The following recipe can be used:
  - **If the number of frames is large enough,**
    - \* Check the drift of the background level during a pointing listed in \*.vsky and comment out any high background MIR-L frames from “irclog” and run the pipeline again. If the CoaddLusingS tool is used, the frames with the same frame number must be also commented out, i.e., if F0000001\_L002 is commented out, F0000001\_S002 must be also commented out.
    - \* Use rej\_sky=yes option in order to ignore the bad frames:
 

```
irc,> pipeline2 rej_sky=yes
```
  - **If the target is a point source,**
    - \* Use submedsky option to remove the diffuse background:
 

```
irc,> pipeline2 submedsky=yes
```
    - \* Adjust the median kernel size in the submedsky option:
 

```
bluebox> epar adjust_sky
```

 (x.box = 20) If submedsky=yes, x box car size  
 (y.box = 20) If submedsky=yes, y box car size
  - **Else,**
    1. Make a template of EL using make\_e1 and data from adjacent pointings
    2. Subtract the template from object frames using sub\_e1

These modules are in `IRC_TOOL` (§5.13).

- **Problem with short exposure frames with IRC:** A problem exists with the contiguous short-exposure frames of the MIR-S and MIR-L data taken in IRC00, IRC04, and IRC05. At present the cause is uncertain, however, it is advised not to use short-exposure frame data for scientific purpose. They may be used to check the saturation in long-exposure frame data. Specifically, the IRC MIR pointing is composed of several exposure cycles, filter changes and dithers. Each exposure cycle is made up of 1 short and 3 long frames. For AOT IRC02, IRC03, exposures are always separated by dithers etc., and the problem does not arise, however, for IRC05, IRC00, IRC04 they are not necessarily separated. The problem is occurring on contiguous exposure cycles (i.e. nothing in between). For example;

```
(short1,long1,long1,long1)(short2,long2,long2,long2)
```

The bad frames are the short2 frames, i.e. those following a previous contiguous exposure cycle. This effect extends to the short frame of the final dark even. This problem may be critical for spectroscopy of bright sources with IRC04, however, for IRC00 & IRC05 users, the effect may not prove critical since users may disregard the short frame since these AOTs are intended for deep imaging. **The processing of short frames can be disabled by commenting out in “irclog” or by pipeline2 coaddshort=no (default).**

- **PSF:** As described in §4.4, the extended shape of PSF, which depends on the filter, makes the comparison of images with different filters difficult.
- **Temporal variation of NIR and MIR-S flat:** As already described in §4.2, the flat for NIR and MIR-S changed on January 7th, 2007. A noticeable pattern (so-called “soramame”) in the bottom right corner of the MIR-S field disappeared on this date. Recently, Murata et al. (2013) found that the “soramame” pattern was not stable, i.e., its shape and position changed with time.

However, the current toolkit cannot provide flatfield frames for each pointed observation due to lack of S/N. Instead, it includes one and four “soramame” patterns for each of NIR and MIR-S filters, respectively.

- **Coadd frames from multiple pointed observations:** In principle, the IRC toolkit will attempt to process all the frames in the working directory. However, please note that under certain circumstances dark and flat calibrations should be done for each pointed observation due to their variation. (If using superdark, dark subtraction is not a problem. If observation dates are after January 7th, 2007, the flat variation should be negligible.)

As a consequence, we recommend to run prepipeline and pipeline1 for each pointed observation and then to run pipeline2 for coadding frames from multiple pointed observations. However, coaddLusingS may not work properly for such data sets.

## 5.15 Error messages when running the pipeline and Troubleshooting

Please note that the error messages shown in this section may be obsolete and will not appear with the latest (ver. 140003 or later) toolkit.

1. The pre-pipeline stage sometimes give an error message such as `ls: ../rawdata: No such file or directory` or `cat: slice_tmp0: No such file or directory`, etc, although the pre-pipeline seems to run correctly. Typing `unlearn_all` should clear these error messages.

2. The distortion processing (green box processing) can give the following error message, causing the pipeline crash:

```
### DISTORTION ###
Making the input file list...
Correcting distortion...
#This may take a while...
ERROR on line 56: Cannot open file
(~/iraf/irc/lib/distortion/DARK_distortion_database.dat)
distortion (ircconst=constants.database, logfile=irclog, prefixs=mslnDwa,
verbose=no)pipeline ()
This is because the DARK entries should be removed from the irc log file.
```

3. The coadd stage can result in the following error:

```
### COADD ###
Making the input file list...
Extracting sources...
Calculating XY shift...
Adjusting sky level...
Coadding images...
ERROR on line 148: parameter 'direction' not found
This problem may be caused when using versions of IRAF earlier than IRAF 2.12.2. The
problem is with geoxytran task. epar images.immatch.geoxytran can be typed in the
IRAF shell to see if the parameter exists. Even after installing the newer version of IRAF
it is necessary to type unlearn geoxytran before the toolkit runs correctly.
```

4. The pre-pipeline run can apparently miss some perl scripts and end with an empty or non existing *irclog* file.

```
### MKIRCLOG ###
Making the file list...
Reading header...
#This may take a while...
tcsh: ~/iraf/irc/perl/formatlog.pl: Command not found.
tcsh: ~/iraf/irc/perl/checkname.pl: Command not found.
### MKIRCLOG finished!! ###
```

Primarily, it has to be checked that the toolkit is being run from the working directory and not, for example in `~/iraf/`. If the problem persists then it may be because *perl* is in the wrong place! *Perl* should be in `usr/local/bin/perl`, therefore a symbolic link should be set up from the perl library to `usr/local/bin/perl` (type *which perl* to find out where *perl* is currently hiding).

5. If a new version of the toolkit crashes, as a first fix, `unlearn_all` should be typed within `irc`.
6. The IRC toolkit does not run on the new Intel Mac machines, due to differences in the IRAF build in the intel binaries. Replacing the intel binaries with the original binaries causes `iraf` to run under emulation but solves the problem. IRAF 2.13 has been successfully running on the intel machines.
7. The `coaddition` process or the `coaddLusingS` function, can cause the crash of the toolkit with the error:  
`ERROR on line 128: Attempt to access undefined local variable 'filter'.`  
This error will occur if the pre-pipeline is attempted to run twice on a given data set. As a check the files (and their counterpart corresponding MIR-L images) listed in the pair file (e.g. `pair0001_S7.list_long`) should be examined to see if they have the appropriate "FILTER" keywords in their header.
8. The "Matching failed" error message that could appear in the `putwcs` process is not an intrinsic pipeline error. It is due to the fact that the 2MASS data format changes from time to time. Appropriate updates or patches are made to the pipeline. The updates will be recorded in the Observer's page.

## 5.16 Toolkit structure

The structure of the IRC imaging toolkit for Phase 1&2 (ver. 140003 or later) is shown in Figure 5.16.16.

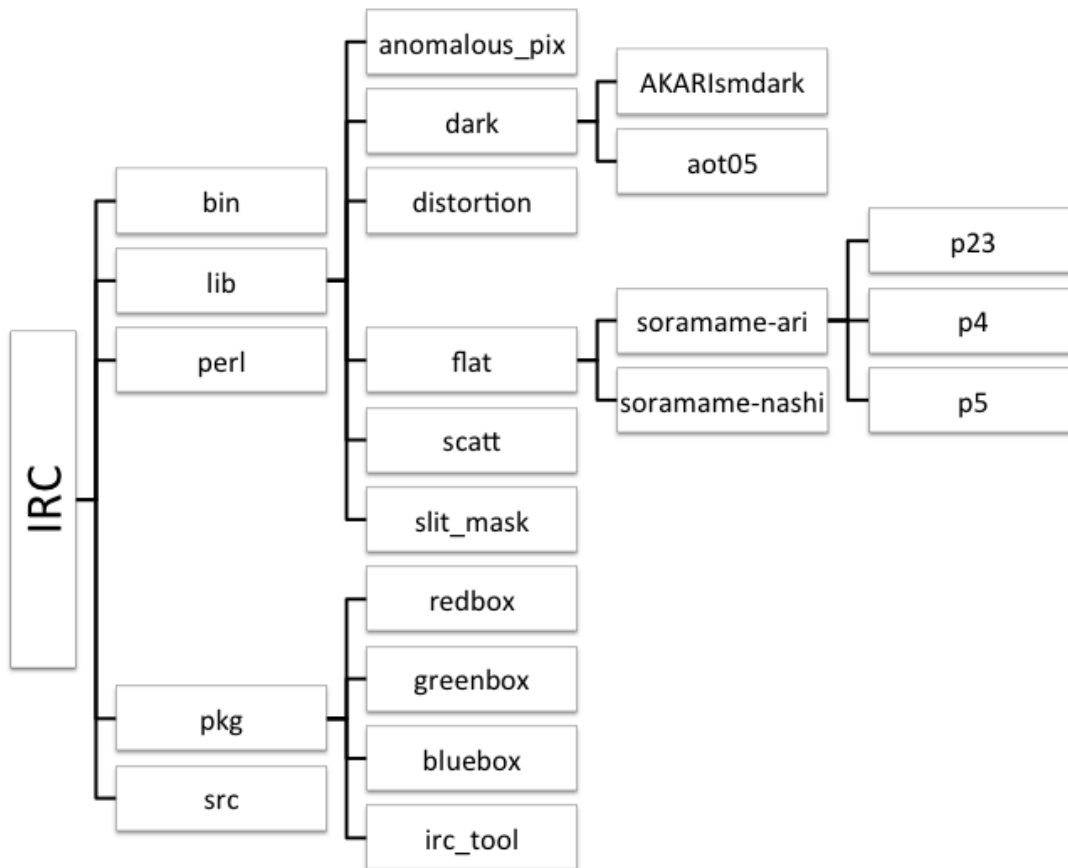


Figure 5.16.16: The configuration of the IRC imaging toolkit for Phase 1&2 (ver. 140003 or later).

# Bibliography

- K. Arimatsu, T. Onaka, I. Sakon, S. Oyabu, Y. Ita, T. Tanabé, D. Kato, F. Egusa, T. Wada, and H. Matsuhara. Characterization and Improvement of the Image Quality of the Data Taken with the Infrared Camera (IRC) Mid-Infrared Channels on Board AKARI. *PASP*, 123: 981–995, August 2011. doi: 10.1086/661201.
- F. Egusa, T. Wada, I. Sakon, T. Onaka, K. Arimatsu, and H. Matsuhara. Interstellar Dust Properties of M51 from AKARI Mid-infrared Images. *ApJ*, 778:1, November 2013. doi: 10.1088/0004-637X/778/1/1.
- K. Murata, H. Matsuhara, T. Wada, K. Arimatsu, N. Oi, T. Takagi, S. Oyabu, T. Goto, Y. Ohyama, M. Malkan, C. Pearson, K. Malek, and A. Solarz. AKARI North Ecliptic Pole Deep Survey. Revision of the catalogue via a new image analysis. *A&A*, 559:A132, November 2013. doi: 10.1051/0004-6361/201321505.
- T. Tanabé, I. Sakon, M. Cohen, T. Wada, Y. Ita, Y. Ohyama, S. Oyabu, K. Uemizu, T. Takagi, D. Ishihara, W. Kim, M. Ueno, H. Matsuhara, and T. Onaka. Absolute Photometric Calibration of the Infrared Camera (IRC) aboard AKARI. *PASJ*, 60:375–388, December 2008.
- K. Tsumura and T. Wada. A New Method of Dark-Current Estimation for Diffuse Sky Measurements with the AKARI Infrared Camera. *PASJ*, 63:755–762, August 2011.

## Chapter 6

# Spectroscopy pipeline cookbook

The spectroscopy pipeline is being developed and maintained by the IRC spectroscopy data reduction team. It is mostly written in IDL, and uses the IDL ASTRO library (maintained at the GSFC) among others. Although it is developed under Linux environment, it may be portable to other platforms after some modifications (though we have no plan to increase the exportable platforms by ourselves). The toolkit also uses the `ds9` FITS viewer, and the `xpa` package for communication between the `ds9` and the IDL main program.

The spectroscopy data reduction requires a calibration database (FITS images and ascii tables) distributed and updated by the IRC spectroscopy data reduction team. The database is based on observations of calibration objects and calibration frames taken during PV/DT phase observations, as well as pre-launch calibration experiments in our laboratory. Therefore observers do not have to make their own calibration observations.

### 6.1 General overview of the pipeline processing

The main pipeline processing consists of several well defined steps, which are explained in the following sections.

In general terms, the IRC slitless spectroscopy differs from more standard slit spectroscopy in that in the latter case, the pixel position and the wavelength are closely correlated. The IRC spectroscopy does not follow this relation and needs to be applied in three steps:

- Many spectroscopic flats have been combined to form a "super-flat" which can be used to remove the pixel to pixel variation of the monochromatic response of the detector.
- After subtracting the background, extracting the sources and performing the wavelength calibration, the wavelength flat can be used. The wavelength dependency of the flats is due to the same mechanism to that of imaging mode, and is corrected by interpolating/extrapolating the imaging super-flat taken with two different filters for every pixel and the wavelength (colour correction).
- Finally, the spectral response specific to the spectroscopic mode observation is corrected by the spectral response function obtained from the observations of standard stars. More detailed explanations can be found in following subsections.



### 6.1.1 Dark subtraction

Scaled super-dark images are subtracted from the raw data. For the scaling, dark count offset is calculated within the pipeline, by comparing average counts at the slit-mask-covered portion of the pre-dark image, and the corresponding area on the super-dark image.

Additionally the average dark counts of the mask-covered portion of each observed sub-frame is measured, except for LG2 for which there is no good dark area on the spectroscopy images for measuring the dark level. The averaged offset is added to (or subtracted from) the super-dark to make the scaled super-dark.

### 6.1.2 Linearity correction/Saturation Masking

Linearity correction is made following the method adopted for imaging data reduction.

The saturation masking is also performed as in the imaging pipeline: the toolkit first checks the short-exposure images, and find regions where expected counts in longer-exposure frame exceeds the saturation limit based on the exposure time ratio of short-/long-exposure frames (see table 4.6.5). Then, the regions are masked in the longer-exposure frames. The user should check the masking in the edges of the saturated regions, due to the drift between short and long exposures pointing.

### 6.1.3 (monochromatic) Flat-fielding

In the case of the slit-less spectroscopy, the entire FOV is the aperture for the background sky, but the object image itself is the aperture for the object. This aperture size difference makes difficulties in flat-fielding the slit-less spectroscopy images since, unlike a conventional long-slit spectrograph, a given pixel can be illuminated by background photons with a range of wavelengths within the disperser's passband, and the mixing fraction of photons of different wavelengths depending on the spatial distributions and spectra of sources. We need 3D flat information (X, Y along space, plus Z along the wavelength) for full flat calibration. However it is impossible to obtain such a detailed flat since there are no good monochromatic flat light nor a series of narrow-band filters covering the passband of the disperser. Because of these difficulties, we will make a flat calibration in two steps, starting with the monochromatic correction.

To correct for the pixel-to-pixel variation of the monochromatic response (response or flat that does not depend on wavelength), the whole image is divided by the 'super-flat'. The super-flats are made by combining a larger number of background spectroscopy images. Note that the background sky image is not flat along Y or the wavelength axis, i.e., there are several spectral features on the 'super-flats' due to, e.g., contributions of zero-th or higher-order light in cases of grism spectroscopy images. Although the features should be removed to correct for the pixel-to-pixel variation of the response, we first divide the dark-subtracted images by the super-flat with the spectral features. As shown below in equation 6.1.1, this process makes the background flat, facilitating the sky subtraction.

Assume that the dark-subtracted images are represented by the following equation:

$$obs = sky \times F_1(x, y) \times spectral\_feature(x, y) + obj(\lambda) \times F_2(x, y, \lambda) \times R(\lambda) \quad (6.1.1)$$

where  $F_1(x, y)$  is the flat in which the background spectral features are not present,  $F_1(x, y) \times spectral\_feature(x, y)$  is the 'super-flat',  $F_2(x, y, \lambda)$  is the wavelength-sensitive flat (see below for color-term correction), and  $R(\lambda)$  is the spectral response. Since the super-flat is only a function of the position in the detector, this step is called monochromatic flat-fielding. If we divide the observation by the 'super-flat', we obtain:

$$obs' = sky + obj(\lambda) \times F_2(x, y, \lambda) \times R(\lambda) / [F_1(x, y) \times spectral\_feature(x, y)] \quad (6.1.2)$$

#### 6.1.4 Background subtraction (from individual sub-frames)

After monochromatic flat-fielding, the background should be flat over the aperture. However, in real data, this is not occurring in most of the cases. For NP, NG, and SG1, outlier-tolerant low-order polynomial surface fitting is performed for each sub-frame, and is subtracted off from the flat-fielded images. For SG2 and LG2, background suffers from straylight (from the Earthshine) contamination, and the flat-fielded images are much more structured. To make good sky subtraction, a median running-box filter is applied to estimate the local sky, and is subtracted off from the 'stray light-covered' background. Such background should be removed from individual sub-frames, since the contribution of the Earthshine depends on the telescope pointing angle from the earth direction, and the amount of straylight changes within a single pointing maneuver (or within a single AOT operation).

In the first pass of the processing within the pipeline, source masking will not be applied in determining the background, because no source position information is available at the stage. In the second pass, after processing through section 6.1.9 once, the background is measured again while considering the source masks.

The image obtained after background subtraction has the following expression:

$$obs'' = obj(\lambda) \times F_2(x, y, \lambda) \times R(\lambda) / [F_1(x, y) \times spectral\_feature(x, y)] \quad (6.1.3)$$

#### 6.1.5 Image screening

Some sub-frames may be severely damaged by cosmic-ray shower, a satellite passing in front of the telescope, etc. If this is the case, one can interactively set the flag, by using `ds9`, for any sub-frames to be discarded in the following processes.

#### 6.1.6 Image registration (among sub-frames)

Relative image shift due to satellite attitude drift among spectroscopy sub-frames is measured by means of cross-correlation technique. This can be made only with NP and NG due to the number of spectra present in NIR images. For SG1, SG2, and LG2, pixel offsets measured with NP/NG are used for matching, rather than measuring their own shifts, since all cameras take images simultaneously.

Similar shift-and-add technique is also needed for the reference sub-frames, except for N3, where there is only a single reference sub-frame. To find the shift values for L18W, we first detect point sources in S9W, measure their positions, and calculate the shift by using the list of target coordinates, and shift both S9W and L18W images.

#### 6.1.7 Imaging stacking

After registering all the sub-frames, all the selected (screened) sub-frames are combined to make higher S/N stacked images. For spectroscopy images, a three-sigma clipping averaging method is used. For reference images, a simple median averaging is used due to the small number of sub-frames.

Some sub-frames are removed due to satellite maneuver. When the toolkit recognizes that the last exposure frame (cycle) was taken during this maneuvering period, the frame is automatically

removed from the stacking list. Note that, although the observing manual says that 8 sub-frames will be taken for spectroscopy in AOT04 operation, it turned out that one additional frame (9th frame) can often be taken without suffering from satellite maneuvering. You may add the frame for stacking.

### 6.1.8 Target detection/position measurement

Target positions can be provided by the user in the form of a source table (see below), or automatically computed within the toolkit, using the `daofind` method for target detection. Even if the target positions are set by users, the toolkit performs re-centering of the source positions by means of Gaussian peak search. (This functionality can be disabled with the command line option.) This process is coupled with the following step (background subtraction).

### 6.1.9 Background subtraction (from stacked image)

Although background subtraction has been already applied before stacking images, any remaining background is removed at this step.

The background subtraction and target detection/position measurement (explained in the previous section) are made iteratively in the following way. First, the target is tentatively detected by the automatic source detection program (not based on the user-supplied source table), and source masks will be created for all detectable sources. Then the background is measured while considering the source masks, and is subtracted off from the original stacked image. The background-subtracted image is used for better source detection/position measurement, and better source masks will be created for better background subtraction.

When sources are detected, source masks are created for better background subtraction from individual sub-frames (section 6.1.4) in the second pass of the pipeline processing.

### 6.1.10 Extracting 2D spectra

By using the reference image positions and pre-defined coordinates offsets in the calibration database, rectangle areas around the source spectra are extracted on the spectroscopy images. For NP, spectral distortion (see below) is taken into account along the dispersion direction to find best Y offset when extracting 2D spectra.

#### **X-offset adjustment in spectroscopy image extraction**

In real data, one need to further adjust the offset of the source extraction boxes. One may sometimes find 2D spectra slightly away from the expected position (at the center of the extraction box) along X axis. This kind of shift cannot be corrected in the previous image registration processes, and the correction is made at this stage. The center position of the 2D spectra is measured for each extracted 2D spectra, and the mean X offset from the center of the extraction box is calculated. If the pipeline successfully finds the shift value, the shift will be applied in extracting the 2D spectra. However, for some cases where only very faint objects were detected, calculating this additional shift may fail (and no further shift is applied).

Measuring the X offset and making good source masks (as explained in the previous section) are closely related to each other during the pipeline processing. In the first pass of the source detection, the automatic source detection sub-program works even if the target table is supplied in the pipeline command line. The X offset is measured with the tentatively detected sources at this stage. In the second pass, measured X offset (as well as Y offset found in adjusting

the wavelength zero reference point; see the next section) between spectroscopy and reference images is taken into account in extracting the 2D spectra. Only the sources specified in the source table, or sources detected with the sub-program, will be processed (extracted) in the second pass. This two-stage process ensures good source masking for better sky subtraction and good offset measurement with brighter and larger number of sources, even for the cases in which the observer is only interested in small number of faint sources.

Measurement of the center position of the 2D spectra can be made easily for NP, NG, and SG1 spectra for which larger number of brighter sources can be detected even in blank sky regions. Therefore, the toolkit measures the X offset at NP and NG for correcting both NP and NG, and at SG1 for correcting SG1, SG2, and LG2. Therefore, the user must start pipeline processing for NP/NG first, then SG1, and finally SG2 and LG2. See section 6.4.1 for more explanations.

### 6.1.11 Wavelength calibration

In the case of grism spectra, the dispersion equation is almost linear theoretically and a linear equation for expressing the wavelength is assumed. Therefore, once the 2D spectra extraction is made with sufficient accuracy, it is straightforward to make a wavelength calibration.

For prism (NP) spectra, since the dispersion equation is highly non-linear one especially at shorter wavelength end, it is better not to transform images to avoid introducing extra uncertainties in the image interpolating/extrapolating processes. Rather, a separate array (whose length is equal to the Y length of the extracted 2D spectra) will be created to store the wavelength values for each Y pixel. One wavelength array is applicable for all the extracted spectra within the FOV. This kind of wavelength array is also used for grism spectra (NG/SG1/SG2/LG2).

### Finding wavelength zero reference point

Some problems arise for accurate wavelength determination. One is the satellite attitude stability problem. If the satellite pointing moves between reference and spectroscopy images, the reference image does not provide good wavelength zero reference point any more.

The NP spectrum (before flux calibration) shows a notable peak around  $2.4 \mu\text{m}$ , and there are lots of fairly bright stars with almost identical spectra, regardless of the type of stars within a single FOV. Therefore it is possible to find the best offset of the wavelength zero reference point, by measuring the NP peak positions with respect to the spectral template that was taken when the satellite attitude stability was good enough, by averaging the offsets measured for many stars. Once the offset is measured, extraction of the 2D spectra is made again, after considering the Y offset (as well as X offset as explained earlier).

The zero reference point is much difficult to be found in NG spectra, due to lack of notable spectral features before applying the flux calibration. Therefore, although the toolkit can estimate the reference point by examining the observed spectroscopy images, it is strongly recommended to check the zero-th order light images for more accurate wavelength calibration.

The chance of detecting zero-th order light image at significant level for SG1, SG2, and LG2 is not so large. Therefore the drift of the wavelength zero reference point is calculated by using the drift measured in NP or NG for MIR-S/L grisms, after correcting the pixel scale difference.

Another issue related to measuring the wavelength zero reference point is the finite pixel resolution. Although the source positions can be measured with an accuracy of less than one pixel size unit on the reference image, the extraction of 2D spectroscopy images can only be made on integer pixel number to avoid erroneous image interpolation. This means that a pixel error as large as  $\pm 0.5$  could be introduced in the wavelength calibration process if not corrected, and is not so small comparing with the full length of the dispersed spectroscopy images ( $\sim 50$

pixel). As a first-order correction, we shift both the wavelength array and spectral response curve, both of which should show rather smooth change along Y (or wavelength) axis, and not perform sub-pixel shifting of the images. As a result, since object positions change slightly among different pointing observations, the wavelength at the same Y pixel of the extracted 2D spectra (or the wavelength array) also changes with different pointing observations.

### 6.1.12 Flat color-term correction

The presence of significant color variation in the flat images can be found in the ratio images of the broad-band flats (e.g., S7 flat / S15 flat). Therefore, although monochromatic flat-fielding can flat the background, the object spectrum is affected by the color term of the sensitivity. The correction for this could be done after extracting the 2D spectra for each target and applying the wavelength calibration. However, since we have only two broad-band filters for MIR-S/MIR-L (S7 and S15 for MIR-S, and L15 and L24 for MIR-L) and three for NIR (N2, N3, and N4), we can derive only global trends of wavelength-dependence of the flats. (Note that the wide-band filters, S9W and L18W, are not suitable for deriving the color dependence of the flat within the spectral coverage of the channel). Two broad-band flat images are interpolated to estimate the flats for a given wavelength in the following way:

$$F_2(x, y, \lambda) = [F(x, y, \lambda_2) - F(x, y, \lambda_1)]/(\lambda_2 - \lambda_1) \times (\lambda - \lambda_1) + F(x, y, \lambda_1) \quad (6.1.4)$$

where  $\lambda_2$  and  $\lambda_1$  are effective wavelength for broad-band filters.

Therefore the color term in equation 6.1.3 is expressed as:

$$\frac{F_2(x, y, \lambda)}{\text{spectral\_feature}(x, y) \times F_1(x, y)} = \frac{\left[ \frac{F(x, y, \lambda_2) - F(x, y, \lambda_1)}{\lambda_2 - \lambda_1} \times (\lambda - \lambda_1) + F(x, y, \lambda_1) \right]}{\text{spectral\_feature}(x, y) \times F_1(x, y)} \quad (6.1.5)$$

Therefore the color-term correction is calculated by two broad-band super-flats and one spectroscopy super-flat. Note that the product  $F_1(x, y) \times \text{spectral\_feature}(x, y)$  always appears together, i.e., we do not have to separate *spectral\_feature* term from the 'super-flat'.

After the color-term correction the image is as follows:

$$\text{obs}''' = \text{obj}(\lambda) \times R(\lambda) \quad (6.1.6)$$

For the NG spectra with the point source aperture (Np), flat-fielding will be made in a similar way to the slit spectroscopy of diffuse sources, since the aperture size is much smaller than the size of dispersed spectroscopy images. For spectroscopy with NG at Np and other slit spectroscopy data calibration, the super-flat is normalized to be unity at each wavelength (or Y) pixel, and there are no spectral features in the flats. On the other hand, NG spectra at Nc will be reduced in the same way as for other slit-less spectroscopy.

### 6.1.13 (local) Background subtraction (from extracted 2D spectra)

Although the background has been subtracted and it should be close to zero at this stage, any remaining background on the extracted 2D spectroscopy images is subtracted at this stage. Here we consider source masks for better determination of the local background. The background is measured and subtracted off, assuming a constant value across the images for all dispersers.

### 6.1.14 Spectral tilt correction

Although we do not reform the image 'shape' along the wavelength direction during the course of wavelength calibration because of simple linear grism dispersion, we do reform along X (or space) direction to correct spectral tilt. The tilt occurs due to misalignment of grism insertion direction with respect to chip orientation. The tilt is notably seen in NG images in which a pixel shift as large as  $\Delta X \simeq 2$  is observed over the longer dispersed image length ( $\Delta Y \simeq 250$  pixel). Similar tilt is also observed for other prism/grisms (NP, SG1, SG2, and LG2), although the tilt looks very small due to short dispersed image length. However, a tilt correction will be made for spectra of all types of dispersers.

### 6.1.15 Spectral response calibration

The spectral response calibration  $R(\lambda)$  depends exclusively on the wavelength. Therefore the response calibration table is a 1D vector ( $\lambda$  vs. ADU/s/mJy). This means that response variations of individual pixels have been removed beforehand by flat-fielding processes. Being different from the spatial flat correction, the spectral response varies significantly with wavelength due to change in quantum efficiency of chip and change in optical transmission along the camera optical trains, including the disperser.

The observed wavelength-calibrated 1D spectrum in ADU is just divided by the spectral response table. Since the wavelength for a given pixel in the observed spectrum is slightly different from that in the response table, simple interpolation will be performed to match the wavelength of the observed wavelength-calibrated spectrum with that in the response table.

The spectral response function used in the pipeline was defined at the centre of the field of view and checked at the periphery of the field for consistency.

### 6.1.16 Notes on slit spectroscopy

The same pipeline can be used for both slit-less and slit spectroscopy data reduction. Although the reduction of the slit spectroscopy data can be made in a similar way as for the slit-less spectroscopy data, there are some differences in some processing steps between the two. Here we summarize these differences.

- The slit spectroscopy flat-fielding consists of a normalized feature-less flat image. Therefore no color-term correction is necessary.
- Background subtraction is made on extracted 2D spectra in the case of point sources slit spectroscopy (Np), after stacking sub-frames. If dealing with slit spectroscopy for diffuse sources, the background subtraction is not performed since entire slit is expected to be filled with the object that is diffuse and there is no pure background area in the image.
- Shift-and-add feature of sub-frames will be disabled. Therefore any spectral change along the slit could not be related to a real change in the spatial dimensions of the extended source in case of large telescope jitter motion is observed. To measure such motion, run the pipeline for slit-less mode (without any slit-processing option in the pipeline command).
- In the wavelength calibration, measurement of the reference image positions will not be made, and pre-defined slit positions will be used as a wavelength zero reference point.

## 6.2 How to install and to set-up the IRC spectroscopy pipeline

The package has been tested in a Linux environment. It seems to run on the MAC OS-X environment, though it is not officially supported.

- Ask you local computer administrator for the IDL installation. There are no special requests in the IDL installation.
- Ask you local computer administrator for the ds9/xpa installation. There are no special requests in the ds9/xpa installation.
- Get the `irc_specred` package from the AKARI Observer's web site (see section 1.3). Extract and store it under your favorite directory.
- Set the following environment variables in your command-line shell. Below is an example for `cs`:

```
setenv IRC_SPECRED_ROOT <somewhere>
setenv IRC_SPECRED_LIB ${IRC_SPECRED_ROOT}/LIB/
setenv IRC_SPECRED_HOME ${IRC_SPECRED_ROOT}/ASTRO-F/
setenv IRC_SPECRED_CALIBDIR ${IRC_SPECRED_HOME}/IRC_SPECRED/CALIBDIR/
setenv IRC_SPECRED_DATADIR <anotherwhere>
setenv IDL_PATH +<IDL system path>:+${IRC_SPECRED_HOME}:+${IRC_SPECRED_LIB}
```

`IRC_SPECRED_ROOT`, `IRC_SPECRED_DATADIR`, and `IDL_PATH`, have to be modified by substituting `<somewhere>`, `<anotherwhere>`, and `<IDL system path>`, according to your local system settings <sup>1</sup>.

### 6.2.1 Data preparation

As explained in Chapter 3, when de-packing the data from the archive under `IRC_SPECRED_DATADIR`, the raw data will be stored in `IRC_SPECRED_DATADIR/<targetid>.<targetsubid>/rawdata`. `IRC_SPECRED_DATADIR`, `<targetid>`, and `<targetsubid>` will be used in the command line of the pipeline command.

All the reduced data and related information will be stored in a separate directory called `<root_dir>/<targetid>.<targetsubid>/irc_specred_out`. When the directory is missing, the toolkit will create it.

## 6.3 Calibration data

When de-packing the toolkit, the following calibration directories are created:

### 6.3.1 Calibration files

- `${IRC_SPECRED_CALIBDIR}/DARK` contains dark images with high S/N, combined with pre-compiled dark images, which can be applied for all the observations, after performing a small correction in the count offset. There are several 'super-darks' for NIR/MIR-S/MIR-L (as specified in the following list files).

---

<sup>1</sup>In the following, contents within the parentheses `<something>` should be changed according to user's interests.

- DARK/DARK\_NIR\_long.lst, DARK/DARK\_NIR\_short.lst
- DARK/DARK\_MIRS\_long.lst, DARK/DARK\_MIRS\_short.lst
- DARK/DARK\_MIRL\_long.lst, DARK/DARK\_MIRL\_short.lst

- $\${IRC\_SPECRED\_CALIBDIR}$ /FLAT contains two types of flats: super-flats for spectroscopy and reference images. These super-flats are made by combining a large number of blank sky images:

For slit-less spectroscopy:

- FLAT/SPEC2DFLAT\_NP.lst
- FLAT/SPEC2DFLAT\_NG.lst
- FLAT/SPEC2DFLAT\_SG1.lst
- FLAT/SPEC2DFLAT\_SG2.lst
- FLAT/SPEC2DFLAT\_LG2.lst

For slit spectroscopy:

- FLAT/SPEC2DFLAT\_NP\_slit.lst

For reference images and color-term correction of the flats:

- FLAT/IMAG2DFLAT\_N3.lst
- FLAT/IMAG2DFLAT\_N4.lst
- FLAT/IMAG2DFLAT\_S7.lst
- FLAT/IMAG2DFLAT\_S9W.lst
- FLAT/IMAG2DFLAT\_S11.lst
- FLAT/IMAG2DFLAT\_L15.lst
- FLAT/IMAG2DFLAT\_L18W.lst
- FLAT/IMAG2DFLAT\_L24.lst

- $\${IRC\_SPECRED\_CALIBDIR}$ /MASK contains images of known bad pixels (hot pixels, cold pixels, etc.). Masked area are marked by NaN (Not a Number) in the mask images.

- MASK/SLITMASK\_NIR.lst
- MASK/SLITMASK\_MIRS.lst
- MASK/SLITMASK\_MIRL.lst
- MASK/OUTLIERMASK\_NIR.lst
- MASK/OUTLIERMASK\_MIRS.lst
- MASK/OUTLIERMASK\_MIRL.lst

- $\${IRC\_SPECRED\_CALIBDIR}$ /COORDOFFSET contains a table of coordinate offsets in pixels ( $dX$ ,  $dY$ ) used to extract spectroscopy images for each object based on target positions on the reference image for all dispersers. The table also includes sizes of source extraction boxes ( $\Delta X$ ,  $\Delta Y$ ) on reference and spectroscopy images, and offsets ( $dX$ ,  $dY$ ) for zero-th order light image position.



– COORDOFFSET/IRCCOORDOFFSETPAR.dat

- $\${IRC\_SPECRED\_CALIBDIR}/WAVEPAR$  contains the wavelength calibration tables.

For gratings (NG/SG1/SG2/LG2), the wavelength ( $\mu\text{m}$ ) is expressed by a 1st order polynomial (linear) equation, and parameters are (1) dispersion ( $d\lambda/dY$ ), (2) wavelength at origin ( $\lambda_0$ ), and (3) position of the origin ( $Y_0$ ). In the toolkit, the position of the origin is fixed at the center of the extracted spectroscopy image. Therefore, only dispersion and wavelength at the origin are set in the calibration database files. The parameters can be applied for all the spectra within the FOV (i.e., the parameters are constant across the FOV). Effective wavelength ranges for each disperser are also set in the table (there are two kinds of range definitions: 'sensitive' and 'reliable' ranges).

For NP, the pixel position for a given  $\lambda$  is expressed in a 2nd-order polynomial equation, defined through three parameters (0th, 1st, and 2nd-order coefficients). Note that, for data analysis convenience, the equation is in pixel=function( $\lambda$ ) form, being in inverse form for the gratings. Effective wavelength ranges are also set in the table.

Only for NP, significant spectroscopy distortion exists, i.e., reference positions on the spectroscopy images cannot be represented by a constant pixel shift ( $dX$ ,  $dY$ ) from reference image positions. The deviation of pixel shift along wavelength axis (or Y axis) from the case of constant pixel shift is expressed in 3rd-order polynomial equation of reference position ( $dY_{\text{distortion}}=\text{function}(X_{\text{ref}}, Y_{\text{ref}})$ ). Polynomial coefficients are tabulated in a separate ascii table, and are stored under the same directory. Note that spectroscopy distortion along X ( $dX_{\text{distortion}}$ ) is not so significant, and constant pixel shift works rather well for NP, as in the same way for NG/SG1/SG2/LG2.

– WAVEPAR/IRCWAVEPAR\_COMMON.dat

– WAVEPAR/IRCWAVEPAR\_NP.dat

– WAVEPAR/IRCWAVEPAR\_NG.dat

– WAVEPAR/IRCWAVEPAR\_SG1.dat

– WAVEPAR/IRCWAVEPAR\_SG2.dat

– WAVEPAR/IRCWAVEPAR\_LG2.dat

– IRCSPECBOXDYPAR\_NP.dat

- $\${IRC\_SPECRED\_CALIBDIR}/RESPONSE$  contains ascii files tabulating  $\lambda$  vs. ADU/long exposure time in seconds/mJy for each disperser. There are five such tables (NP/NG/SG1/SG2/LG2). The spectral response is measured by observing flux standard stars with known flux energy distribution. This directory also contains a NP template spectrum (wavelength-calibrated spectrum, before calibrating spectral response) that will be used to find relative image shift along dispersion direction (or Y) between spectroscopy and reference images.

– RESPONSE/RESPONSE\_NP.lst

– RESPONSE/RESPONSE\_NG.lst

– RESPONSE/RESPONSE\_SG1.lst

– RESPONSE/RESPONSE\_SG2.lst

– RESPONSE/RESPONSE\_LG2.lst

- $\${IRC\_SPECRED\_CALIBDIR}/DISTPAR$  contains ascii tables containing spectral tilt information of the grism insertion angle.
  - `DISTPAR/IRCDISTPAR_NP.dat`
  - `DISTPAR/IRCDISTPAR_NG.dat`
  - `DISTPAR/IRCDISTPAR_SG1.dat`
  - `DISTPAR/IRCDISTPAR_SG2.dat`
  - `DISTPAR/IRCDISTPAR_LG2.dat`
- $\${IRC\_SPECRED\_CALIBDIR}/APCOR$  contains the spectral aperture correction tables.
  - `APCOR/APCOR_NP.dat`
  - `APCOR/APCOR_NG.dat`
  - `APCOR/APCOR_SG1.dat`
  - `APCOR/APCOR_SG2.dat`
  - `APCOR/APCOR_LG2.dat`

## 6.4 Running the pipeline

### 6.4.1 Data reduction order

The pipeline has to be run more than once, for **NP** (AOT0a) or **NG** (AOT0b) first, then **SG1** and **SG2**, and finally **LG2**. We need to start processing the shorter wavelength cameras (**NIR** and **MIR-S**), where larger number of brighter sources are expected to be observed within the FOV as position reference sources. The information derived there will be used for registering the longer wavelength cameras (**MIR-S** and **MIR-L**).

- to measure relative X and Y shift among spectroscopy sub-frames of **NP/NG** for registering spectroscopy sub-frames of **NP/NG/SG1/SG2/LG2**.
- to measure relative X and Y shift among reference sub-frames of **S9W** (with larger number of brighter sources) for registering imaging sub-frames of **S9W** and **L18W**.
- to measure relative X and Y shift of the spectroscopy image with respect to the reference image of **NP** or **NG** for registering reference and spectroscopy images of **NP/NG/SG1/SG2/LG2**.

Therefore the data reduction order should be as follows:

- First run: run the pipeline for **NP** (AOT04a) or **NG** (AOT04b), without a target table for enabling automatic target detection sub-program.

For **NG** data with point source aperture (**Np**), one needs to run the pipeline first without `/Np_spec` option. For other types of slit spectroscopy, one may skip this run because shift-and-add feature is disabled for this observing mode.

- Second run: run the pipeline for your desired targets. Make target tables for **N3**, **S9W**, and **L18W** on the raw images (at this stage only **N3** image has been processed). Run the pipeline again for **NP/NG/SG1/SG2/LG2** with target lists. Image shift database created previously with **NP/NG** will be used for the 2nd run. If your target is compact and bright enough to be detected by the source detection sub-program, you do not have to perform this 2nd run. For the 2nd run, begin processing for **NP/NG** first, then **SG1**, and finally **LG2**.

- Third run: run the pipeline again if you want to revise the target table. This is optional. Now you got processed reference images for revising the target tables. Run the pipeline again with the updated target tables to see final results.

### 6.4.2 Running the pipeline

Type the following in the IDL command line (a command in a single line):

```
irc_specred, <targetid>, <targetsubid>, <ext_source_table>, <refimage_list>,
<specimage_list>, <filter_spec>
```

#### Mandatory arguments:

- **targetid**: ID of the pointing observation. The information will be provided with the data distribution.

Example: 1331048

- **targetsubid**: Sub-ID of the pointing observation. The information will be provided with the data distribution.

Example: 1

- **ext\_source\_table**: An ascii list describing source position (X, Y) in pixel, or the target table.

Example: myobjects.tbl

```
cat myobjects.tbl
 100.0 100.0
 200.5 200.5
 150.0 150.5
```

This will extract spectra of sources located at (100.0, 100.0), (200.5, 200.5), and (300.0, 300.5) in pixel on the reference image.

If **ext\_source\_table** is set to "" (null string), then the pipeline activates its sub-program for automatic source detection.

There are some important tips in preparing the source table:

- Coordinates counts from 1, not 0, i.e., coordinates of the lower left corner of the image is (1, 1), not (0, 0).
  - For NIR the toolkit interprets by default the pixel coordinates as measured in the raw image (before the image rotation). When one measures the source positions in the processed images (after the image rotation), set the **/rotated\_NIR\_source\_table** option at the pipeline command line.
  - For MIR-L, one can use Y range of either 257-512 (for images before detaching MIR-S/L) or 1-256 (for images after detaching MIR-S/L) to set Y position of the targets. The pipeline subtracts 256 from the Y input if Y>256.
- **refimage\_list**: An ascii file listing FITS file names of reference image.

Example: N3.lst

```
cat N3.lst
F000001_N.fits
```

A default list is provided with the data distribution, and is found in **/rawdata** directory.

- `specimage_list`: an ascii file listing FITS file names of spectroscopy images.

Example: `NP.lst`  
`cat NP.lst`  
`F000002_N.fits`  
`F000004_N.fits`  
`F000006_N.fits`

A default list is provided with the data distribution, and is found in `/rawdata` directory.

Even if you find some images being damaged severely and you do not want them to be included in the pipeline processing, you must list all the images in the input list. Then you should specify the sub-frames to be removed on `ds9` within the pipeline. This is because the file names and their order in the list are used to relate FITS files to the exposure timing along the AOT operation sequence.

- `filter_spec`: a string specifying a disperser for the processing. Set one of the following: `N3_NP`, `N3_NG`, `S9W_SG1`, `S9W_SG2`, `L18W_LG2`

### 6.4.3 Options

- `root_dir`: a string specifying a directory in which a set of data is located. If set, this overrides the setting found in the environment variable `IRC_SPECRED_DATADIR`.

Example: `root_dir='/DATA/ASTRO-F/IRC/SPEC/'`

- `/Nh_spec`, `/Ns_spec`, `/Ls_spec`: flags for slit spectroscopy data reduction.
- `/Np_spec`: a flag for `Np` spectroscopy data reduction.  
See section 6.1.16 for more information of slit spectroscopy data reduction.
- `/no_tune_sourcepos`: a flag for disabling source position tuning subprogram within the pipeline. By default, `irc_specred` tries to measure accurate source positions by searching Gaussian peak around the coordinates set in the target table. This flag disables this functionality.
- `/use_short_refimage`: use a short exposure image to measure source positions. By default, `irc_specred` uses the long exposure frame for measuring source positions in the reference image. With this flag set, the toolkit uses the short exposure frame for measuring the source positions. Note that the data reduction will be made for both short and long exposure frames even with this flag set. This flag could be useful for measuring source positions of bright and saturated objects in the long exposure frame.
- `savefile`: set this option to a named variable that will contain the file name of the IDL save file (section 6.5.5). The simplest way to restore the IDL save file is to run `irc_specred` with the `savefile=savefile` option, and issue `restore,savefile` command after `irc_specred` finished and before, e.g., plotting the spectra.
- `/no_slit_flat`: a flag for disabling flat fielding process for slit spectroscopy at NIR. By default, `irc_specred` performs spectroscopy flat fielding with the super-flat image. However, as the natural background is faint in the NIR, the quality of the flat can not be improved so much. As a result, unfortunately, the quality of the processed spectra is limited by

the quality of the flat, not by the dark current nor photon noise. With this option set, `irc_specred` skips performing the flat fielding. Users are recommended to compare the spectra processed with and without the flat fielding process. We expect no big differences among the two spectra, except for random pixel-to-pixel variation of the flux, or some narrow (as narrow as one-pixel size) spike features, meanwhile spectra processed without the flat fielding could look better in terms of S/N. However, it seems a good idea to compare the results processed with and without the flat fielding. If you find that this is also the case for your data, you may adopt the data processed with the option `/no_slit_flat`.

- `/nir_column_pull_down_correction`: a flag for enabling masking column pulled-down regions in NIR images. With this option set, `irc_specred` searches for any pulled-down columns in each sub-frame, by examining dark area pattern at `Nh` slit area where background is minimum, and the pipeline masks out the columns. Furthermore, the pipeline also masks the same region in the next sub-frames in which damage by the column pull-down is still visible for deepest pulled-down columns.

#### 6.4.4 Outputs

- Whole image products:
  - Processed and stacked reference image (and corresponding mask and residual (reference image  $\times$  mask) images). Dark subtraction, flat-fielding, and background subtraction are made:
 

```
<targetid>.<targetsubid>.<filter_spec>.refimage_bg.fits
<targetid>.<targetsubid>.<filter_spec>.refimage_mask.fits
<targetid>.<targetsubid>.<filter_spec>.residual_refimage_bg.fits
```
  - Processed and stacked spectroscopy image (and corresponding mask and residual (spectroscopy  $\times$  mask) images). Dark subtraction, flat-fielding, and background subtraction are made:
 

```
<targetid>.<targetsubid>.<filter_spec>.specimage_bg.fits
<targetid>.<targetsubid>.<filter_spec>.specimage_mask.fits
<targetid>.<targetsubid>.<filter_spec>.residual_specimage_bg.fits
```

These images are in 3D, being the third (Z) dimension for the short (Z=0) and long (Z=1) exposure frames.

NaN (Not a Number) represents masked pixel/area.

- Extracted image products:
  - Extracted reference images for individual targets:
 

```
<targetid>.<targetsubid>.<filter_spec>.refimage_bg_indiv.fits
```
  - Extracted spectroscopy images for individual targets (and corresponding mask images). There are two kinds of images. One is wavelength calibrated (`_WC`) image for which flat color-term correction and wavelength calibration were applied. The other are flux calibrated (`_FC`) images for which flux calibration was applied as well as flat color-term correction and wavelength calibration:

```

<targetid>.<targetsubid>.<filter_spec>.specimage_wc_indiv.fits
<targetid>.<targetsubid>.<filter_spec>.specimage_mask_indiv.fits
<targetid>.<targetsubid>.<filter_spec>.specimage_fc_indiv.fits
<targetid>.<targetsubid>.<filter_spec>.specimage_noisemap_indiv.fits

```

Note that our spectral plotting tool (see below) uses `_WC` image as an input, not the `_FC` image, since the tool does on-the-fly flux calibration after considering various plotting conditions/options. Since the default `_FC` images does not care these, we strongly recommend to use our plotting tool to review the spectra.

In `_wc_indiv.fits` and `_fc_indiv.fits` files, wavelength information is set in the FITS headers with header keywords: `CRVAL`, `CDELTA`, `CRPIX`, and `CD` matrix. Users can plot the spectra with, e.g., the standard spectral plotting tool `SPLIT` on `IRAF`.

Note, however, that there are no such FITS header information for prism `NP` spectra because of their non-linear wavelength solution.

Here is an example to plot the `SG1` spectra with `IRAF/ SPLIT` task.

```

split xxxxxxx.1.S9W_SG1.specimage_fc_indiv.fits
Image line/aperture to plot (0:) (1): 10
Image band to plot (1:) (1): 2

```

In this example, the plot shows flux-calibrated spectrum of the 2nd object along `X` (space) = 10 pixel. Note that 2nd object means source ID 1 on the `IRC_SPECRED` since `IDL` counts from zero while `IRAF` does from one. Note also that no aperture correction can be applied for the spectral plot with the `SPLIT` task.

These images are in 3D, being the third (`Z`) dimension for source id. `NaN` (Not a Number) represents the masked pixel/area.

- Others:

- Target information table: a table of target information, such as positions (after source position tuning), flux, and size (Gaussian FWHM).

```

<targetid>.<targetsubid>.<filter_spec>.target_table.tbl

```

Its format is the following:

```

ID, image_x, image_y, image_mask_dx, image_mask_dy, spec_x, spec_y, spec_mask_dx,
spec_mask_dy, flux, image_FWHM, spec_bgnoise_ADU, spec_x_pos, spec_x_FWHM,
bad_sourcepos_flag

```

- Target table: If the source detection sub-program is used within the pipeline, a target table will be written. The file format is similar to the input target table. When source position tuning option is on, this file contains the updated source coordinates.

```

<targetid>.<targetsubid>.<filter_spec>.source_table.tbl

```

- IDL save file: The output of the pipeline will also be stored in the IDL save file, which is basically a dump file of the IDL memory image at the end of the pipeline processing. See also 6.5.5 to see how to work on the save file.

```

<targetid>.<targetsubid>.<filter_spec>.IRC_SPECRED_OUT.sav

```

- Log of the toolkit processing: a copy of the `irc_specred` logger is saved as an ascii file.
  - `<targetid>.<targetsubid>.<filter_spec>.log`
- DS9 region files: DS9 region files that have been used to locate targets on reference and spectroscopy images on `ds9`.
  - `<targetid>.<targetsubid>.<filter_spec>.refimage.reg`
  - `<targetid>.<targetsubid>.<filter_spec>.specimage.reg`

The region files and saved FITS images of the whole image products can be used to review the targets on `ds9` manually.

- Pipeline work files: The following files will be created by the pipeline. The files will be overwritten without notice. User are asked not to delete any of these files.
  - `NP_SHIFT_XY.dat`: for registering NP/SG1/SG2/LG2 sub-frames in AOT04a
  - `NG_SHIFT_XY.dat`: for registering NP/SG1/SG2/LG2 sub-frames in AOT04b
  - `S9W_SHIFT_XY.dat`: for registering S9W and L18W sub-frames
  - `NP_SPECBOX_SHIFT_X.dat`: for shifting SG2/LG2 along X in AOT04a
  - `NP_SPECBOX_SHIFT_Y.dat`: for shifting the wavelength zero-reference point for NP/SG1-/SG2/LG2 in AOT04a
  - `NG_SPECBOX_SHIFT_X.dat`: for shifting SG2/LG2 along X in AOT04b
  - `NG_SPECBOX_SHIFT_Y.dat`: for shifting the wavelength zero-reference points of NG/SG1-/SG2/LG2 in AOT04b

#### 6.4.5 Summary of interactive operations within the pipeline

Although the pipeline program works as a 'pipeline' (i.e., without interactive operation by users), some operations in the `irc_specred` do require interactive operation.

- Removing one or more sub-frames before combining the sub-frames: In some sub-frames, one may find severe damage by cosmic-ray shower, nearby satellite passing in front of the telescope, etc. To check the sub-frames and remove from the sub-frame combination list, all the dark-subtracted/flat-fielded/sky-subtracted sub-frames will be shown on a `ds9` for reviewing. To remove some sub-frames, use the **Frame -> show/hide frames** pull-down menu of `ds9` to hide the frame(s) you need to remove. The toolkit checks the hidden sub-frames and remove them from the internal sub-frame combination list.
- Retrying automatic source detection with modified detection parameters: If you use automatic source detection sub-program within the pipeline, you can retry source detection after tweaking the detection parameters. You will see the reference image on the `ds9` with detected sources marked, and you are asked to answer if the detection is satisfactory or not. If the answer is no, then another dialog with several detection parameter entries pops up. You can edit the parameters, and press OK to re-find the sources. You can repeat this detection process as many times as you like until you get satisfactory source list. The sub-program uses `daofind` algorithm, with the following parameters:

- `threshold`: Threshold intensity for a point source - should generally be 3 or 4 sigma above background.
- `fwhm`: FWHM to be used in the convolve filter.
- `sharplim`: 2 element vector giving low and high cutoff for the sharpness statistic (Default: [0.2,1.0] ). Change this default only if the stars have significantly larger or smaller concentration than a Gaussian.
- `roundlim`: 2 element vector giving low and high cutoff for the roundness statistic (Default: [-1.0,1.0] ). Change this default only if the stars are significantly elongated.

By default, `threshold` is three times the measured background noise. When too much or too less sources are found, `threshold` change would give better results, and it is not necessary to take care of sharpness/roundness parameters in most of the cases.

#### 6.4.6 Warning messages of the pipeline

Some common and frequently appearing warning messages are listed below.

- **Warning (`irc_specred`): Wrong number of arguments!** Check the command line arguments, and try again.
- **Warning: No <.> was found/set...Stop!** Some files that should be provided for the pipeline seem missing. Check if list files are properly set in the command line. This warning will also appear if you run `SG1/SG2/LG2` data reduction before performing `NP` or `NG` data processing, and some mandatory database files, e.g., describing relative image shifts, are missing.
- **Warning: Offset search box is too small!:** When the telescope drifts too much, the image matching sub-program fails to find the best shift values among sub-frames. Normally the sub-program resumes searching the shift with larger search box. Normally, this message is not so serious.
- **Warning: No data are available for measurement... Returning 0!** or **Warning: Data seems too noisy (sigma=<sigma>)... Returning 0!:** These messages will appear if, e.g., detected sources are too faint and their positions could not be measured with good enough accuracy. Check the source detection parameters for better source detections. This message is not so serious in most of the cases.
- **Warning: sigma of specbox Y shift measurement seems too large!:** This warning appears when the toolkit fails to measure the relative Y shift of `NP` spectra with respect to `N3` reference image. Check the reference image on `ds9` to know if source detection could be made successfully. Sometimes the program might detect only cosmic-ray hits, not stars, if the parameters are not optimized.
- **Warning: sky level is larger than 1.5 times sky sigma!:** After extracting spectroscopy images, remaining sky will be subtracted off locally around the source. If everything works fine, the average of the remaining sky should be very small, and is typically less than 1.5 times sky rms fluctuation. This warning message will appear if sky level is larger than the typical value. When this warning appears, check the `ds9` image to see if there remains large scale sky level variation. Presence of such sky often indicates failure in monochromatic flat-fielding and/or global sky subtraction, or any big unexpected debris. Note that this warning will not appear for slit spectroscopy (including `NG` at `Np`).



- **Warning: Available sky area is too small!:** Due to clouded source masking, the remaining sky area is too small for measuring sky. Check the source detection parameters for fewer source detection. Usually, this message is not so serious.
- **Warning: Cross-correlation peak is weak:** The cross-correlation function will be calculated while registering sub-frames and/or short and long exposure frames. The peak value of the cross-correlation function is a good measure of the frame registration. The value is 1 for ideal image matching, and is typically 0.6 or larger for real data with noise, but peak of 0.3 is still good. When this warning appears, check the quality of the registered and stacked images. So far registration of the short exposure frame can not be made with good enough accuracy, and one should ignore this warning for short exposure frames. This message is not so serious in most of the cases.
- **Warning: ROB\_MAPFIT: Too few points!:** This message comes from the fitting routine ROB\_MAPFIT called from some of the toolkit programs. The routine tries to fit the image region robustly (e.g., excluding outliers, iteratively, etc.), but it sometimes fails when the fitting area is heavily masked out for some reason. However, it somehow return the result (even if the results are not reliable in terms of statistics). Users may ignore the messages.
- **Warning: strange spec file list... Stop!:** The `irc_specred` reads list of FITS files to be processed (NP.lst/NG.lst/SG1.lst/SG2.lst/LG2.lst). When something wrong happens during data acquisition (i.g., too much time before stabilizing the telescope pointing), telemetry downlink (e.g., loss of telemetry), and/or data handling at ground (e.g., disk storage failure), the listed available FITS files are not in a proper order. Observers may notice that the list misses one or more FITS files due to some of these reasons. The toolkit analyze the file list before actually processing the data, and warns the uses if it detects something strange. Upon this warning messages, users are requested to check the input file lists or contents of distributed FITS files, and report any problems to the AKARI/IRC Helpdesk for more support. Although the `irc_specred` skips this list checking routine if a flag `/no_database_check` is set to the toolkit, use of this option without noting problems is dangerous, and usually is not recommended.

## 6.5 Working on the pipeline output

### 6.5.1 Displaying the whole images on ds9

Here we explain the region marks on the `ds9` that are shown in the processed whole image products, e.g., spectroscopy and reference images before source extraction.

In the spectroscopy image side (left),

- The blue rectangle shows spectroscopy image extraction area.
- The green rectangle shows area reserved for the object (or masked area for other objects).
- The red rectangle shows plotting area as defined by the spectral plotting tool.
- The yellow circle shows the expected positions of the zero-th order light.

In the reference image side (right), marked circles correspond to source positions (with diameter of the source FWHM).

- Green circles show sources with good position measurements.

- Red circles show sources with less accurate position measurements.

Source identification numbers are also indicated by the region marks.

For clear view of the image under complicated region marks, check out the `region -> show regions` check box in the `ds9` pull-down menu.

To display these images manually, issue

```
show_aperture_on_ds9, <image>, source_table (,/imag) 2
```

where `<image>` could be `refimage_ff[*,* ,1]` or `specimage.bg`, etc. on the IDL command line. When `/imag` option is set, the image is shown on the right side of the `ds9`, with region marks for reference image. The default (no option) is for spectroscopy image. See appendix for more on array name conventions.

### 6.5.2 Displaying the extracted images on ATV

ATV is a general-purpose interactive array image-displaying tool. The array should be in 2D. See ATV web page (<http://www.physics.uci.edu/barth/atv/>) for more information on the program <sup>3</sup>.

Command line syntax:

```
atv,array(,/block)
```

Here are some ATV tips:

- To display whole images, issue  

```
atv,<array>[* ,* ,1]
```

1 means long exposure frame (and 0 for short). Here, `<array>` should be something like `refimage.bg` or `specimage.bg`.
- To display extracted images of your desired `source_id`, use  

```
atv,<array>[* ,* ,source_id]
```

Here, `<array>` should be something like `specimage.n.bg`. To check mask area, use  

```
atv,<array>[* ,* ,source_id]*mask[* ,* ,source_id]
```
- When color table looks abnormal, type `set_color` at the IDL prompt before launching the `atv`.

### 6.5.3 Checking for wavelength zero reference point with the zero-th order light image

The toolkit calculates the wavelength zero reference point based primary on positions of the objects on the reference image. It also takes into account a wavelength zero-point drift due to satellite attitude drift, as well as coordinate rounding effect when extracting 2D spectra. In most cases, these methods work well to estimate the wavelength zero reference point with accuracy of 0.5 pixel or less. Since positions of the zero-th order light image are also calculated in the same way as for the wavelength zero reference point, one may check the wavelength

<sup>2</sup>Items in parentheses () are optional.

<sup>3</sup>In some systems, `/block` option may be required for interactive operation on the ATV. The conditions for which `/block` requirement seems to depend on local Linux or X11 system settings. The author does not have any good ideas on the correct usage of this option.

zero reference point accuracy by comparing positions of expected zero-th order light image and actually observed ones. Unfortunately, this check can be made only when bright sources with measurable zero-th order light images are observed at some part of the FOV by chance.

When a shift is found, the `change_wave_offset` command can correct for the estimated wavelength shift in pixel. The shift is calculated from the current position. This command changes the internal variable that records the wavelength offset, updates an offset database on disk, and re-draws the images on `ds9` with updated zero-th order light marks. This command can be used as many times as needed until getting satisfactory result. Then one can use the spectral plot tool for reviewing spectra with updated wavelength and spectral-response calibration. See below for the plotting tools.

Command line syntax (a command in a single line):

```
change_wave_offset,<wave_offset>,source_table,
space_profile,spec_profile,wave_array,specimage_fc_1d,
refimage_bg,specimage_bg,
refimage_n_bg,refimage_n_bg_short,
specimage_n_sff,specimage_n_sff_short,
specimage_n_wc,specimage_n_wc_short,
specimage_n_fc,specimage_n_fc_short,
res_refimage_bg,res_specimage_bg,
mask_refimage,mask_specimage,mask_specimage_n,
imagheader,speheader,imagheader_extract,speheader_extract,
noisemap,noisemap_n,noisemap_short_n,noise_mask,
dir=!IRC_SPECREC_DIR.workdir,savefile=savefile,/write_indiv_spec
```

where `<wave_offset>` is a pixel number (e.g., 1.0, 0.5, -0.5) to be shifted. <sup>4</sup>

#### 6.5.4 Spectral plotting tool

The toolkit's spectral plotting tool can handle many IRC-spectroscopy-specific features, and we recommend to use it for creating spectral plots. These are some of the functionalities of the tool:

- source masks can be considered. (see also `/no_mask` option)
- error bars (statistical plus systematical ones) can be plotted.
- simple image filters for removing isolated 'spike' pixels can be applied.
- aperture stacking along spatial direction and smoothing along wavelength direction can be applied for higher S/N spectra.
- shifting aperture positions along spatial direction (X axis) can be made.
- aperture correction.

Command line syntax (a command in a single line):

---

<sup>4</sup>Since this is a very long command, it seems better to copy the command that is written in the ``${IRC_SPECREC_HOME}/IRC_SPECREC/irc_spectrec.pro` program.

```
plot_spec_with_image,wave_array,specimage_n_wc,mask_specimage_n,
source_table,<source_id>
```

and for short exposures:

```
plot_spec_with_image,wave_array,specimage_n_wc_short,mask_specimage_n,
source_table,<source_id>,/short
```

with the following options:

- **nsum**: Number of pixels along X axis combined for plotting. Default is 3. For slitless spectroscopy, larger **nsum** (wider aperture) collects more photons from the object, but this also collects more background noise. Therefore, the best **nsum** for highest S/N is typically 2 or 3 for point sources (corresponding typical full-width of image PSF). In the case of slit spectroscopy, the range to plot the spectrum is:

- NP/NG: up to the edge of the extracted region
- SG1:  $\text{nsum} \leq 10$
- SG2:  $\text{nsum} \leq 8$
- LG2:  $\text{nsum} \leq 8$

If **space\_shift**  $\neq 0$  (see below) then the range should be smaller in order to prevent from extracting the spectrum out of the slit area.

- **smooth**: Boxcar smoothing width (in pixel) along wavelength direction. Default is **smooth=0** (no smoothing). For spectra with higher S/N without losing spectral resolution, **smooth** should be 3 (corresponding typical full-width of image PSF). Larger boxcar smoothing window will lose the spectral resolution. Note that when even number is set in the **smooth** (e.g., **smooth=2**), the actual smoothing box size would be **smooth+1** (e.g., **smooth=3**).
- **/sigma\_filter**: This option enables **sigma\_filter** operation (at 3 sigma significance level) over 2D spectra to remove spatially isolated high or low count pixels. Default is off. If you find too narrow emitting/absorbing features in your plots, try this option to see if this is a real feature or not. Note that, if there is a cosmic ray hit at the position in one of the sub-frames, such count should be removed as an outlier while combining sub-frames with sigma-clipping averaging method. However, if there are temporal hot pixels or weaker hot/cold pixels that are not shown in the hot pixel mask database, you will find outliers (hot or cold pixels) even after sub-frame combination. Users should take care not to remove real narrow features.
- **space\_shift**: shift of the plot extracting box along X (spatial) axis in pixel. Default is zero. Although the pipeline adjusts the X coordinates of spectrum extraction box by measuring positions of spectra, one may find remaining X offset in some cases. Change this offset to find peak position of the flux. If one changes **nsum** and **space\_shift**, issue the display command to see the modified spectrum extraction boxes graphically on the spectroscopy images over the **ds9**.

```
show_aperture_on_ds9,specimage_bg,source_table,
space_shift=<space_shift>,nsum=<nsum>
```

(a command in a single line)

- **/no\_mask**: by default, plots are shown after applying spectral overlapping masks by nearby sources. The **/no\_mask** option disables this masking functionality and plot spectra regardless of the possible source overlapping. Since masks are created without examining the

source brightness and/or spectral shape (e.g., line emitters, continuum emitters with break, etc.), one may often find the situation where no significant change in plots is found when comparing plots with and without the masking. If this is the case, you can just disable the masking by setting `/no_mask` option.

This option is especially relevant when the source of interest is much brighter than the overlapping ones.

- `ps`, `png`, `ascii`: Plots will be recorded on the files, not on the IDL plot window.
  - `ps=<filename>` creates a postscript file (`filename.ps`) of the plot in the working output directory (under `/irc_specred.out`).
  - `png=<filename>` creates a png image (`filename.png`) of the plot in the working output directory.
  - `ascii=<filename>` creates an ascii file ( $\lambda$  vs flux and flux errors) (`filename.spc`) of the plot in the working output directory. This file can be used for further analysis, for example using `gnuplot` program, with the command of `plot 'filename.spc' with yerrorbar`.
- `/with_image`, `tvbottom=<tvbottom>`, `tvtop=<tvtop>`: The 2D image will be shown on TV (an IDL graphic window) below the spectrum plot. Extraction box for plotting 1D spectrum is overlaid. The default is `with_image=0` (i.e., no TV display). The top and bottom ADU counts for displaying image can be specified with `tvtop` and `tvbottom`. These options are active only when `/with_image` is set.
- `/diffuse`: For slit spectroscopy data, spectra will be shown in units of MJy/str, rather than mJy with this option. The diffuse flux calibration is not yet fully established. Before this flux scale conversion, both `nsum` and `space_shift` parameters are taken into account to specify the spectral extraction aperture to create the spectrum for plotting.
- `/no_aperture_correction`: Aperture correction for point-like sources will be applied automatically within the plotting tool. The aperture size, set by `nsum`, is taken into account to find the correction factor. When the `/no_aperture_correction` option is set, the correction will be disabled. To perform good aperture correction, the aperture is centered on the source, and `nsum` should be 3 or more. Note that the aperture can be shifted by `space_shift` parameter.
- Other generic plot options useful in the plotting tool: The plotting tool accepts any kind of IDL-generic plot options for spectral plotting. See `plot` manual in the IDL documents for full information.

Following are some frequently used options.

- `xrange`: plot range along the X (wavelength) axis. By default, plots are shown within the wavelength range set in the wavelength calibration database file along the X axis. If set explicitly in the plotting tool command line, the default settings will be overridden.
- `yrange`: plot range along the Y (flux) axis. By default, plots are shown in auto-scale mode along Y. One can limit/fix the plot range by setting `yrange`.
- `/xlog`, `/ylog`: plotting in log scale along x or y.

### 6.5.5 Working on saved data

All the processed data are saved as an IDL save file, as well as FITS output files. The IDL save file is actually a dump record of the IDL memory image at the end of the data processing. Therefore, one can recall the pipeline results by simply issuing the following command: `restore,<savefile>`. Here the `<savefile>` is a string of the save file name. To recall other save file image, issue `.reset_session` first to clear the current IDL memory contents, and then issue another `restore` command with another save file name. See IDL manual to know more on the IDL save file, `restore`, and `.reset_session` commands.

After restoring the IDL memory, one can use, for example, the following `irc_specred` commands to review the results.

- `show_aperture_on_ds9, specimage_bg,source_table`
- `show_aperture_on_ds9, refimage_bg,source_table,/imag`
- `plot_spec_with_image,wave_array,specimage_n_wc,mask_specimage_n,source_table,<source_id>`

## 6.6 (Hopefully) Useful Tips

### 6.6.1 Getting best S/N spectra in slit ( $N_s$ , $N_h$ ) or $N_p$ spectroscopy data

Due to the higher dispersion of NG spectra, through narrower slit area ( $N_p$ ,  $N_s$ ,  $N_h$ ), at near infrared where the natural background light is faintest, the S/N of the NG slit flat image is rather poor, and this often limits the quality of the processed spectra. There is an option to disable the slit flat correction (`/no_slit_flat` option of `irc_specred`). We recommend processing the same data, with (default) and without (with the option) flat correction, for comparison. If one finds little noticeable differences in spectral features, (except for quality of the spectra), as we expect, one may accept the spectra processed without flat correction as a final calibrated data. See also section 6.4.3.

### 6.6.2 Tackling narrow spikes seen in NIR spectra (especially in slit spectra)

Even if one is interested in the slit area, any anonymous bright stars that happened to be within the big aperture may cause the column pull-down effect of the array, damaging even the slit spectroscopy data. To check this possibility, examine not only the 1D-extracted spectra but also the entire 2D-images, even outside of the slit area, so as to locate damaged columns (or rows, since NIR images are rotated during the toolkit processing).

With the toolkit version 2, new option `/nir_columnpulldown_correction` was introduced, and the pulled-down columns will be masked out. See also section 6.4.3.

### 6.6.3 Examining strange/fake features in NP spectra, especially around 2.4-3.5 $\mu\text{m}$

Sometimes an error in wavelength calibration leads to errors in the spectral response calibration, creating funny/fake spectral features in NP. In this case, the features resemble the response curve (or more exactly, its change per pixel along wavelength). Because of lowest spectral resolution and rather structured response-curve shape, this effect is most clearly seen in NP spectra. Note that even small wavelength offset (say, a mere 0.5 pixel) would produce noticeable pseudo spectral

features, especially around 2.4-3.5  $\mu\text{m}$ . We recommend to check the spectra of nearby field stars as well as your object to see if the funny features are common to all objects. If they look similar, the features are likely to be fake.

To see how the features change with wavelength offset, try the procedure described in section 6.5.3. Although there are no zero-th order light images available for NP, the command `change_wave_offset` works even for NP for testing how the spectral features change with the offset. Note that, for NP, there are no guidelines, such as zero-th order light, to find the best wavelength zero point in general. Therefore the user should justify the amount of offset entered with this command. Remember that nominal error of the wavelength zero-point calculation is 1.0 pixel or less.

#### 6.6.4 Examining flux level (in)consistency among different disperser data

Sometimes one may find jumps in flux level between SG1 and SG2 spectra (or other pairs of adjacent wavelength) for a single source. There are possible reasons for the jump, and tips to solve the problem.

- Source contamination: Degree of contamination changes with wavelength and, hence, with dispersers, causing flux change across the dispersers. User needs to check the reference image as well as spectroscopy images to find possible contaminating sources. There are no good recipes to remove the contamination.
- Aperture centering: Check the aperture position (along X or space) to see if the aperture is really at the peak of the dispersed images. The toolkit tries to put it at the right position by tracking the telescope jittering motion, but it is not always perfect. Use `space_shift` option of the plotting tool along with `/with_image` option to find the best position. See section 6.5.4 for actual operation.
- Aperture correction uncertainties: Aperture correction is not always perfect because one needs to adopt rather narrow aperture (`nsum=3` or so) for achieving the best S/N. If this is the case, even a small shift of the aperture position on sky (even at a scale of sub-pixel, although `space_shift` should be given in an integer pixel unit) gives rather large uncertainties in the flux aperture correction. Note that spectroscopy data relies on 1D spatial PSF of the source, and the pixel scale is not high enough to sample the PSF at good enough accuracy. So, with these limitations in mind, one needs to check the flux level, by changing the `nsum` and/or `space_shift` parameters, for your own source and its brighter neighbours, to find the accuracy of the absolute flux calibration. See section 6.5.4 for actual operation.
- Wavelength offset error: Because of the very low spectral resolution, the spectral response curves show rather sharp change near the band edge. If the wavelength offset is not properly set, a systematic error in the flux level is expected near the band edge due to wrong wavelength assignment in the spectral flux calibration process. If this happens, the spectrum looks brighter and fainter (or fainter and brighter) at the shortest and longest wavelength coverage of the disperser in a systematic manner. The way the shape change depends on the sign of error in wavelength offset (plus or minus). See section 6.5.3 for checking the wavelength offset error.

## 6.7 Appendix

### 6.7.1 Variable name conventions

As a general rule, the extension of the IDL variables (`_ff`, `_bg`, `_wc`, `_fc`) indicates the finally processed calibration status. Examples:

- `_ff` means that the data is processed all the way to flat-fielding.
- `_bg` means that the data is processed all the way to background subtraction, i.e., flat-fielded and background subtracted.
- `_wc` means that the data is processed all the way to wavelength calibration, i.e., flat-fielded, background subtracted, and wavelength calibrated.
- `_fc` means that the data is processed all the way to flux calibration, i.e., flat-fielded, background subtracted, color-term corrected, wavelength calibrated, and flux calibrated.

Whole image products: `_ff` and `_bg` are in 3D format (X, Y, short/long ID). Short exposure frame is in Z=0, and long exposure frame is in Z=1.

Extracted image products: `_n_` images are in 3D. The third dimension is for indicating the source id. The following extensions refer to different processing stages:

- `_n_bg`: background subtracted on extracted images.
- `_n_wc`: wavelength calibrated, after color-term corrected, residual background subtracted.
- `_n_fc`: flux calibrated, after color-term corrected, residual background subtracted, and wavelength calibrated.

Finally, these are the most frequently referred arrays:

- `refimage_bg`: Flat-fielded, background-subtracted whole reference image in 3D (X, Y, short/long ID)
- `specimage_bg`: Flat-field, background-subtracted whole spectroscopy image in 3D (X, Y, short/long ID)
- `specimage_n_wc`: Wavelength calibrated extracted 2D spectra in 3D (X, Y, source\_id)
- `specimage_n_fc`: flux calibrated extracted 2D spectra in 3D (X, Y, source\_id)

### 6.7.2 Summary of Commands and their Options

This is a broad outline of the main commands related to the pipeline together with their general syntax. For arguments encompassed by `<>` and `<>`, you need to specify your own processing parameters. Options starting with `/` are flags or switches to enable some functionality of the routine. For other options, you can set your parameters in numerals or ascii characters (that should be encompassed with single quotations).

- Running the pipeline

Usage:

```
irc_specred, <targetid>, <targetsubid>, <ext_source_table>, <refimage_list>,
<specimage_list>, <filter_spec>
```

Options



- `<targetid>`: pointing id of your observation. Typically, '1234567'. Check your data distribution.
  - `<targetsubid>`: pointing sub-id of your observation. Typically, '1'. Check your data distribution.
  - `<ext_source_table>`: an ascii file that specifies the source coordinates in X and Y in units of pixels. If this is set to be " (null), then automatic source detection program will be enabled within the pipeline.
  - `<refimage_list>`: an ascii file that specifies the FITS file names of the reference images to be processed. Typically, either 'N3.lst', 'S9W.lst', or 'L18W.lst'
  - `<specimage_list>`: an ascii file that specifies the FITS file names of the spectroscopy images to be processed. Typically, either 'NP.lst', 'NG.lst', 'SG1.lst', 'SG2.lst', or 'LG2.lst'
  - `<filter_spec>`: an code to specify the data processing mode, or a pair of filter and disperser names for the processing. This should be one of the following: N3\_NP, N3\_NG, S9W\_SG1, S9W\_SG2, or L18W\_LG2.
  - `/Nh_spec`, `/Ns_spec`, `/Np_spec`, `/Ls_spec`: flags to specify the slit spectroscopy data reduction.
  - `/no_tune_sourcepos`: a flag to disable source centering functionality (fine tuning of source positions with local Gaussian fitting around the user-specified source locations) when the toolkit is run with user-specified source table.
  - `/use_short_refimage`: a flag to use short reference image, rather than long reference image, for source detection. This is good for bright, saturated sources.
  - `/no_slit_flat`: a flag to disable flat-field correction for slit spectroscopy data (for `Np_spec`, `Ns_spec`, `Nh_spec`, `Lc_spec`). Use of this switch is recommended for slit spectroscopy with the current version of the toolkit/calibration database.
  - `/nir_columnpulldown_correction`: a switch to enable correction for column pull-down effect for `Np` spectra.
  - `savefile`: an ascii variable that store the file name of the IDL save file that records the `irc_specred` output.
- Displaying whole image products
 

Usage:

```
show_aperture_on_ds9,specimage.bg,source_table
```

or

```
show_aperture_on_ds9,refimage.bg,source_table,/imag
```

options

    - `nsum`: width of source extraction apertures in units of pixel, corresponding to the width of red rectangles shown on `ds9`.
    - `space_shift`: number of pixels by which to shift the source extraction apertures along spatial direction.
    - `/imag`: a flag to display reference images. Without this flag, the procedure assumes that the data to be displayed are spectroscopy images.

- Plot spectra

Usage:

```
plot_spec_with_image, wave_array, specimage_n_wc, mask_specimage_n,
source_table, <source_id>
```

options

- `<source_id>`: a number that specify the source to be plotted. You can find the number by looking at the `ds9` window that displays whole image products.
- `/short`: a flag to display short-exposure spectra. One needs to set `specimage_wc_short`, instead of `specimagen_n_wc` in the `plot_spec_with_image` command.
- `nsum`: number of pixels along X axis combined for plotting. This `nsum` parameter also works for `/diffuse` option.
- `smooth`: boxcar smoothing width (in pixel) along wavelength direction.
- `/sigma_filter`: a flag to enable `sigma_filter` operation (at 3 sigma significance level) over 2D spectra to remove spatially isolated high or low count pixels.
- `space_shift`: shift of the plot extracting box along X (spatial) axis in pixel.
- `/no_mask`: a flag to disable masking functionality, i.e., plotting spectra regardless of the possible source overlapping.
- `ps`: root filename of the PS graphical output (`<ps>.ps`) of the spectral plot.
- `png`: root filename of the PNG graphical output (`<png>.png`) of the spectral plot.
- `ascii`: root filename of the ASCII numerical output (`<ascii>.spc`) of the spectra.
- `/with_image`: a flag to display 2D image below the spectral plot.
- `/diffuse`: a flag to convert flux scale to MJy/str for slit spectra.
- `/no_aperture_correction`: a flag to disable aperture correction factor in plotting the spectra.
- `xrange`, `yrange`: parameters to specify plot ranges in X and Y axes, respectively.
- `/xlog`, `/ylog`: a flag to plot spectra in logarithmic scale along X and Y axes, respectively.

- Tweak wavelength zero-point manually

Usage:

```
change_wave_offset, <wave_offset>, source_table,
space_profile, spec_profile, wave_array, specimage_fc_1d,
refimage_bg, specimage_bg,
refimage_n_bg, refimage_n_bg_short,
specimage_n_sff, specimage_n_sff_short,
specimage_n_wc, specimage_n_wc_short,
specimage_n_fc, specimage_n_fc_short,
res_refimage_bg, res_specimage_bg,
mask_refimage, mask_specimage, mask_specimage_n,
imagheader, specheader, imagheader_extract, specheader_extract,
noisemap, noisemap_n, noisemap_short_n, noise_mask,
dir=!IRC_SPECRED_DIR.workdir, savefile=savefile, /write_indiv_spec
```

- `<wave_offset>`: offset along wavelength direction in pixel units.

## 6.8 Error messages when running the pipeline and Troubleshooting

- In general **double quotation mark (“) can cause problems** when calling the toolkit in IDL. For example:

```
restore,"12345678_some_more_information.sav"
```

or

```
irc_specred,"12345678_some_more_information.tbl",'SG1.lst','SG2.lst',S9W_SG1
```

give IDL syntax error, We suggest to use ' (single quotation mark), rather than " (double quotation mark) anytime when you work with the IRC\_SPECRED toolkit. For more, check the IDL manual (search 'quotation').

- When **one of the input parameters of the toolkit is a null string**, no space between single quotation marks should be given. For example:

```
irc_specred,' ','SG1.lst','SG2.lst','S9W_SG1'
```

will give an error message, because the toolkit tries to find the source table whose name is ' ' (blank space), and it fails. The correct syntax is:

```
irc_specred','','SG1.lst','SG2.lst','S9W_SG1'
```

- If **IDL complains about some undefined procedures/functions**, probably something is wrong in the setting:
  - Check `.cshrc` carefully, and/or.
  - After launching the IDL, issue `print,!path` on the IDL command line. This command shows all the paths for the IDL to search the libraries. See if all the TOOLKIT directories are included in `!path`.

- If after running the pipeline several times successfully, it fails with some unknown reasons, try resetting the IDL session, by issuing `.reset` command at the IDL command line. This resets everything stored in the IDL memory, including IDL common and environmental variables that are referred/updated during the toolkit session. Some old settings might cause the trouble. We recommend to reset every time the toolkit is restarted after a pipeline processing failure to avoid any confusion regarding old IDL variables. Remember, however, that the `.reset` command will destroy even the main IDL memory contents that contain information for, e.g., plotting the spectra. Of course, users can restore the IDL save file contents back to the main IDL memory to resume the data analysis.

- The filename where the toolkit saves the information is always `<targetid>.<targetsubid>.<filter_spec>.IRC_SPECRED_OUT.sav`. Therefore the `savefile` is a string variable output that records the save file name, not an input to specify the save file name. If the pipeline is run more than once with different options, the savefile should be renamed before the second run in order to be able to recover the previous results. You can recall the record even if you rename the save file name, by issuing:

```
restore,<renamed_save_file>.
```

- If you want **to see the results of previous toolkit run**, recalling the save file, and you do not remember the ID of your source, issue:  
`show_aperture_on_ds9, <image>, source_table, (/imag)` as instructed at section 6.5.1. This launches a `ds9` and displays image and region marks on it. Do not forget to include `source_table` after `<image>`.
- **There are no good ways to run more than two pipeline processes** at a same time on a single computer as a single user, because more than two toolkit processes share some same `ds9` windows. Please use other computers or other user account.
- There are no good tools to **coadd data taken over multiple pointings**. This is beyond the purpose of the toolkit right now. The simplest way is to average/combine extracted 1D spectra after dumping the results on ASCII files, with the `ASCII` option of the `plot_spec_with_image` command and coadd them with any available tool. Note that the wavelength for a given pixel is different from pointing to pointing for slit-less spectroscopy data, even if the same target was observed with the same pointing coordinates. One may need to rebin the spectra for a common grid for proper stacking.
- There are no good tools for **plotting spectra for a given source taken with different dispersers at once**. One needs to dump the spectra with the `ASCII` option when plotting the individual spectra, and then use your favorite plotting software for plotting multiple spectra once.
- If **the spacecraft attitude shifts after the reference frames have been taken**, the effect will be apparent in the wavelength calibration. A shift of more than 1-2 pixels can happen. For NP only, the signal at the peak of the RSF is used to correct the wavelength reference by default. The result will be inserted into the log file which will be further used to correct the drift in SG1/2 and LG2. Therefore the NIR data should be processed first. Similarly, for NG in the point source aperture (Np), the NG slitless spectroscopy field should be processed first. The actual correction is made by shifting the wavelength array rather than the image array.
- **Strange features found in the NG spectra taken at Np aperture** can be due either to flat-field problem or column pull-down. See section 6.6.1 or 6.6.2.
- **Strange features in the NP spectra taken with the big aperture (for Nc pointing)** will be due to wrong calibration only if the features are seen not only in your target object but also in nearby field stars. See section 6.6.3 for more information.
- There are several kinds of difficulties in **matching the flux level of the same source across the dispersers**, especially in slit-less spectroscopy mode, and jumps in flux level can be found between spectra from different dispersers in the same source. See section 6.6.4 for more details.
- If **unexpected narrow emission-line objects are found**, it could be due to zero-th order light images of nearby brighter stars. See the `ds9` window carefully since it shows the expected location of such features with yellow circles.